TECHNISCHE UNIVERSITÄT MÜNCHEN

Wissenschaftszentrum Weihenstephan für Ernährung, Landnutzung und Umwelt

Lehrstuhl für Pflanzenzüchtung

Genetic analysis of resistance to the three fungal plant pathogens *Blumeria graminis*, *Zymoseptoria tritici*, and *Pyrenophora tritici-repentis* using a multiparental winter wheat population

Melanie Stadlmeier

Vollständiger Ausdruck der von der Fakultät Wissenschaftszentrum Weihenstephan für Ernährung, Landnutzung und Umwelt der Technischen Universität München zur Erlangung des akademischen Grades eines

Doktors der Naturwissenschaften (Dr. rer. nat.)

genehmigten Dissertation

Vorsitzender:	Prof. Dr. Ralph Hückelhoven
Prüfer der Dissertation:	1. apl. Prof Dr. Volker Mohler
	2. Prof. Dr. Chris-Carolin Schön
	3. Prof. Dr. Andreas Graner

Die Dissertation wurde am 24.06.2019 bei der Technischen Universität München eingereicht und durch die Fakultät Wissenschaftszentrum Weihenstephan für Ernährung, Landnutzung und Umwelt am 18.11.2019 angenommen.

Wenn die Menschen nur über das sprächen, was sie begreifen, dann würde es sehr still auf der Welt sein.

(Albert Einstein)

Summary

Common wheat (*Triticum aestivum* L.) is one of the most important staple crops in the world. However, in temperate climates wheat grain yield and quality can be extremely decreased by fungal plant pathogens, such as *Blumeria graminis*, *Zymoseptoria tritici*, and *Pyrenophora tritici-repentis*. These pathogens are causal agents of powdery mildew (PM), septoria tritici blotch (STB), and tan spot (TS), respectively, and represent major fungal threats to wheat production in Europe. Factors like the ongoing wheat-pathogen coevolution and fungicide resistances that emerged in the pathogens have complicated the control of these diseases. Hence, elucidating the potential of breeding for resistance to multiple pathogens would be a significant contribution to accelerate wheat breeding and secure wheat grain yield and quality.

A highly diverse eight-founder multiparent advanced generation intercross (MAGIC) population with a modified mating design was developed. A subset of 394 $F_{6:8}$ recombinant inbred lines were genotyped with a single nucleotide polymorphism (SNP) array composed of 17,267 SNPs and with a functional PCR marker for PM resistance gene *Pm3a*. Population structure, linkage disequilibrium, the total and unique number of recombination events, and the parental genomic proportion were analyzed and a dense genetic map including 5436 markers was constructed. It could be shown that the used crossing design is equivalent to a labor-intensive mating design of an eight-founder MAGIC population regarding the analyzed population properties, the established linkage map, and high precision quantitative trait loci (QTL) mapping. The constructed MAGIC population captured over 70% of the allelic diversity present in the German wheat breeding gene pool and serves as an excellent source for analyzing multiple traits in the same genetic background.

Resistance to PM was evaluated under natural infection, whereas STB resistance was studied under artificial inoculation at two locations in Germany in the season 2016 and 2017, respectively. Disease severity of TS was assessed under natural infection in Germany in 2016 and under artificial inoculation in Germany and Denmark in 2017. Additionally, the agro-morphological traits plant height (PH), ear emergence time, and leaf angle distribution (LAD) were assessed at most locations. To identify genomic regions involved in resistance to the three diseases, quantitative trait locus analysis was conducted using four different genetic mapping methods. Interval mapping was carried out with and without cofactors (CIM and SIM). Single marker regression was performed using bi-allelic SNP calls and multi-point founder probabilities as predictors. In SIM, six,

seven, and nine QTL were identified for resistance to PM, STB, and TS, respectively. Fifteen QTL were detected for the agro-morphological traits using SIM. Most QTL were also detected with the other approaches. The QTL support interval overlapped two times for STB – TS and STB – LAD, respectively, and once for PH and LAD. A genetic region on chromosome 1AS simultaneously conferred resistance to all three diseases and the genetic region on 7AL showed contrary allelic effects for resistance to PM/STB and TS. However, most detected QTL were trait-specific implying that simultaneous breeding for resistance to PM, STB, and TS appears feasible. Marker identified as candidates for marker-assisted resistance breeding were suggested for validation. Multiple candidate genes described to be involved in plant immunity were identified for resistance QTL. The gene products belonged to various protein classes pointing to the involvement of different resistance mechanisms in durable resistance.

Zusammenfassung

Weichweizen (*Triticum aestivum* L.) ist eines der bedeutendsten Grundnahrungsmittel der Welt. In gemäßigten Klimazonen kann der Kornertrag und die Qualität des Weizens jedoch stark durch pilzliche Pathogene beeinträchtigt werden. Bedeutende Krankheiten in europäischen Weizenanbaugebieten sind zum Beispiel Mehltau, Septoria (STB)-Blattdürre und *Drechslera tritici-repentis* (DTR)-Blattdürre. Sie werden durch die Pathogene *Blumeria graminis*, *Zymoseptoria tritici* und *Pyrenophora tritici-repentis* hervorgerufen. Die Krankheitsbekämpfung wird erschwert durch Faktoren wie die anhaltende Weizen-Pathogen Koevolution und die entstandenen Fungizidresistenzen. Die Möglichkeit zeitgleich auf Resistenz gegenüber mehreren Erregern zu züchten, würde eine deutliche Beschleunigung der Weizenzüchtung mit sich bringen und langfristig Weizenerträge bei hoher Qualität sicherstellen.

Es wurde eine hoch diverse multiparentale („Mulitparental Advanced Generation Intercross“; MAGIC) Population basierend auf acht Eltern und einem modifizierten Kreuzungsschema erstellt. Insgesamt wurden 394 $F_{6:8}$ rekombinante Inzuchtlinien mit einem “Single Nucleotide Polymorphism“ (SNP) Markerarray, der 17.267 SNPs umfasst, und mit einem funktionalen PCR Marker für das Mehltauresistenzgen *Pm3a* genotypisiert. Die Populationsstruktur, das Kopplungsphasenungleichgewicht, die spezifische Anzahl und Gesamtanzahl der Rekombinationsereignisse und der Anteil im Genom, der von jedem der acht Eltern vererbt wurde, wurden untersucht. Zudem wurde eine genetische Kopplungskarte mit 5436 Markern erstellt. Die Ergebnisse weisen darauf hin, dass das verwendete Kreuzungsschema gegenüber einem arbeitsintensiven MAGIC Kreuzungsablauf als äquivalent zu betrachten ist. Dies gilt sowohl für die populationsspezifischen Eigenschaften, die genetische Kopplungskarte als auch für die Genauigkeit in der „quantitative trait loci“ (QTL)-Kartierung. Die erstellte MAGIC Population beinhaltete über 70% der im Deutschen Weizen-Genpool vorhandenen allelen Diversität und stellt damit eine sehr gute Ressource da, um viele Merkmale im gleichen genetischen Hintergrund zu untersuchen.
Die Resistenz gegenüber Mehltau wurde unter natürlicher Infektion, gegenüber der STB-Blattdürre mit Hilfe einer Inokulation an je zwei Standorten in Deutschland in den Jahren 2016 und 2017 erfasst. Die Befallsstärke der DTR-Blattdürre wurde in Deutschland 2016 unter natürlichem Infektionsdruck und 2017 an zwei Standorten (Deutschland und Dänemark) nach künstlicher Infektion erhoben. Zusätzlich wurden die agronomischen Merkmale Pflanzenhöhe (PH), Zeitpunkt des Ährenschiebens und Blattstellung (LAD)

bonitiert. Es wurden vier verschiedene Kartierungsmethoden angewendet, um eine Assoziation zwischen genomischen Regionen und den Phänotypen zu detektieren. Die Intervall-Kartierung wurde ohne und unter Berücksichtigung von Kofaktoren (SIM und CIM) durchgeführt. Die Einzelmarker-Regression wurde unter Verwendung des binären Markergenotyps beziehungsweise den Wahrscheinlichkeiten, dass das Allel von einem der acht Eltern vererbt wurde, durchgeführt. Mit der SIM Methode wurden sechs, sieben und neun QTL jeweils für die Resistenzen gegenüber Mehltau, STB-Blattdürre und DTR-Blattdürre detektiert und fünfzehn QTL für die agronomischen Merkmale. Die meisten QTL wurden auch mit den anderen Kartierungsmethoden identifiziert. Das QTL-Vertrauensintervall überlappte je zweimal für STB-Blattdürre – DTR-Blattdürre und STB-Blattdürre – LAD und einmal für PH und LAD. Die genetische Region auf Chromosom 1AS vermittelte Resistenz gegenüber allen drei untersuchten Krankheiten, wohingegen in der Region auf Chromosom 7AL die allelen Effekte für Mehltau/STB-Blattdürre und DTR-Blattdürre umgekehrte Vorzeichen aufwiesen. Die meisten QTL waren merkmalsspezifisch, was die Möglichkeit einer zeitgleichen Resistenzzüchtung gegen die drei Krankheiten impliziert. Mehrere Marker, die für die markergestützte Resistenzzüchtung von Bedeutung sein könnten, wurden zur Validierung vorgeschlagen. Zudem wurden in den detektierten Regionen Kandidatengene gefunden, deren Rolle in der Pflanzenabwehr bekannt ist. Die Genprodukte gehörten verschiedenen Proteinklassen an, was die Vermutung nahelegt, dass verschiedene Resistenzmechanismen an der Ausprägung dauerhafter Resistenzen beteiligt sind.

List of Figures

List of Tables

List of Abbreviations

AGO	ARGONAUTE
bp	DNA base pairs
B.C.	Before Christ
BMWpop	Bavarian MAGIC winter wheat population
BTB/POZ	Broad-complex, tramtrack, and bric-a-brac/poxvirus, zinc finger
Cas9	CRISPR-associated protein 9
CIM	Composite interval mapping
CIMMYT	International Maize and Wheat Improvement Centre
cm	Centimeter
cM	CentiMorgan
CRISPR	Clustered regularly interspaced short palindromic repeats
DE	Germany
DK	Denmark
DNA	Deoxyribonucleic acid
DTR	*Drechslera tritici-repentis*
EET	Ear emergence time
EU	European Union
FLS2	FLAGELLIN-SENSITIVE2
GPS	Global positioning system
HIFs	Heterogeneous inbred families
IBD	Identical by descent
IBS	Identical by state
iid	Independent and identically distributed
KASP	Kompetitive allele specific
LAD	Leaf angle distribution
MAGIC	Multiparent advanced generation intercross
MAS	Marker-assisted selection
Mbp	DNA mega base pairs
MLO	MILDEW RESISTANCE LOCUS
NB-LRR	Nucleotide-binding leucine-rich repeat
NILs	Near isogenic lines
PAMP	Pathogen-associated molecular pattern
PCR	Polymerase chain reaction

PH	Plant height
PM	Powdery mildew
PR5	Pathogenesis-related protein 5
PTI	PAMP-triggered immunity
QTL	Quantitative trait locus/loci
r^2	Squared correlation coefficient
R^2	Explained phenotypic variance
rf	Recombination frequency
RILs	Recombinant inbred lines
RLK	Receptor-like kinase
RNA	Ribonucleic acid
RNAi	RNA interference
ROS	Reactive oxygen species
SIM	Simple interval mapping
SNP	Single nucleotide polymorphism
SOD	Superoxid dismutase
SSD	Single seed descent
STB	Septoria tritici blotch
TALENs	Transcription activator-like effector nucleases
TE	Test environment
TILLING	Targeting induced local lesions in genomes
TS	Tan spot
ZFNs	Zinc finger nucleases

Publications included in this thesis

Stadlmeier et al. (2018)

Stadlmeier, M., Hartl, L., and Mohler, V. (2018). Usefulness of a multiparent advanced generation intercross population with a greatly reduced mating design for genetic studies in winter wheat. *Front Plant Sci.* 9, 1825. doi: 10.3389/FPLS.2018.01825.

Abstract

Background

Genetic marker information and high-throughput genotyping methods are no longer limiting factors for genetic studies in plant breeding. The focus is now on developing next generation mapping resources, such as NAM and MAGIC populations, and to exploit their potential. Recently, huge efforts were made to develop MAGIC populations for several plant species. So far, no information has been available about the impact of a greatly reduced MAGIC mating design on population properties and QTL analyses.

Results

We developed an eight-founder MAGIC population in winter wheat with a modified mating design. The population comprising 394 $F_{6:8}$ lines was genotyped with the 15K + 5K Infinium® iSelect® array containing 17,267 SNP markers. The lines showed no significant signatures of population structure and increased relationship between individuals. The founder contributions of the eight parents were nearly equally distributed over the genome with average genome-wide values of 7.0 to 9.6%. The constructed genetic linkage map included 5435 polymorphic high-quality SNPs distributed over 2804 loci with a total map length of 5230 cM. Congruency to other linkage maps and to physical marker positions of the IWGSC RefSeq v1.0 showed appropriate marker ordering of the genetic map. On average, 73 recombination events per line were detected. This was twice as many as reported for a four-founder MAGIC and similar to observed values of an eight-founder MAGIC population with a full mating design. Our MAGIC population captured 71.7% of the allelic diversity present in the German breeding gene pool as suggested by simulation studies using a complete eight-founder MAGIC mating design and randomly selected founders. As a proof of principle, we mapped five quantitative trait loci explaining more than 70% of the total phenotypic variance for the trait seedling resistance to powdery mildew.

Conclusion

In this study, the impact of a labor- and cost-efficient MAGIC mating design on various population properties, on the construction of a linkage map, and on trait mapping was analyzed. It appears that such a design is equivalent to a labor-intensive MAGIC mating design with simultaneous reduction of costs and efforts during development.

Candidate's contribution

Analysis of genotypic data, construction and validation of the genetic linkage map, design and execution of the seedling resistance trial, phenotypic data analysis, QTL mapping, creation of all figures and tables, discussion of the results, writing the first draft of the manuscript, revision of the paper.

Stadlmeier et al. (2019)

Stadlmeier, M., Jørgensen, L. N., Corsi, B., Cockram, J., Hartl, L., and Mohler, V. (2019). Genetic dissection of resistance to the three fungal plant pathogens *Blumeria graminis*, *Zymoseptoria tritici*, and *Pyrenophora tritici-repentis* using a multiparental winter wheat population. *G3 Genes|Genomes|Genetics*. 5, 1745-1757. doi:10.1534/g3.119.400068.

Abstract

Background

Common wheat (*Triticum aestivum* L.) is one of the most important food crops in the world. However, wheat grain yield and quality can be extremely decreased by fungal plant pathogens. In Europe, the three pathogens *Blumeria graminis*, *Zymoseptoria tritici*, and *Pyrenophora tritici-repentis* are major fungal threats to wheat cultivation. Therefore, new resistance loci and simultaneous genetic analysis of resistance to these pathogens is of great interest for resistance breeding.

Results

We assessed resistance to powdery mildew (PM), septoria tritici blotch (STB), and tan spot (TS) in field trials at six locations over two years. Additionally to the disease traits, the agro-morphological traits plant height, ear emergence time, and leaf angle

distribution were assessed. Different mapping methods were applied to detect quantitative trait loci (QTL) associated with the traits of interest. Six, seven, and nine QTL for resistance to PM, STB, and TS, respectively, were identified. Additionally, 15 QTL were mapped for the agro-morphological traits. Environmentally stable and strong QTL were mapped with all methods in most cases. A QTL for PM and STB each was assigned to a gene based on functional markers. For three PM QTL and one TS QTL, candidate genes were suggested based on published genetic studies. Resistance to STB and TS was conferred by the same genetic region in two cases. Two genetic regions associated with all three analyzed diseases were detected on chromosomes 1AS and 7AL.

Conclusion

The value of MAGIC populations for investigating genetic relations between various traits within the same genetic background was shown. Promising resistance loci for all three diseases were identified with the potential to establish diagnostic markers. Parallel marker-assisted breeding for resistance to PM, STB, and TS appears feasible, although knowledge of specific genetic regions with contrary allelic effects for the different diseases such as on chromosome 7AL should be considered.

Candidate's contribution

Conceiving and executing the field trials, phenotypic data analysis, QTL mapping, creating all figures and tables, discussion of the results, writing the first draft of the manuscript, revision of the paper.

1 INTRODUCTION

1.1 Background

Wheat (*Triticum* spp.) was one of the first cereal crops cultivated about 10,000 years ago in the Neolithic period (Lev-Yadun et al., 2000). Multiple disciplines, including archaeobotany, phytogeography, genetics, and genomics, acted jointly to determine the most probable area where cultivation and, later on, domestication of small cereal crops started. They concluded that the cradle for today's agriculture is in the Fertile Crescent (Fig. 1), a region that includes today's Lebanon and parts of Turkey, Iran, Iraq, Syria, Jordan, and Israel (Gopher et al., 2001; Lev-Yadun et al., 2000). Farmers soon started to make an investment in farming activities leading to a long-term transition of wild to domesticated plant forms.

Figure 1 Origin and spread of *Triticum* spp..

The origin of wheat is in the Fertile Crescent (grey shaded area, according to Salamini et al., 2002). The suggested provenance of *T. monococcum*, *T. dicoccum*, *T. durum*, and *T. aestivum* is encircled with orange, green, brown, and purple, respectively (according to Dubcovsky and Dvořák, 2007). The probable distribution of wheat over the Mediterranean route is indicated with a blue line (according to Badaeva et al., 2015). The geographic map is based on scribble maps (Anonymous, 2019a).

The wild diploid wheat *T. monococcum* spp. *aegilopoides* (genome A^mA^m), also called einkorn, was the first cultivated wheat species (Fig. 1). However, its intensive cultivation lasted only a few thousand years until it became less important (Salamini et al., 2002). Recently, the einkorn wheat *T. monococcum* spp. *monoccocum* experienced a renaissance due to its high content of health-promoting ingredients like minerals, carotenoids, and other secondary metabolites (Miedaner and Longin, 2012). The tetraploid wild wheat *T. turgidium* spp*. dicoccoides* (genome AABB) was also domesticated in the early Neolithic times (Harlan and Zohary, 1966). It is assumed that the tetraploid status was based on an allopolyploidization event between *T. urartu* (genome AA) and a close relative of *Ae. speltoides* (genome BB) (Blake et al., 1999; Dvořák et al., 1998). The domesticated emmer wheat *T. turgidium* spp*. dicoccum* (genome AABB) (Fig. 1) evolved to one of the most important crops in the beginning of the Neolithic period, and was still grown in ancient Egypt (Salamini et al., 2002). It is characterized by hulled seeds and a non-brittle rachis, which might have been important factors for its early success. Genetic studies indicated that the major genes *brittle rachis 1-3* located on the chromosomes of homoeologous group 3 mainly control the constitution of the spike rachis (Nalam et al., 2006). A reduced spikelet shattering may be seen as the most important indicator of wheat domestication as it extended the possible harvest time point and strongly reduced yield loss. The formation of the hexaploid wheat (genome AABBDD) is based on a hybridization event between a subspecies of *T. turgidium* and the wild grass *Ae. tauschii* spp. *strangulata* presumably in the southern Caspian basin (Dvořák et al., 1993, 1998). It is assumed that the first hexaploid wheat already showed a non-brittle rachis but hulled seeds. A further important breakthrough in the domestication of the *Triticum* spp. was the development of the free-threshing tetraploid wheat species *T. turgidium* spp*. durum* and the hexaploid species *T. aestivum* spp. *aestivum* (Fig.1). Nowadays, it is supposed that the free-threshing hexaploid wheat emerged by a further hybridization event between *T. aestivum* ssp. *compactum* and the domesticated emmer wheat *T. turgidum* ssp. *dicoccum* (Yan et al., 2003). Genetic studies showed that the trait free-threshing is caused by several loci located *inter alia* on the long arm of chromosome 5A and on the short arm of chromosomes 2A and 2D (Simons et al., 2006; Sood et al., 2009). Once the naked wheat species had emerged, the foundation was laid for the expansion of the tetra- and hexaploid wheats over the Mediterranean route to southwest Europe (Fig. 1) and the northern foothills of the Alps about 4,000 B.C. (Maier, 1996). Since that time, a continuous evolution of wheat under domestication has taken place, affecting a broad range of morphological, physiological,

and qualitative traits. This process has been dramatically accelerated by modern plant breeding since the 1940s, for example, by the establishment of the International Maize and Wheat Improvement Centre (CIMMYT).

Today, common wheat (*Triticum aestivum* L.) is one of the most important staple crops in the world with a harvest area of over 218 million hectares and a production of over 770 million tons worldwide (FAOSTAT, 2017). In the European Union (EU) more than 142 million tons of wheat are produced (Eurostat, 2018) on a cultivated area of over 26 million hectares (Eurostat, 2017). Thus, wheat accounts for almost half of all cereals produced within the EU.

One major threat to wheat cultivation in Europe is the attack by fungal plant pathogens. It is assumed that pathogens first evolved in the same area as their respective host species and spread along the routes of host domestication (McIntosh, 2009). Whether the spread of pathogens depended on wind dispersal or directly on seed, straw, and hay transport remains unclear. A prerequisite for the successful coevolution of pathogens in response to changes in the host is a large genetic diversity and a high evolutionary potential in the pathogen population (McDonald and Linde, 2002). It was shown that major fungal wheat pathogens, such as *Blumeria graminis*, *Zymoseptoria tritici*, and *Puccinia striiformis*, are highly polymorphic fungi harboring a diverse pool of haplotypes with significant genetic variation for virulence and the possibility of chromosomal rearrangements (Plissonneau et al., 2018; Schwessinger et al., 2018; Wicker et al., 2013). Population geneticists consider mutation, gene flow, genetic drift, reproduction system, and selection as the five core evolutionary forces to rapidly evolve virulence on resistant hosts (McIntosh, 2009). Furthermore, temporal, spatial, and environmental aspects of the host-pathogen life history (Burdon and Thrall, 2008; Chen et al., 2017) as well as agricultural practices, such as large field sites, monoculture, and reduced genetic diversity of cultivated varieties (Burdon and Thrall, 2008), can have a significant impact on pathogen outbreaks as the selection of virulent pathotypes is strengthened. Changes in pathogen populations can reach dramatic extents whenever widespread varieties carry single major resistance genes. Such breakdowns of major resistance genes with large effects have been reported in wheat mainly for rusts and powdery mildew (Bennett, 1984; Hovmøller et al., 2010; Miedaner and Flath, 2007; Olivera Firpo et al., 2017; Singh et al., 2008). To achieve a more durable resistance, multiple quantitative resistance genes with ideally complementary modes of action have to be pyramidized in a single plant genotype additionally to qualitative resistances (Pilet-Nayel et al., 2017).

For wheat cultivation in Europe the three diseases powdery mildew (PM), septoria tritici blotch (STB), and tan spot (TS) caused by *B. graminis*, *Z. tritici,* and *Pyrenophora tritici-repentis*, respectively, are major fungal threats (Lucas et al., 2015). The ascomycete *B. graminis* of the order Erysiphales is an obligate biotrophic fungus that infects wheat at almost every growth stage (Bürstmayr et al., 2016). It can colonize the complete aboveground part of the plant. Early in the year, the cleistothecium releases the sexually produced haploid ascospores (Götz and Boyle, 1998), which are dispersed by wind and rain splash. Cool and moist conditions favor the germination of the spores and the infection of susceptible wheat cultivars. After the fungus has developed haustoria, which are established to feed the fungus and to control the host's metabolism and immunity (Hückelhoven and Panstruga, 2011; Panstruga and Dodds, 2009), the fungus builds conidiophores. These structures release conidia for a second cycle of infection within a week. The fast and massive reproduction through asexual cycles is a major strategy of *B. graminis* (Dean et al., 2012). At the end of the cropping season, the fungus carries over on infected crop debris, volunteers, and autumn sown wheat plants in cleistothecia and as mycelia clusters. Currently, more than 100 PM resistance alleles are described in the literature, distributed over nearly the whole wheat genome (Bürstmayr et al., 2016; Li et al., 2018). In addition, quantitative trait loci (QTL) associated with resistance to PM were described (Li et al., 2014b). However, many PM resistance genes are race-specific and already ineffective due to successful adaptation of the fungus.

Z. tritici (anamorph *Septoria tritici*) is a necrotrophic ascomycete belonging to the Dothideales and causes STB, which is one of the most damaging fungal diseases of wheat in regions with humid climates (Fones and Gurr, 2015). *Z. tritici* is a necrotrophic fungus. Its wind-dispersed sexual propagules, the ascospores, penetrate the plant through open stomata during early developmental stages without the establishment of appressoria (Dean et al., 2012). In a second stage of the fungal life cycle, infection mainly occurs by splash-dispersed asexual pycnidiospores from basal leaf layers (Suffert et al., 2011). The lengthy latent period with symptomless intercellular colonization of the plant tissue, which typically lasts 3-4 weeks, is a major challenge to react sufficiently early to STB disease (Orton et al., 2011). The fungus can overwinter as mycelium, pycnidia, and pseudothecia on the same reservoirs as *B. graminis*. Genetic analyses investigating STB resistance have previously identified 21 major genes and a large number of QTL (Brown et al., 2015). However, there is still a lack of widely commercially relevant wheat germplasm with adequate resistance to *Z. tritici* infection (O'Driscoll et al., 2014).

TS is another economically significant residue-born wheat disease, caused by the necrotrophic ascomycete *P. tritici-repentis* of the order Pleosporales. Primary infection takes place in autumn and spring through ascospores, which are formed during the sexual stage and overwinter as pseudothecia mainly on crop debris but also on volunteer plants. In a second infection stage, heavy rain splash moves the asexual conidia from lower to upper leaf layers (Schilder and Bergstrom, 1992), resulting in first symptoms within a week after infection. Main symptoms are yellow to brown leaf spots surrounded by chlorotic and necrotic areas (Lamari and Bernier, 1989). The symptoms are mainly associated with the three fungal protein effectors ToxA, ToxB, and ToxC (Strelkov and Lamari, 2003), with further effectors assumed to be involved (Faris et al., 2013). *P. tritici-repentis* isolates are classified into eight different races based on their ability to produce the three virulence factors (Strelkov and Lamari, 2003). Besides seven qualitative race-specific resistance loci (Faris et al., 2013) also race-nonspecific QTL have been detected for TS resistance (Juliana et al., 2018; Kollers et al., 2014).

The attack of wheat through each of these pathogens can lead to loss of grain quality and to dramatically yield loss. Therefore, in some European countries over 95% of winter wheat acreage is treated with fungicides (Jørgensen et al., 2008). A study, conducted over a period of 10 years in three European countries, reported a reduction in yield and quality of winter wheat of up to 9% if only one fungicide class, the azoles, were omitted and up to 26% if no fungicides were applied (Blake et al., 2011). However, fungicide applications are under continuous pressure from several sides: first, because of acquired fungicide resistances and second, due to the increased demand for more sustainable agriculture. Since the 1970s, fungicide resistances have been reported for various fungicide classes such as the benzimidazoles (Griffin and Fisher, 1985; Sanders et al., 1986), the demethylation inhibitors (Leroux and Walker, 2011; Stammler and Semar, 2011), the quinone outside inhibitors (also called strobilurins) (Cheval et al., 2017; Drabešová et al., 2013; Jørgensen et al., 2018), and the azoles (Cools and Fraaije, 2008, 2013; Jørgensen et al., 2018; Mullins et al., 2011) – all of these fungicide classes are applied in wheat cultivation. However, even more alarming is the dramatically reduced time from seven to two years, during which pathogens evolved resistance (Lucas et al., 2015). It was suggested that this development was linked to classes of selective fungicides showing a specific mode of action at a single-site target in the pathogen combined with applications at lower concentrations (Lucas et al., 2015). In contrast, most former fungicides represented multi-site target chemicals, which interfered with a range of different cellular processes making it less likely that the fungus adapts to the fungicide

(Klittich, 2008). However, former fungicides were applied at high doses and often showed strong adverse effects on cultivated plants and the users (Morton and Staub, 2008). To counteract this issue, often mixtures of multiple site-specific active compounds are used. The development and release of fungicides with novel active substances will probably remain on a low level in the EU: first, because of high costs of usually more than 200 million Euros for development and license (Anonymous, 2019b) and second, due to the stricter legal regulations in the framework of Regulation (EC) No 1107/2009 (Anonymous, 2019b). Furthermore, fungicide applications often do not fit well to the concept of sustainability. The United Nations released the UN 2030 Agenda for Sustainable Development in September 2015. This is the first global resolution considering sustainability as a holistic approach including society, economy, and environment. The agenda defines 17 objectives, called the Sustainable Developmental Goals, which should be reached by 2030 (United Nations, 2015). The second objective of this agenda aims at ending hunger, achieving food security, improving nutrition, and promoting sustainable agriculture (United Nations, 2015). A long-term sustainable agriculture requires changes in various aspects of the agricultural sector. This includes *inter alia* technical progress in agriculture, a deeper understanding of composition and interactions in the soil and of humus formation, altered strategies for field management practices, as well as a shift in the focus of breeding.

Facing these challenges, breeding wheat varieties resistant to multiple fungal pathogens is important. For establishing durable resistance, new wheat cultivars must comprise not only qualitative resistance genes, which act in a race-specific manner, but also polygenic race-nonspecific resistances. To supply wheat breeders with knowledge about such loci, the scientific community should intensify its efforts to find novel quantitative resistance and multi-resistance loci by establishing new resources and utilizing cutting edge technologies and knowledge.

1.2 Outline

In plant breeding, the quality and power of genetic studies mainly depends on the genetic material employed and the quality of the genotypic and phenotypic data. In the last years, huge efforts were made to develop low-cost marker technologies that are able to cover the entire genome with high density. Examples are genotyping by sequencing (He et al., 2014) and high density genotyping arrays, like the Wheat660K SNP array introduced by Cui et al. (2017). Additionally, advances in whole genome sequencing led

to high-quality annotated reference genome, like the recently published genome of Chinese Spring (International Wheat Genome Sequencing Consortium, 2018). This opens new possibilities such as the comparison of different genetic studies based on different marker systems and better understanding of genes on a functional genetic basis. Both will accelerate the understanding of wheat genetics and genomics. Therefore, genetic studies are no longer limited by available genotyping techniques, markers, and sequence data.

To take full advantage of these capacities in high-resolution QTL mapping, an expanded genetic diversity in mapping populations is required. The most widely used population type for complex trait mapping is the classical bi-parental population. The substructure is well-known, and the effect of rare alleles can be properly estimated with high statistical power. However, biparental crosses exhibit a narrow genetic base and therefore, cannot fully break down the complex genetic structure underlying phenotypic variation. In addition, only few traits can be investigated simultaneously. The limited number of recombination events, which occur during population construction (Flint-Garcia et al., 2003), leads to large linkage blocks with poor mapping precision in linkage analysis (Holland, 2007; Xu et al., 2017; Zhu et al., 2008). In contrast, association mapping (AM) panels encompass a great allelic diversity and make use of the large number of historical recombination events by random sampling of diverse lines. Marker-trait association analysis based on historically evolved linkage disequilibrium can be much more powerful in terms of genetic resolution and mapping accuracy (Ewens and Spielman, 2001) although a sufficiently large sample size is required (Flint-Garcia et al., 2003). Further constraints of AM panels are the reduced statistical power in detecting association for low-frequency allelic variants (Asimit and Zeggini, 2010; Gibson, 2012) and the risk of detecting false positives due to population structure (Vilhjálmsson and Nordborg, 2013; Zhao et al., 2007). As a next-generation mapping resource, multiparental populations, such as the *Arabidopsis* multi-parent recombinant inbred line (AMPRIL) population, the nested association mapping (NAM) panels, and the multiparent advanced generation intercross (MAGIC) populations have emerged. In crops, the latter population type was first discussed by Mackay and Powell (2007) and Cavanagh et al. (2008). To date, MAGIC populations have been developed in many plant species including *Arabidopsis* (Kover et al., 2009), wheat (Huang et al., 2012; Mackay et al., 2014; Sannemann et al., 2018; Shah et al., 2019; Stadlmeier et al., 2018), rice (Bandillo et al., 2013), tomato (Pascual et al., 2015), faba bean (Khazaei et al., 2018; Sallam and Martsch, 2015), maize (Dell'Acqua et al., 2015), barley (Sannemann et al., 2015), and sorghum (Ongom and Ejeta, 2018). In

MAGIC designs, diverse genetic founders are intercrossed during several rounds in a defined funnel crossing scheme. This results in highly diverse genotypes with a unique mosaic of founder alleles and known pedigree (Cavanagh et al., 2008). MAGIC populations combine the advantage of known relatedness and structure with a high recombination rate and genetic diversity. Therefore, they constitute a powerful resource for high resolution and multiple trait mapping. However, realizing and establishing a full MAGIC cross design is an expensive, time-, and labor-consuming task. Therefore, it is of great interest whether expenditures can be reduced during MAGIC population creation while concurrently preserving the above stated benefits. In Stadlmeier et al. (2018) the effect of a modified labor- and cost-saving mating design on kinship, population structure, founder probabilities, and linkage disequilibrium, and on genetic linkage map construction was analyzed using an eight founder winter wheat MAGIC population comprising 394 recombinant inbred lines (RILs). Based on the results, recommendations were given for the establishment and crossing scheme of prospective MAGIC designs. An appropriate genetic linkage map is crucial for high confidence QTL mapping and for reliable statements on marker-phenotype associations. The genetic map presented in Stadlmeier et al. (2018) was validated via multiple comparisons with physical and genetic maps. As a proof of concept, QTL mapping was conducted for the trait seedling resistance to powdery mildew, which was assessed in a controlled environment.

The reaction of different host genotypes to a specific pathotype or an isolate mixture of a pathogen can be assessed accurately in controlled environments. Thus, such an experimental design is well-suited to test and prove established resources and methods. However, the main limiting factor under controlled conditions is the area necessary to carry out experiments with large population sizes and replicated entries from seedling to the adult plant stage. Another concern is that controlled experimental setups do not reflect the complex situation present in the field and therefore, the results are sometimes not easily transferable to field conditions. Another advantage of field trials is the ability to assess the reaction to a naturally occurring mixture of various isolates of a pathogen at a specific location. This allows detecting resistance loci that have not been overcome yet and to map both, race-specific and race-nonspecific resistance loci, which are considered important to establish durable resistance in cultivars. Therefore, for the study of Stadlmeier et al. (2019) the above-introduced MAGIC population was grown in replicated field trials over several years to assess resistance to PM, STB, and TS, which represent important fungal diseases in European winter wheat cultivation (Lucas et al., 2015). Different mapping approaches were applied to detect genomic regions conferring

resistance to the three diseases. The positions of the identified resistance loci were compared to QTL mapped for agro-morphological traits within the same population to distinguish between cellular, molecular, and morphological escape resistance mechanisms. Furthermore, the relation between the three fungal disease resistances were analyzed at the genetic level with high accuracy and possible strategies for resistance breeding in winter wheat were suggested.

Here, the results presented in Stadlmeier et al. (2018) and Stadlmeier et al. (2019) are supplemented by additional findings important for the deeper understanding of MAGIC crossing designs and the molecular plant mechanisms involved in incompatible wheat-pathogen interactions.

2 MATERIAL AND METHODS

2.1 Development of the Bavarian MAGIC winter wheat population

The BMWpop was constructed from eight European winter wheat lines at the Bavarian State Research Center for Agriculture in Freising, Germany (Fig. 2). The founders 'Event' (A), 'Format' (B), 'BAYP4535' (C), 'Potenzial' (D), 'Ambition' (E), 'Bussard' (F), 'Firl3565' (G), and 'Julius' (H) were selected based on phenotypic diversity for a broad range of agronomic traits, including yield potential, grain quality, and disease resistance, as well as affiliation to different breeding programs (Stadlmeier et al., 2018).

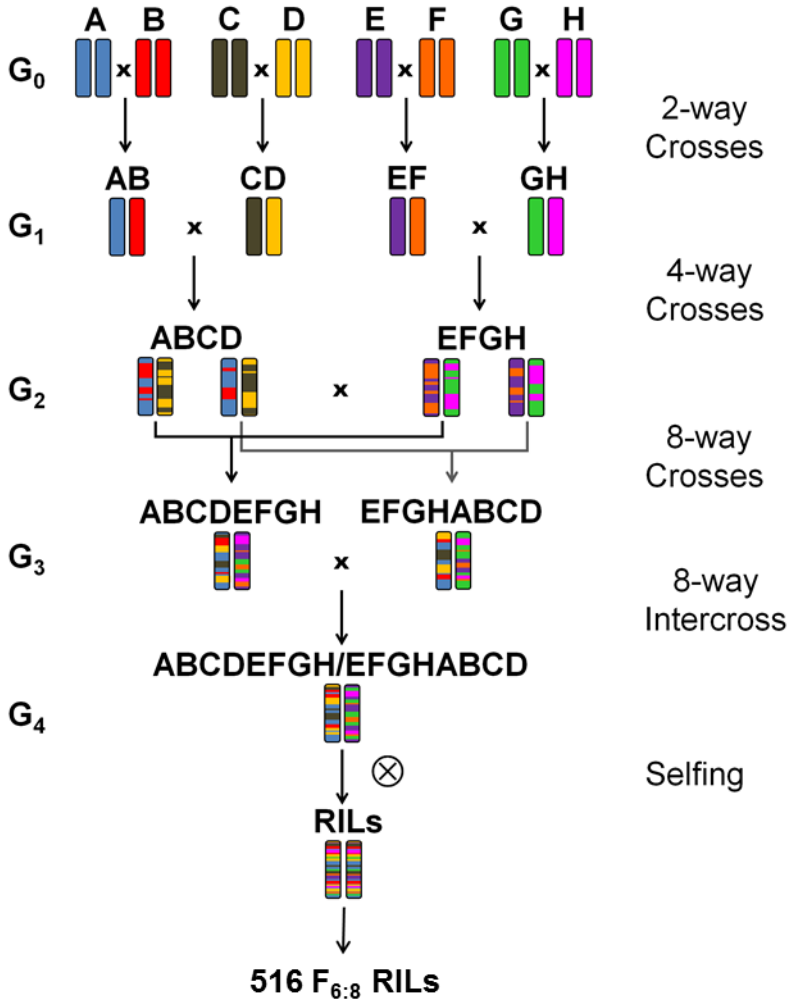

Figure 2 Crossing design of eight-founder Bavarian MAGIC winter wheat population.

(A) 'Event', (B) 'Format', (C) 'BAYP4535', (D) 'Potenzial', (E) 'Ambition', (F) 'Bussard', (G) 'Firl3565', and (H) 'Julius' (graphic based on Cavanagh et al. (2008) and adapted from Stadlmeier et al. (2018)).

For the construction of BMWpop, the number of unique cross combinations, which are possible in an eight-founder MAGIC design, was greatly reduced. Four two-way cross combinations (AB, CD, EF, and GH) were generated using one ear per founder. One randomly selected F_1 grain of each two-way cross was grown. Egg cells and pollen, respectively, of the F_1 plants were used for 16 independent crosses for each of the two four-way cross combinations ABCD and EFGH. Out of these 16 available grains per four-way cross combination, eight seeds were randomly selected for further mating. Four seeds of the eight selected ABCD and EFGH crosses, respectively, were raised and used as female crossing partner, while plants from the remaining seeds acted as the male crossing partner in the eight-way cross combination to obtain four ABCDEFGH and four EFGHABCD eight-way crosses. Each of the four ABCDEFGH plants acted as female and was crossed with each of the four reciprocal EFGHABCD plants to obtain 16 independent eight-way intercrosses (ABCDEFGH/EFGHABCD; Table 1).

Table 1 Eight-way intercross in Bavarian MAGIC winter wheat population

♀ \ ♂	**L1_EFGHABCD**	**L2_EFGHABCD**	**L3_EFGHABCD**	**L4_EFGHABCD**
L1_ABCDEFGH	Subgroup 1	Subgroup 2	Subgroup 3	Subgroup 4
L2_ABCDEFGH	Subgroup 5	Subgroup 6	Subgroup 7	Subgroup 8
L3_ABCDEFGH	Subgroup 9	Subgroup 10	Subgroup 11	Subgroup 12
L4_ABCDEFGH	Subgroup 13	Subgroup 14	Subgroup 15	Subgroup 16

Therefore, the population was built up of 16 highly related subgroups. The F_1 seeds of the 16 subgroups were selfed to the F_6 generation by single seed descent (SSD), followed by two generations of bulk propagation. It was intended to establish subgroups of equal size within the framework of population development. All analyses mentioned below refer to a subset of 394 $F_{6:8}$ recombinant inbred lines (RILs) that were selected based on seed availability and suitability for experimental field trials, with special consideration of plant height.

2.2 Genotypic data analysis

2.2.1 Investigation of population and kinship structure

Plant genomic DNA was extracted from a bulk of ten plants per line as described by Plaschke et al. (1995). The BMWpop and the eight founders were genotyped using the

15K + 5K Infinium® iSelect array and a functional PCR marker for the powdery mildew resistance allele *Pm3a* (Tommasini et al., 2006). Quality control and filtering of markers was based on the synbreed package V0.12-6 (Wimmer et al., 2012) in R (R Development Core Team, 2017). SNPs that were monomorphic, showed more than 5% of missing data, and had a minor allele frequency lower than 5% were discarded. Additionally, it was taken care that no duplicated SNPs remained and that for each marker genotype all founders showed a homozygous call. After filtering, 6717 markers were available for further analysis.

The genetic distance between the 394 RILs and the eight founders was calculated using Rogers' distance (Rogers, 1972). To graphically display the genetic distance between the RILs and the parents, the genetic distance matrix was submitted to a principle coordinate analysis as described by Gower (1966) using the R package ape V5.0 (Paradis et al., 2004). The genomic relationship matrix K was calculated with the Genomic Association and Prediction Integrated Tool V3.0 (Lipka et al., 2012) according to the method 1 of VanRaden (VanRaden, 2008).

2.2.2 Construction and validation of the genetic linkage map

In multiparental population designs, it is not possible to clearly define the parental origin of an allele when using bi-allelic marker systems. This makes the statistical methods to estimate the recombination frequency between a pair of markers used for bi-parental populations difficult to apply to MAGIC designs. For RILs, which were derived from eight-way designs, Broman (2005) calculated two-locus haplotype probabilities. These two-locus haplotype probabilities are a function of the recombination frequency (rf) and were calculated for a grid of potential recombination values (from 0.0 to 0.1 in steps of 0.005 and from 0.1 to 0.5 in steps of 0.01). The observed pattern of allelic segregation at two loci in BMWpop was compared with these theoretical haplotype probabilities. The most probable rf between two markers in BMWpop was estimated using the maximum likelihood method resulting in an estimated rf-matrix of dimension m x m, where m represented the number of markers (Huang and George, 2011). Missing values in the rf-matrix resulted from parental allelic combinations of two markers that were (nearly) uninformative because of (nearly) identical allelic combinations in the population, independent of the rf (Shah and Huang, 2017). This means that compared to the founders the probability of allelic combinations of a marker pair remained the same or

almost similar in the population no matter which rf was assumed. Therefore, no rf could be assigned to such a marker pair. Based on the rf-matrix, the markers were distributed to 300, 250, and 200 linkage groups. The grouping was carried out with hierarchical clustering using a distance matrix that was built from a combination of the rf and the corresponding log-likelihood ratio. Using lg=200, linkage groups were assigned to chromosomes based on the information of published maps (Cavanagh et al., 2013; Marcotuli et al., 2017; Wang et al., 2014a) and adjusted where necessary using the grouping results of the more stringent settings (lg=250 and lg=300). Markers were excluded from linkage groups when (i) the location on a particular chromosome was not confirmed by one of the reference maps and concurrently at least two other maps suggested a location on another chromosome and (ii) the missing values in the rf matrix exceeded a threshold of 20%. Marker ordering within linkage groups was carried out in two steps using two-point ordering. In the first step, an overall path order was constructed to minimize the total map length. In the second step, fine ordering was performed starting with the overall path order. The latter algorithm is a simulated annealing method, also called “Anti-Robinson seriation”, where at the beginning a pair of random markers is permuted and a single marker is subsequently moved to a random position (Shah and Huang, 2017). After marker ordering, all linkage groups belonging to the same chromosome were assembled based on the consensus map of Cavanagh et al. (2013). Finally, the validity of the marker order over the whole chromosome was examined with respect to a minimized number of crossovers by investigating local permutations of the marker order using a window size of three markers. The genetic map distances were calculated according to Haldane’s mapping function (Haldane, 1919).

The genetic linkage map was established with the two R packages mpMap V2.0.2 (Huang and George, 2011) and mpMap2 V0.0.3 (Shah and Huang, 2017).

The congruency of marker order was examined between the established linkage map and the three genetic maps of the eight-founder MAGIC design NIAB 2015 (Gardner et al., 2016; Mackay et al., 2014), the four-founder MAGIC population 9kMAGIC (Cavanagh et al., 2013; Huang et al., 2012), the bi-parental backcross progeny L19 BC1 (Geyer et al., 2018), and the physical marker positions of the IWGSC RefSeq v1.0 (International Wheat Genome Sequencing Consortium, 2018). Common markers between BMWpop map and the respective genetic and physical map formed the basis for the comparison. For further validation of the established linkage, the chromosome length and the number

and distribution of markers and loci over the genome were compared to the linkage maps of the three above-mentioned populations.

2.2.3 Population genetic analysis

Genome- and chromosome-wide linkage disequilibrium was calculated as the squared correlation coefficient (r^2) between all pairs of 5436 mapped markers using the R package genetics V1.3.8.1 (Warnes et al., 2013). The 95th percentile of the distribution of the square root transformed r^2 values between unlinked markers was taken to determine the population-specific critical r^2 value. LD was assumed to be caused by genetic linkage if a r^2 value was above this threshold (Breseghello and Sorrells, 2006). Smoothing curves were fitted to the plots of LD decay estimation by least square regression using a smoothing span parameter of 0.1 (R/stats V3.4.3, R Core Team, 2007).

In an eight-founder MAGIC design, each parent should theoretically contribute 12.5% to the genetic material represented in the population. To calculate the realized contribution of each founder line, it was necessary to define the parental origin of each marker allele. The estimation was based on a multi-point founder haplotype construction using the information of all linked marker loci (Huang and George, 2011). The algorithm, which was implemented in R/mpMap, estimated for each genotype multi-point founder probabilities that a marker allele was inherited from the eight founders, respectively. Based on these founder probabilities, the origin of an allele was assigned to one of the eight founders if the probability exceeded a threshold of 70%. The assignments were used to calculate the contribution of each founder per chromosome. Additionally, the founder assignments also were the basis to compute the number of recombination events per line in BMWpop. If the parental origin of an allele changed along the chromosome, a recombination event was assumed. The number of recombination events in BMWpop was compared to the number of recombination events in the two MAGIC populations NIAB 2015 and 9kMAGIC and the bi-parental cross L19 BC1. For both multiparental designs, the calculation of the number of recombination events followed the one already described for BMWpop (Huang et al., 2012, Stadlmeier et al., 2018). In the backcross population, a recombination event was counted if the allele call changed from heterozygote to homozygote along the chromosome and *vice versa*.

The allelic diversity present in the BMWpop was compared to a panel of 524 German winter wheat breeding lines derived from six breeding companies (Geyer et al., 2016).

2.3 Genetic analysis of resistance to *B. graminis*, *Z. tritici*, and *P. tritici-repentis*

2.3.1 Experimental design

Seedling tests

Seedling resistance to PM was assessed in the glasshouse under controlled conditions with a temperature of 18°C, a relative humidity of 67%, and 16 h light per day in two independent experiments. For each experiment, the RILs and the parents were sown in multi-pot plates with 10 grains per line in a randomized complete block design with two replicates.

Field trials

Field trials were conducted during 2016 and 2017 in Germany and Denmark under natural pathogen attack and artificial infestations to assess reaction to PM, STB, and TS (Table 2). Two field trials were carried out for PM and STB, whereas three experiments were conducted for TS. The experimental design at each location was an incomplete block design with two replications and a block size of 10 to 47 lines depending on the field site. The lines were sown in double-row plots of 30 plants except in Roggenstein, where 1300 plants per line were sown in 4.5 m^2 plots. The founders and a set of check varieties with known disease susceptibility to the three pathogens were included as duplicated entries in each trial. Additionally, three checks with a low, medium, and high degree of susceptibility to the respective pathogen were included in each block, except in Roggenstein, where only the parental lines were included. Field trials were managed according to standard agronomic cultivation practices at each location, with the exception that no fungicide was used to control the pathogen that caused the trait of interest.

Table 2 Field trial environments and traits scored

Year	Location	GPS[a]	Abbreviation	Inoculation	Traits scored[b]					
					PH	EET	LAD	PM	STB	TS
2016	Freising (DE)	48°24'45.3"N 11°43'21.1"E	16FS1	*Z. tritici* conidia	x[c]	x	x		x	
2016	Freising (DE)	48°24'01.8"N 11°42'46.4"E	16FS2	None	x	x	x			x
2016	Roggenstein (DE)	48°10'51.9"N 11°19'07.3"E	16RG	None				x		
2017	Freising (DE)	48°24'43.9"N 11°43'20.1"E	17FS1	*Z. tritici* conidia	x	x	x	x	x	
2017	Freising (DE)	48°24'38.6"N 11°43'27.9"E	17FS2	*P. tritici-repentis* infected straw	x	x				x
2017	Slagelse (DK)	55°25'06.9"N 11°22'54.7"E	17SL	*P. tritici-repentis* infected straw	x	x	x			x

Table modified after Stadlmeier et al. 2019.

[a] Global Positioning System (GPS) coordinates.

[b] Traits are plant height (PH), ear emergence time (EET), leaf angle distribution (LAD), powdery mildew (PM), septoria tritici blotch (STB), and tan spot (TS).

[c] The respective trait was scored.

2.3.2 Inoculation method

Powdery mildew

In seedling tests, trials were inoculated with conidia of two *B. graminis* isolates by shaking heavily infected wheat seedlings 30 to 40 cm above the plants when the primary leaves reached a length of 5 cm. The isolate mixture was known to be virulent against the PM resistance genes *Pm2*, *Pm4b*, *Pm5a*, *Pm6*, and *Pm8* (Mohler et al., 2013).

In the field trials in 2016 and 2017, PM infection occurred naturally during tillering stage.

Septoria tritici blotch

A collection of *Z. tritici* single-spore isolates (Table 3) was screened comprising ten current isolates provided by the company EpiLogic GmbH (Freising, Germany) and two historical ones, kindly shared by the Julius-Kühn-Institute (Quedlinburg, Germany). Isolates were selected based on a high sporulation rate on cultivation medium and virulence to the eight founders at seedling stage. The four selected single-spore isolates St-SN-002, St-SN-004, BAZ 6/1/04, and BAZ 8/8/04 were cultivated in petri dishes on a yeast-malt agar for five to seven days with 8 h in darkness at 12°C followed by 16 h under white and ultraviolet light at 20°C in a MLR-351 incubator (Sanyo Electric Co., Osaka, Japan). The yeast-malt agar consisted of 4 g yeast, malt, and glucose,

respectively, and 15 g agar per liter of distilled water. Well-cultured plates were used as starter cultures for mass propagation in a liquid growth medium consisting of 4 g yeast, malt, and glucose, respectively, per liter of distilled water. The conidia of one plate were used to incubate 150 ml of the liquid yeast-malt-glucose medium using 500 ml Erlenmeyer flasks. The flasks were incubated under natural light at 20°C on a reciprocal shaker with 175 rpm (Risser et al., 2011). The conidia suspension was concentrated with a separating funnel and the conidia concentration was determined with a Fuchs-Rosenthal hemocytometer. The inoculum was adjusted to $1x10^6$ conidia per ml with equal shares per isolate and, finally, Tween 80 solution (0.05% v/v) was added to the inoculum. The experiments were inoculated twice with 660 l inoculum per hectare at an interval of seven days during cloudy afternoons when the flag leaf of more than half of all lines was fully developed. An hour after first inoculation, mist irrigation was applied from 8:00 am to 6:00 pm for eleven days in cycles of two hours irrigation followed by a one-hour break with 12 l m^{-2} d^{-1} on average.

Table 3 Screened isolates of *Z. tritici* for field inoculation

Isolate ID	Origin	Year of sampling	Organization of sampling
St-BB-003	Germany, Brandenburg	2015	EpiLogic GmbH
St-BB-007	Germany, Brandenburg	2015	EpiLogic GmbH
St-ST-001	Germany, Saxony-Anhalt	2015	EpiLogic GmbH
St-ST-006	Germany, Saxony-Anhalt	2015	EpiLogic GmbH
St-TH-001	Germany, Thuringia	2015	EpiLogic GmbH
St-SN-002*	Germany, Saxony	2015	EpiLogic GmbH
St-SN-004*	Germany, Saxony	2015	EpiLogic GmbH
St-BY-008	Germany, Bavaria	2015	EpiLogic GmbH
St-BY-010	Germany, Bavaria	2015	EpiLogic GmbH
St-BY-027	Germany, Bavaria	2015	EpiLogic GmbH
BAZ 6/1/04*	Germany, Lower Saxony	2008	Julius-Kühn Institute
BAZ 8/8/04*	Germany, Mecklenburg-West Pomerania	2008	Julius-Kühn Institute

* Isolate used for field inoculation.

Tan spot

The field trial in Germany in 2016 was sown at a field site with wheat mono-cropping and reduced tillage for more than ten years. At this field, natural *P. tritici-repentis* infection occurred annually. The field trials in Germany and Denmark during the cropping season 2017 were inoculated with 50 g m^{-2} naturally *P. tritici-repentis* infected straw. In both countries, the straw was collected from fields heavily infected with this pathogen.

Inoculation was carried out in Denmark in December 2016 and in Germany in March 2017 at the two- to five-leaf stage.

2.3.3 Trait assessment

Powdery mildew

In seedling experiments, disease severity was scored based on the primary leaf two weeks after inoculation. In field trials, PM infestation of whole plants was assessed before the flag leaf was fully developed. In both cases, PM was assessed on a plot basis using a rating scale from 1 (no disease) to 9 (severe disease).

Septoria tritici blotch

Five weeks after inoculation, disease severity was assessed three times at seven-day intervals until a maximum of differentiation was reached. STB infestation of the flag leaf was visually rated on a plot basis as the percentage of leaf area covered by lesions exhibiting pycnidia (small black dots) from 0% (no symptoms) to 100% (severe disease).

Tan spot

Tan spot infestation was visually assessed two times at seven-day intervals until a maximum of variation was visible. The percentage of leaf area showing brown to black spots surrounded by chlorotic and necrotic areas was evaluated as described for STB.

Agro-morphological traits

Additionally to the three disease traits, the three agro-morphological traits PH, EET, and LAD were recorded (Table 2). At the end of the cropping season, PH was measured in cm from the ground level to the top of the ear. EET was assessed when half of the ear emerged above flag leaf ligule for half of all plants per plot in days after 1st May. The trait LAD was scored to investigate the potential effect of LAD on STB development due to spray inoculation. The LAD score was a combination of the leaf angle between the stem and the proximal third of the leaf and the overhanging of the distal part of the leaf (Fig. 3). LAD was recorded in odd numbers from 1 (erectophile, <45°; no overhanging) to 9 (planophile, >45°; overhanging).

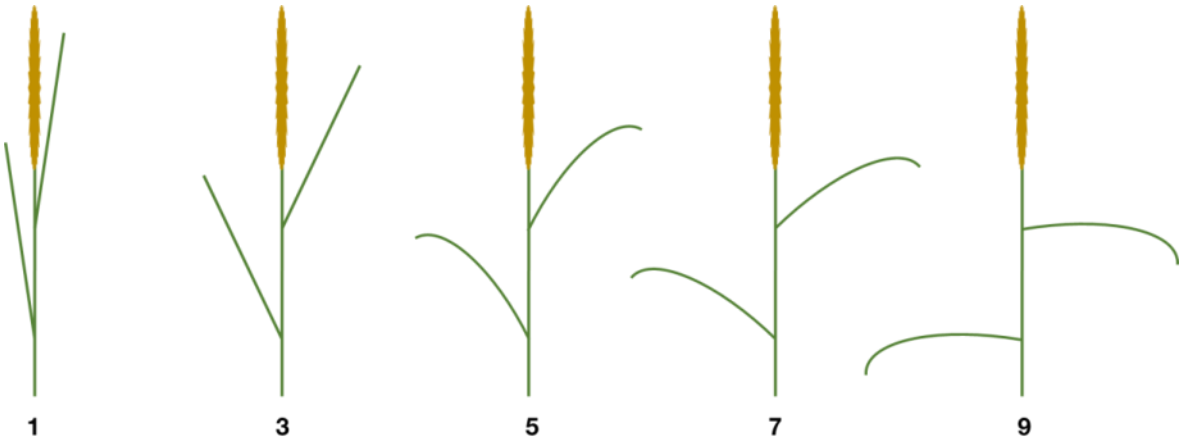

Figure 3 Scoring scheme of the trait leaf angle distribution.
Scoring was carried out in odd numbers from 1 (erectophile, <45°; no overhanging) to 9 (planophile, >45°; overhanging).

2.3.4 Phenotypic data analysis

Scoring exhibiting maximum differentiation in the BMWpop was used for the following analyses of traits STB and TS. Observations were identified as outliers according to Grubbs (1950). Outliers were removed only if incorrectly scored or when obvious problems were observed for a specific plot. Phenotypic data analysis was performed in R/lme4 V1.1-14 (Bates et al., 2015). All residuals were investigated with residual diagnostic plots for deviations of normality and homoscedasticity. The analysis of seedling resistance to PM across trials was based on the following model, with the term 'location' referring to the two independent experiments in the greenhouse:

$$y_{ijk} = \mu + g_i + l_j + gl_{ij} + r_{kj} + e_{ijk} \quad (1)$$

y_{ijk}	Trait observation
μ	Overall mean
g_i	Fixed effect of the genotype i
l_j	Random effect of the location j
gl_{ij}	Random interaction effect of genotype i and location j
r_{kj}	Random effect of the replication k nested within location j
e_{ijk}	Random residual error; $e_{ijk}\ iid \sim N(0, \sigma_e^2)$

The phenotypic data at individual field environments, also referred to as test environment (TE), was analyzed with the following model:

$$y_{ikm} = \mu + g_i + r_k + b_{mk} + e_{ikm} \quad (2)$$

y_{ikm} Trait observation
μ Overall mean
g_i Fixed effect of the genotype i
r_k Random effect of the replication k
b_{mk} Random effect of incomplete block m nested within replication k
e_{ikm} Random residual error; $e_{ikm}\ iid \sim N(0, \sigma_e^2)$

Data analysis across the TEs was carried out according to the statistical model:

$$y_{ijkm} = \mu + g_i + l_j + gl_{ij} + r_{kj} + b_{mkj} + e_{ijkm} \quad (3)$$

y_{ijkm} Trait observation
μ Overall mean
g_i Fixed effect of the genotype i
l_j Random effect of the location j
gl_{ij} Random interaction effect of genotype i and location j
r_{kj} Random effect of the replication k nested within location j
b_{mkj} Random effect of incomplete block m nested within replication k nested within location j
e_{ijk} Random residual error; $e_{ijk}\ iid \sim N(0, \sigma_e^2)$

To obtain variance components, genotype was fitted as random in the above-mentioned models. The single-plot repeatability of seedling resistance to powdery mildew was based on a reduced model (1) without considering the effect of the location and the genotype-by-location interaction effect. The repeatability of each trait in each field environment was based on model (2). In both cases, the repeatability was calculated as the ratio of the genotypic variance component and the sum of the genotypic and residual error variance components. The heritability was estimated on a progeny mean basis according to Hallauer and Miranda (1981):

$$\hat{h}^2 = \frac{\hat{\sigma}_g^2}{\hat{\sigma}_g^2 + \frac{\hat{\sigma}_{gl}^2}{L} + \frac{\hat{\sigma}_e^2}{L * R}} \quad (4)$$

$\hat{\sigma}_g^2$ Estimate for the genotypic variance component

$\hat{\sigma}^2_{gl}$	Estimate for the genotype-by-location variance component
$\hat{\sigma}^2_{e}$	Estimate for the residual error variance component
L	Number of test environments
R	Number of replications per test environment

Pearson's phenotypic correlation coefficients between the disease and agro-morphological traits in the field were calculated based on adjusted means across TEs. Genotypic correlations between traits that were evaluated in the same location were estimated in PLABSTAT Version 3Awin (Utz, 2011) fitting genotype and TE as random.

2.3.5 QTL mapping

Four different methods were used to analyze the association between the marker data and (i) the seedling resistance to PM across experiments, and (ii) the six traits PM, STB, TS, PH, EET, and LAD scored in the field in individual environments and (iii) across environments. Interval mapping that was implemented in R/mpMap V2.0.2 was carried out with and without cofactors (composite interval mapping: CIM and simple interval mapping: SIM). Single marker regression was performed using bi-allelic SNP calls (identical by state: IBS) and multi-point founder probabilities (identical by descent: IBD) as predictors.

For interval mapping, 2804 markers and their positions on the genetic linkage map of BMWpop (Stadlmeier et al., 2018) were used. Each marker represented a unique locus on the genetic map. The interval approach was based on the multi-point founder probabilities, estimated as described above (section 2.2). For each trait, an empirical threshold at the 0.001 genomewise significance level was determined from 1,000 permutation runs according to Churchill and Doerge (1994). The QTL were detected at marker positions. All detected QTL were fit simultaneously in a full model. In a final fit, only QTL with a p-value < 0.1 were included and the additive effects of each QTL relative to the founder 'Julius' and the proportion of the explained phenotypic variance (R^2) of the individual QTL (partial R^2) and the full model (total R^2) were estimated. The QTL support interval (SI) in interval mapping was defined as the chromosomal region surrounding a QTL peak at a $-\log_{10}(p)$ fall-off of ±1.0. A coinciding QTL (cQTL) was defined when the SIs of QTL overlapped. Because cofactor selection remained challenging, in CIM, only linkage groups, which were associated with the trait of interest in SIM, were considered.

The number of cofactors to be selected was set to the number of QTL detected in SIM. Cofactor selection was based on a forward selection regression model using the Akaike information criteria (Huang and George, 2011) ensuring a minimum genetic distance of 10 cM between two selected markers.

For the single marker regression, all 5436 mapped markers of BMWpop were used. For the IBS and IBD method, QTL were detected according to the following statistical model in R/lme4:

For IBS:

$$\boldsymbol{y} = \mathbf{1}\mu + \boldsymbol{x}_m\boldsymbol{\beta}_m + \boldsymbol{S}\boldsymbol{\alpha} + \boldsymbol{\varepsilon} \quad (5)$$

$\boldsymbol{y}$	$N \times 1$ vector of adjusted means across TEs of the N genotypes
$\mathbf{1}$	N-dimensional vector of ones
μ	Common intercept
$\boldsymbol{x}_m$	$N \times 1$ vector assigning marker genotype at marker m
$\boldsymbol{\beta}_m$	1 × 1 vector containing additive effects of the bi-allelic marker genotype at marker m
$\boldsymbol{S}$	$N \times$ (16-1) matrix assigning the MAGIC subgroup
$\boldsymbol{\alpha}$	(16-1) × 1 vector containing random effects of the fifteen MAGIC subgroups relative to ‘Subgroup 16’
$\boldsymbol{\varepsilon}$	N-dimensional vector of residuals; $\varepsilon \sim N(0, I\sigma_\varepsilon^2)$

For IBD:

$$\boldsymbol{y} = \mathbf{1}\mu + \boldsymbol{X}_m\boldsymbol{\beta}_m + \boldsymbol{S}\boldsymbol{\alpha} + \boldsymbol{\varepsilon} \quad (6)$$

$\boldsymbol{y}$	$N \times 1$ vector of adjusted means across TEs of the N genotypes
$\mathbf{1}$	N-dimensional vector of ones
μ	Common intercept
$\boldsymbol{X}_m$	$N \times$ (8-1) matrix assigning the multi-point founder probabilities at marker m
$\boldsymbol{\beta}_m$	(8-1) × 1 vector containing the additive effects of the seven parental alleles relative to ‘Julius’ allele at marker m
$\boldsymbol{S}$	$N \times$ (16-1) matrix assigning the MAGIC subgroup
$\boldsymbol{\alpha}$	(16-1) × 1 vector containing random effects of the fifteen MAGIC subgroups relative to ‘Subgroup 16’
$\boldsymbol{\varepsilon}$	N-dimensional vector of residuals; $\varepsilon \sim N(0, I\sigma_\varepsilon^2)$

In equation (5) the additive effect of the minor allele and in equation (6) the additive founder effects relative to 'Julius' were estimated. The random term accounting for the MAGIC subgroup was excluded from the final analysis if it was not significant at $p < 0.05$. The estimated p-values were corrected for multiple testing according to Benjamini and Hochberg (1995) using a false discovery rate of 0.01. Adjoining significant SNPs in a chromosomal region were assumed to represent the same QTL as long as the sign of the additive effect was the same. A second QTL proximal or distal to a detected one was defined at a minimum distance of 30 cM. The most significant SNP was chosen as the QTL peak position. The QTL support interval in single marker regression was defined by all significant SNPs in the respective genetic region. All detected QTL were fit simultaneously to estimate the total phenotypic variance explained.

Although CIM has more power than SIM, SIM was used as the main QTL detection method as cofactor selection in CIM remained challenging (Stadlmeier et al., 2019). QTL mapped with SIM were named following the recommendations for gene symbolization in wheat (McIntosh et al., 2013). A QTL detected by SIM was considered to be mapped with another method if the SIs overlapped. To define the physical position of QTL mapped by SIM, the sequence of the QTL peak marker was blasted against the reference sequence IWGSC RefSeq v1.0 using the BLASTn basic search tool (International Wheat Genome Sequencing Consortium, 2018).

2.3.6 Candidate gene search

The physical position of each QTL peak marker was analyzed in the database EnsemblePlants (http://plants.ensembl.org/index.html), which is a genomic portal for various plant species including *T. aestivum*. First, it was investigated if the peak marker coincided with a high confidence protein-coding gene based on the IWGSC RefSeq v1.0 (International Wheat Genome Sequencing Consortium, 2018). Second, ten-thousand base pairs (bp) were added up- and downstream of the peak marker sequence and within this interval additional candidate genes were searched. This narrow genetic region around the peak marker was expected to be appropriate, as MAGIC populations are considered to lead to precise mapping results (Cockram and Mackay, 2018). In addition, generally small SIs were detected. If no candidate gene was found in this region, the number of bp were extended to up to 1 mega base pairs (Mbp) depending on the proximity of the QTL peak marker to the next candidate gene. The detected high confidence protein-coding genes were submitted to the Triticeae Toolbox (T3) database

(https://triticeaetoolbox.org/wheat/genes/) to search for gene description and functional annotation available from IWGSC.

3 DISCUSSION

The development of new varieties resistant to major fungal diseases, such as PM, STB, and TS, is an ongoing task in winter wheat breeding driven by host-pathogen coevolution, fungicide resistance evolved in pathogens, and sustainability aspects of crop production. The objective of the study was to analyze the usefulness of a modified MAGIC mating design, to identify genomic regions conferring resistance to PM, STB, and TS, and to investigate the potential of combining resistance to these diseases in one genotype. This chapter presents a comprehensive discussion of the results of the two publications underlying this thesis complemented by additional findings and recommendations.

3.1 Future prospects of MAGIC designs

3.1.1 Crossing scheme

The multiparent advanced generation intercross was first introduced and applied to mice, named “heterogeneous stock”, to dissect QTL with large effect into numerous linked QTL with small effects (Mott et al., 2000). Since Mackay and Powell (2007) and Cavanagh et al. (2008) proposed this population type for crops, MAGIC designs have been established in several plant species. The number of founders used in most studies is either four or eight, with a higher number of founder lines enhancing the allele and gene diversity (Huang et al., 2012; Ladejobi et al., 2016). The main reason for using a lower number of founder lines may be the increased workload and costs associated with crossing designs that involve multiple founders. One approach to counteract this issue was to simplify the crossing scheme. A full eight-founder MAGIC design is built of 28 two-way crosses, 210 four-way crosses, and 315 eight-way crosses. Each of the 315 eight-way crosses represent a unique funnel of the form {[(A x B) x (C x D)] x [(E x F) x (G x H)]}, where the matched brackets define the two-way, four-way, and eight-way crosses of the eight parents denoted with the letters. To analyze the usefulness of a modified mating design, an eight-founder winter wheat MAGIC population was established (Stadlmeier et al., 2018). The crossing design was based on only one of the 315 possible funnels and the number of two-way, four-way, and eight-way crosses was kept low with four, 32 and eight, respectively. It was assumed that at least multiple funnels should be used to sample a high diversity among the founder lines and to enhance the number of recombination events to reduce the extent of LD (Ladejobi et al., 2016). To preserve the

propagated advantages of such a population type (section 1.2 Outline), an eight-way intercross step was introduced including 16 crosses.

Despite the reduced mating design, only very mild population structure and relatedness between individuals was observed indicating that genomic regions of all parents were captured in the population. This was supported by nearly equally distributed genome-wide founder representations. The mild structure could be caused by the final eight-way intercross step as suggested by principal coordinate analysis. Lines sharing the same father clustered more closely. It is also likely that the mild effect occurred just by chance because in single marker analysis the initially included fixed effect for MAGIC group assignment (Stadlmeier et al., 2019), which accounts for the observed structure, was not significant at $p < 0.05$ for all analyzed traits.

In a fully realized eight-founder MAGIC design, a higher number of recombination events per line compared to a simplified mating design is expected. However, the mean number of recombination events per line in BMWpop was 1.3 times higher compared to the eight-founder MAGIC population NIAB 2015, which included all possible 210 four-way crosses. The range of the mean recombination events per line in NIAB 2015 (2-130) exceeded the one of BMWpop (49-100) (Fig. 4). However, it appears that the extreme values in NIAB 2015 represented outliers (Fig. 4).

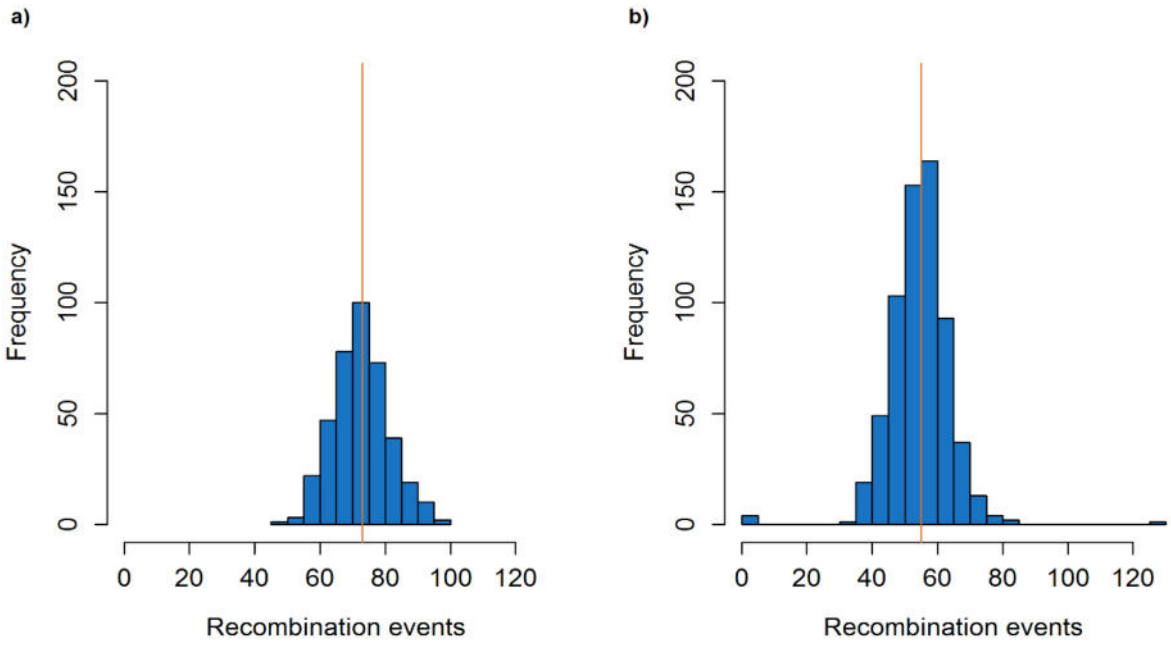

Figure 4 Distribution of the number of recombination events per line.

a) BMWpop and b) NIAB 2015. The orange vertical line indicates the arithmetic mean.

BMWpop showed fewer unique recombination events compared to NIAB 2015 with values of 2812 and 4140, respectively. However, after correcting for the different population sizes of 394 (BMWpop) and 643 (NIAB 2015), the mean number of unique recombination events per line was 7.1 for BMWpop compared to 6.4 for NIAB 2015. Therefore, it seems that the higher total number of unique break points in the NIAB 2015 mating design was a consequence of the larger population size.

The reduced mating design showed no adverse effect on marker ordering as the congruency of marker order with the IWGSC RefSeq v1.0 (International Wheat Genome Sequencing Consortium, 2018) and various genetic maps (Cavanagh et al., 2013; Gardner et al., 2016; Geyer et al., 2018) was high. A strict inspection and manual curation in each step of map construction was applied, which was also necessary for genetic map creation of the NIAB 2015 (Gardner et al., 2016). The resolution of the D genome map remained unsatisfactory in both eight-founder MAGIC maps BMWpop and NIAB 2015. The application of a more comprehensive SNP chip, like the Wheat660K array, most likely would not improve saturation of the D genome (Cui et al., 2017), presumably due to the origin of hexaploid *T. aestivum* wheat. Although different lines may have contributed their D genomes to bread wheat (Ogbonnaya et al., 2005), it appears that hexaploid wheat shares a single D genome gene pool (Dvořák et al., 1998), leading to the low allelic diversity of the D genome. To overcome this limitation, MAGIC populations involving synthetic wheat lines may be a promising approach. Primary synthetics (Mujeeb-Kazi et al., 1996) would be the best choice to maximize D genome diversity but they suffer from a high genetic load. A significant number of synthetic backcross-derived wheats are available (Dreisigacker et al., 2008) and may be used in combination with elite lines in MAGIC designs to exploit an increased proportion of untapped D genome diversity.

Based on marker data generated with the Illumina® Infinium® 15K SNP array, 71.7% of the polymorphic markers present in a panel of 524 common wheat breeding lines (Geyer et al., 2016) segregated in BMWpop. This is consistent with simulation studies using randomly selected founders and a fully realized eight-founder mating design. Thus, the captured allelic diversity does not appear to be influenced by the crossing design used.

It can be concluded, that a simplified MAGIC mating design with an additional eight-way intercross step, as described in Stadlmeier et al. (2018), shows no drawbacks regarding population structure, linkage disequilibrium, total and unique number of recombination events, and genome-wide founder representations and does not reduce the power of further applications, but simultaneously reduce effort and costs. It would be interesting to see whether these results can be validated by other wheat MAGIC populations produced

by a simplified mating design such as the WM-800 population (Sannemann et al., 2018). In such a comparison it would be possible to analyze the impact of the eight-way intercross step because the WM-800 mating design lacks this step. The results from a recently published eight-founder MAGIC population in wheat supports the assumption that additional generations of intercrossing considerably increase the number of recombination (Shah et al., 2019). Thus, it can be recommended to use a simplified crossing design with at least one additional intercross step, a high number of founders (≥ 8) selected for a maximum of segregating alleles, and a large population size to increase the number of recombination events and allele diversity within a MAGIC population.

3.1.2 Benefit of MAGIC designs for practical breeding

The attractiveness of a MAGIC population for breeders is that a breeding variety could emerge, which already combines favorable alleles for a wide range of traits like resistance, yield, and quality parameters. This was recently postulated for a genetically diverse eight-founder cowpea MAGIC population comprising 305 F_8 lines (Huynh et al., 2018). However, to find superior lines with high probability, a large enough population with several thousand progenies should be generated. A further challenge is the required time for the establishment of MAGIC populations. Ongom and Ejeta (2018) reported that it lasted over 15 years to establish a multiparental population using 19 founders in *Sorghum bicolor* L. Four-, eight-, and 16-way MAGIC populations have two, three, and four crossing rounds, respectively, before selfing. Following the above stated recommendation to include at least one additional round of intercrossing, the number of crosses would be further increased. Thus, compared to bi-parental designs, the development of MAGIC populations entails a delay of one (four founders) to three years (16 founders). Speed breeding could be used to accelerate crossing and selfing during population establishment (Watson et al., 2018).

Because of these limitations, it is rather probable that breeders will cooperate with research institutions to develop MAGIC populations in the context of pre-breeding programs. Linkage of favorable and unfavorable genes are expected to be broken with a high probability in such designs and promising MAGIC lines can be selected and used in bi-parental crosses. In addition, considering primary or backcross derived synthetics as MAGIC founders may introduce novel untapped genetic diversity into elite breeding material. Furthermore, breeders can take advantage of investigated relationships

between multiple traits in a single genetic background. This would be especially beneficial for disease resistance traits because natural infection often does not occur each year. Hence, assessment of disease resistance traits may imply huge efforts. Moreover, the establishment of diagnostic markers suitable for marker-assisted selection is relatively easy to accomplish because of the high-precision QTL mapping in MAGIC populations. Cockram et al. (2015) used an eight-founder MAGIC winter wheat population for fine-mapping the wheat *Snn1* locus, which confers sensitivity to the effector SnTox1 of *P. nodorum*. They converted the QTL peak SNP marker for the *Snn1* locus to a diagnostic KASP marker publically available for breeders and researchers.

3.2 Experimental design and phenotyping

Resistance to PM and STB was assessed in two field trials in Germany in the season 2016 and 2017. Disease severity of TS was assessed two times in Germany in 2016 and 2017 and at a field trial in Denmark in 2017. Measuring the phenotype in several locations and years aims to reduce the genotype × environment interaction effect and to figure out the true genetic value of a genotype. Thus, a high number of TEs is expected to provide a nearly unbiased estimate for the genetic value of a genotype. Although the total number of trials carried out for each disease was limited, medium to high heritabilities of 0.64, 0.79, and 0.70 for PM, STB, and TS, respectively, were estimated.

Both PM trials depended on natural infection and showed the full range of reaction scores. However, the population mean of the trial in Roggenstein in 2016 (score 2.0) differed significantly ($p < 0.05$) from the mean of the trial in Freising in 2017 (score 3.5). Both TEs showed a medium correlation of 0.56. To ensure even and heavy infestation with *B. graminis*, it would have been advantageous to include highly susceptible varieties as spreaders. Immediately after assessment of PM at the field trial in Freising in 2017, a fungicide against PM was applied several days before the inoculation with STB. It was taken care that no genotype suffered severely due to PM infection and that plants were healthy before STB inoculation. Similar correlations between STB scored in 2016 and PM scored in 2016 and 2017 and between STB scored in 2017 and PM scored in 2016 and 2017 (Table 4) suggested that PM infestation had no influence on STB disease development at the field trial in Freising in 2017.

Table 4 Correlations between PM and STB assessments

	STB 16FS1[c]	**STB 17FS1[d]**
PM 16RG[a]	0.14	0.12
PM 17FS1[b]	0.23***	0.19***

[a] Powdery mildew scored in Roggenstein in 2016.

[b] Powdery mildew scored in Freising in 2017.

[c] Septoria tritici blotch scored in Freising in 2016.

[d] Septoria tritici blotch scored in Freising in 2017.

*** Significant at $p < 0.001$.

The STB field trials were inoculated with four isolates, which were virulent to all founders at seedling stage. The motivation was to avoid the effect of qualitative resistance genes, which may have negatively influenced the detection of quantitative resistance loci with small effects. However, McDonald and Martinez (1990) suggested that a high genetic diversity of the fungus is present at field sites naturally infected with STB. They identified 22 different haplotypes of *Z. tritici* from a single wheat field of the size 40 m × 40 m based on 19 different leaf samples. It is assumed, that in 2016 also a natural infection occured because first STB symptoms appeared a week earlier than expected based on the artificial inoculation. This assumption is supported by the significantly ($p < 0.05$) higher mean infestation rate in 2016 compared to 2017 and the medium correlation of 0.63 between the two field trials despite the use of the same isolate mixture. In retrospect, it would have been appropriate to use all available isolates regardless of their effect on seedling resistance. Possible strong QTL could have been modeled as fixed effects in the final QTL model.

In 2016, the TS trial was not artificially inoculated, whereas in both TS trials in 2017 straw, which was heavily infected with *P. tritici-repentis,* was spread as a source of inoculum. Although the mean TS infestation in Freising in 2016 was significantly higher ($p < 0.05$) compared to infestation in Freising in 2017, repeatability values were lower with 0.39 compared to 0.67, respectively. This indicates that infection triggered by a field site where wheat after wheat was sown repeatedly over ten years was generally a good source for TS inoculation; however, a more consistent inoculation was achieved by artificial inoculation with TS infected straw. The extremely high mean TS infestation in Slagelse in 2017 (58.0%) compared to the German field trials (33% and 25%) may be explained by more aggressive pathogen isolates present in Denmark. It is supposed that the genetic constitution of isolates from both countries is different because effector tests revealed the absence of ToxB in all German samples, but not in Denmark (data

unpublished). Despite this finding, the phenotypic correlation between both countries was significant ($p < 0.05$) with values of up to 0.61.

The scoring of PM, STB, and TS infestation was carried out visually using different rating scales. The visual assessment of traits can lead to bias. To enhance objectivity, precision, and to be able to deal with large population sizes (>1000), automation of phenotypic evaluation can be a promising approach. In recent years, huge efforts have been invested in the development of quantitative, high-throughput plant phenotyping networks, such as the Jülich Plant Phenotyping Centre (JPPC; https://www.fz-juelich.de/ibg/ibg-2/DE/Organisation/JPPC/JPPC_node.html), and analysis tools like HTPheno (Hartmann et al., 2011), IAP (Klukas et al., 2014), and PhenoBox (Czedik-Eysenberg et al., 2018). Image-based phenotyping methods are non-destructive, they are able to detect spatial patterns of heterogeneity, and they can capture data not visible to the human eye (Mutka and Bart, 2015). Different image-based methods are available for the assessment of plant diseases: visible light, chlorophyll fluorescence, hyperspectral, thermal, and 3D sensor imaging. The automated, high-throughput digital imaging allows for collection of extensive and accurate data. Additionally, different dimensions of disease symptoms, like percent leaf area infected and density and size of pycnidia, can be quantified as shown in a study for STB (Stewart and McDonald, 2014). Chlorophyll fluorescence and thermal imaging capture changes in the chlorophyll fluorescence emission and altered leaf surface temperatures, respectively, which can occur early during or in the course of infection. The hyperspectral imaging even allows distinguishing between different plant diseases present at the same time (Mahlein et al., 2012). Thus, image-based phenotyping methods dramatically widen the phenotyping capabilities. Studies already showed high correlations between data from automated and manual phenotyping (Hartmann et al., 2011; Sugiura et al., 2016; Thoen et al., 2016) suggesting that this technology may be trendsetting. However, there are some challenges that have to be addressed: first, it has to be analyzed how the recorded data has to be interpreted regarding biological functions and reactions (Lindenthal et al., 2005, Rodríguez-Moreno et al., 2008). Second, it is necessary to develop adequate designs of machines, which can be used for various crops. Third, the computer-based processing of the image-based phenotypes needs to be accurately calibrated and trained to transform images with high reliability into quantitative data that are appropriate for genetic studies. The newly arising field of machine learning may help to support and accelerate the efforts for training of such algorithms. Fourth, the whole process of automated high-throughput plant imaging requires large storage and computer capacities. Since these requirements

are generally not easy to achieve, a possible solution may be the blockchain technology. Blockchain is a distributed ledger technology, comparable with a decentralized database structure, which allows storing vast amounts of data including *e.g.* origin, assessment, and updates of data (Wright and De Filippi, 2015; Zheng et al., 2017). One advantage for the use in science is the transparency and integrity of data; this means it is nearly impossible to manipulate data once stored in this system and if necessary data can be traced from entry point to the actual status (Irving and Holden, 2016). For the case that data should not be publically available, a consortium blockchain with a selected number of nodes and users can be chosen (Zheng et al., 2017).

3.3 Candidate genes for resistance to PM, STB, and TS

In SIM, which was chosen as the main QTL detection method, six, seven, and nine QTL were identified for the diseases PM, STB, and TS, respectively, across field environments. For seedling resistance to PM, four QTL were detected.

The peak marker sequence of the disease QTL was located in 87% of the cases in the sequence of a protein coding gene of high confidence based on IWGSC RefSeq v1.0 (Table 5). This high hit rate may be explained by the fact that around 80% of the markers from the 15K + 5K Infinium® iSelect array indicating genes based on the IWGSC RefSeq v1.0 (J. Plieske and M. Ganal, personal communication). In 65% of the cases, the peak marker was located in the sequence of a candidate gene involved in plant resistance. Twenty-one additional candidate genes were found when extending the interval up to ±0.01 Mbp. Of these genes, 53% are suggested to be associated with plant disease resistance. Eight candidate genes, of which three are possibly involved in plant resistance, co-located with *QPm.lfl-3D* and *QTs.lfl-7A.1* when extending the window to up to ±1 Mbp.

The QTL *QPm.lfl-6B*, which was detected in the seedling test and in the field, was physically mapped to the genomic region of a gene encoding a putative RING/U-box superfamily protein (Table 5). E3 ubiquitin ligases represent RING-type and U-box proteins that directly transfer ubiquitin to specific substrate proteins. Several RING-type and U-box ubiquitin enzymes were shown to play a role in pathogen-associated molecular pattern (PAMP)-triggered immunity (PTI) and effector-triggered immunity as reviewed in Zeng et al. (2006) and Cheng and Li (2012). Yu et al. (2013) reported that over-expression of the E3 ubiquitin ligase EIRP1 in wild grapevine enhanced resistance to powdery mildew. Additionally, ubiquitination enzymes are involved in the regulation of

the intracellular nucleotide-binding leucine-rich repeat (NB-LRR) R protein-mediated plant immunity (Cheng and Li, 2012). About 2000 bp proximal to this candidate gene, a gene coding for a receptor-like kinase (RLK) was located. Different RLKs were shown to mediate resistance to PM, Fusarium head blight, and stripe rust in wheat (Hu et al., 2018; Rajaraman et al., 2016; Thapa et al., 2018; Zhou et al., 2007). The physical position of the QTL *QPm.lfl-7D*, which was shown to map to the same genetic region as the multi-resistance gene *Lr34/Yr18/Sr57/Pm38* (Stadlmeier et al., 2019), coincided with a candidate gene encoding the CsAtPR5 protein (Table 5). CsAtPR5 is a precursor of the pathogenesis-related protein 5 (PR5) and has been found to be associated with resistance to PM (Niu et al., 2010), common bunt (Bhatta et al., 2018), and yellow rust (Bozkurt et al., 2007) in hexaploid wheat.

The *QTL QStb.lfl-1B* was in the sequence of a candidate gene encoding an ARGONAUTE (AGO) protein. AGO proteins are core components in enzymatic complexes that incorporate none-coding small ribonucleic acids (RNAs) to induce gene silencing caused by complementary sequences (Yang and Huang, 2014). This mechanism, known as RNA interference (RNAi), plays a key role in multiple cellular processes including host immunity (Seo et al., 2013). AGO proteins are primarily known to be involved in viral defense (Carbonell and Carrington, 2015). Apart from this, it was shown that RNA silencing also plays a role in the interaction with bacterial (Navarro et al., 2006) and fungal pathogens (Jin and Wu, 2015; Li et al., 2014a; Shen et al., 2014). Another candidate gene, annotated as a reticulon-like kinase, was located 300 bp distal to AGO. In Arabidopsis, two reticulon-like kinases were found to be involved in the regulation of the intracellular transport and activity of the FLAGELIN-SENSITIVE2 (FLS2) receptor (Lee et al., 2011). FLS2 is a well-known element of PTI for the recognition of the bacterial flagellin. Although there is a lack of studies reporting similar observations for fungal PAMPs, it is still conceivable that related mechanisms are involved in fungal plant defense. The QTL *QStb.lfl-2B.3*, which was suggested to represent a novel adult plant stage resistance locus located proximal to *Stb9* (Stadlmeier et al., 2019), co-located with a gene predicted to encode a histone-lysine N-methyltransferase. Sireesha and Velazhahan (2017) reported the differential expression of a sequence matching to a histone-lysine N-methyltransferase during infection of maize with the fungal pathogen *Peronosclerospora sorghi*.

The QTL *QTS.lfl-2A* on the short arm of chromosome 2A was located at the same physical region as a gene with a described function as a Cu/Zn-superoxide dismutase (Cu/Zn-SOD). During pathogen attack, plants can react with an oxidative burst, which

leads to a release of several reactive oxygen species (ROS). To protect the plant tissue from toxicity and damage by these ROS, plants have evolved efficient antioxidant systems including enzymes such as SOD (Bowler et al., 1992). In pearl millet seedlings, which were inoculated with the downy-mildew pathogen *Sclerospora graminicola*, an over two fold increase of superoxide dismutase activity was detected in the resistant genotypes (Babitha et al., 2002). Additionally, it was shown that over-expression of Cu/Zn-SOD in tobacco plants mediated resistance to bacterial wildfire and crown gall diseases (Faize et al., 2012). The QTL *QTS.lfl-5B* was in the sequence of a candidate gene annotated as a subtilisin-like protease. These proteases are a diverse family of serine peptidases with various biological functions, such as plant development and protein processing. Furthermore, they were found to be involved in plant immunity and plant defense response to a wide range of pathogens in several plant species (Figueiredo et al., 2018). In wheat, Fan et al. (2016) reported an up to three fold increase of a subtilisin-like serine protease activity during infection with *P. triticina* in an incompatible wheat-pathogen interaction. About 8000 bp distal, a gene encoding a BTB/POZ (broad-complex, tramtrack, and bric-a-brac/poxvirus, zinc finger) domain was located. The BTB/POZ domain is a widely distributed structural motif in proteins with various biological processes, such as transcriptional and cytoskeleton regulation. The BTB/POZ domain is also present in proteins involved in the regulation of pathogenesis-related proteins (Fu et al., 2012; Wang et al., 2016). This pathway may be more common for biotrophic pathogens as it is normally activated by salicylic acid. However, in wheat, it was shown that the activation of this pathway is independent thereof (Molina et al., 1999). Recently, in soybean a novel protein containing BTB/POZ domain was found to be up-regulated during infection with *Phytophthora sojae*. Interestingly, over-expression of this novel protein in transgenic soybean plants led to a significantly higher activity and expression level of SOD (Zhang et al., 2019).

The two genomic regions on chromosome 1AS and 7AL were associated with all three diseases. The QTL peak markers spanned a physical distance of 4.6 Mbp (1AS) and 13.9 Mpb (7AL). Within this region 86 and 175 candidate genes were found for chromosomes 1AS and 7AL, respectively. The QTL peak markers in both regions were embedded each in a candidate gene, known to be involved in plant pathogen defense (Table 5; *QStb.lfl-7AL*: calcium-binding EF-hand domain protein). However, it is possible that further genes in these regions contribute to broad-spectrum disease resistance. For example in the region on chromosome 1AS a gene coding for a disease resistance protein RPM1 and a serine/threonine-protein kinase were located a few thousand base

pairs proximal to STB and TS QTL peak markers. In the genetic region on chromosome 7AL, a gene coding for a disease resistance protein of the NBS-LRR class was located around 6500 bp proximal to the PM QTL peak marker. It is possible that on chromosomes 1AS and 7AL gene cassettes are present, which confer resistant to multiple pathogens.

Different candidate genes, which have been shown to be involved in various plant defense mechanisms, were found to co-locate with disease QTL by Stadlmeier et al. (2019). It is possible that candidate genes, which have not been described to play a role in plant immunity up to now, may be of interest as well and that the presented results may lack candidate genes located outside of the investigated physical interval. The broad range of different genes and subsequently mechanisms involved in plant immunity may represent a key factor for durability of quantitative resistance in plants.

Many of the described protein classes are also known to be involved in diverse biological cell processes, such as plant development and growth and response to abiotic stress. Genes involved in plant immunity and growth may represent the genetic basis of reported trade-offs between these two plant reactions (Denancé et al., 2013; Tian et al., 2003).

The candidate gene analysis will be taken to the next step when the IWGSC RefSeq v1.0 is upgraded to a high quality IWGSC Gold Standard reference genome sequence that will be anchored to genetic maps and will incorporate different genetic wheat data resources (IWGSC, 2019).

Table 5 Candidate genes for disease resistance QTL

Trait	QTL	Marker	Candidate gene at QTL peak marker	Gene annotation at QTL peak marker	No. of adjacent genes[a]
PM					
	QPm.lfl-1A	PM3a	TraesCS1A02G008100	Powdery mildew resistance protein PM3CS[d]	1
	QPm.lfl-3D	AX-94444273	-	-	4[b]
	QPm.lfl-4A[c]	IWA1635	TraesCS4A02G438700	Leucine-rich repeat kinase[d]	–
	QPm.lfl-5A	AX-94816504	-	-	2
	QPm.lfl-6B	IWA3268	TraesCS6B02G439800	RING/U-box superfamily protein, putative[d]	1
	QPm.lfl-7A	IWA501	TraesCS7A02G553800	MYB-related protein[d]	1
	QPm.lfl-7D	TA015297.0413	TraesCS7D02G026500	CsAtPR5[d]	–
STB					
	QStb.lfl-1A	IWB29039	TraesCS1A02G017000	RNA binding protein[d]	2
	QStb.lfl-1B	IWA198	TraesCS1B02G480100	ARGONAUTE[d]	1
	QStb.lfl-2B.1	IWB43273	TraesCS2B02G096600	Serine/threonine-protein kinase ATM[d]	1
	QStb.lfl-2B.2	BobWhite_c10215_242	TraesCS2B01G308300	Target of rapamycin complex 2 subunit MAPKAP1	1
	QStb.lfl-2B.3	RAC875_c14885_1184	TraesCS2B02G501300	Histone-lysine N-methyltransferase[d]	1
	QStb.lfl-2D	AX-94384624	TraesCS2D01G022800	Formamidopyrimidine-DNA glycosylase	2
	QStb.lfl-4B	AX-94488964	TraesCS4B01G031600	Phosphatidylinositol N-acetyglucosaminlytransferase subunit P-like protein	2
TS					
	QTs.lfl-1A	IWB29039	TraesCS1A02G017000	RNA binding protein[d]	2
	QTs.lfl-2A	IWB39657	TraesCS2A02G121200	Superoxide dismutase [Cu-Zn] [d]	1
	QTs.lfl-2B	IWA4642	TraesCS2B02G159500	Hepatoma-derived growth factor-related protein 2	–
	QTs.lfl-2D	IWB32049	TraesCS2D02G572700	Importin beta 1[d]	–
	QTs.lfl-3D	IWB50741	TraesCS3D02G197700	Kinesin-like protein[d]	–
	QTs.lfl-4B	Kukri_c3474_395	TraesCS4B02G314000	Methyltransferase-like protein 1	2
	QTs.lfl-5B	IAAV3362	TraesCS5B02G036600	Subtilisin-like protease[d]	2
	QTs.lfl-7A.1	IWB8933	-	-	4[b]
	QTs.lfl-7A.2	IWB38709	TraesCS7A02G533600	Dual specificity phosphatase family protein[d]	1

[a] Number of adjacent candidate genes in interval of ± 0.01 Mbp around QTL peak marker.

[b] Interval extended to up to ± 1 Mbp.

[c] QTL only mapped in seedling stage.

[d] Protein described to be involved in plant defense.

- No candidate gene/protein was located at QTL peak marker.

– No candidate genes in interval around QTL peak marker.

3.4 Follow-up research for investigating resistance to PM, STB, and TS

To investigate a potential role of the suggested candidate genes in resistance to PM, STB, and TS, studies at the genic level need to be undertaken. Disrupting candidate gene expression and, consequently, observing changes in resistance to the pathogens *B. gramins*, *Z. tritici*, and *P. tritici-repentis* would be a strong indication for their participation in the wheat-pathogen interaction.

The classical genetic approach to explore the biological function of a candidate gene and its impact on the phenotype is the analysis of mutants. Non-transgenic and undirected mutations in a genome can be induced by chemical mutagenesis. In such mutagenized populations, point mutations can be detected and analyzed by reverse genetic strategies such as targeting induced local lesions in genomes (TILLING). Several TILLING populations in wheat are available (Chen et al., 2012; Henry et al., 2014; Krasileva et al., 2017; Uauy et al., 2009) and represent useful genetic resources to investigate the function of candidate genes. Genetic engineering is a method to establish mutants with a directed mutation. Today, genome editing is the most frequently used and advanced technology to genetically modify the genome. Techniques, such as zinc finger nucleases (ZFNs), transcription activator-like effector nucleases (TALENs), and clustered regularly interspaced short palindromic repeats (CRISPR)/CRISPR-associated protein 9 (Cas9) systems are available. However, CRISPR/Cas9 is the most commonly used because it shows a high success rate, it is relatively easy to design and implement, and it is inexpensive (Doudna and Charpentier, 2014; Ran et al., 2013). CRISPR/Cas9 applications have already been shown to be successful in enhancing resistance to virus, bacterial, and fungal diseases for several plant species as reviewed by Borrelli et al. (2018). This technology can be applied for the implementation of different mechanisms, which induce mutant phenotypes, including posttranscriptional gene silencing, gene knockout, and gene overexpression. Posttranscriptional gene silencing is based on antisense RNA and RNAi constructs. They are complementary and sequence-specific to RNA transcripts of the target gene. Consequently, double stranded small RNAs are produced, which mediate sequence-specific RNA degradation of target transcripts. Single, multiple, and homoeologous genes can be knocked out by modifying the DNA sequence of the target gene. Wang et al. (2014b) simultaneously modified all three homoeologous mildew resistance loci *TaMLO-A1*, *TaMLO-B1*, and *TaMLO-D1* in wheat that encode the MILDEW RESISTANCE LOCUS (MLO) protein and showed that this

modification leads to a heritable broad-spectrum resistance to PM. Overexpression of wild-type gene can be particularly suitable for functionally redundant genes or deleterious knockout mutants. In wheat, overexpression of specific genes were used to analyze the function of genes involved in resistance to fungal pathogens (Chen et al., 2008; Dong et al., 2010; Mackintosh et al., 2007). Simultaneous overexpression of several genes, which were shown to individually enhance resistance, would be of great interest as results could contribute to a deeper understanding of possible resistance trade-offs (e.g. biotrophic *vs.* necrotrophic pathogen resistance).

Apart from plant transformation, gene expression studies are feasible based on transcriptome analysis during fungal pathogen infection using quantitative real-time polymerase chain reaction, expression microarrays, and RNAseq analysis (San Segundo-Val and Sanz-Lozano, 2016). However, this approach just monitors whether the gene is expressed during infection steps.

In the case where no candidate gene was found in the region of a QTL and the support interval was narrow (e.g. *QTs.lfl-7A.1*), near isogenic lines (NILs) can be generated for a given QTL. Based on genotypic data of the progeny and founders and the additive effects of the founders at the QTL, MAGIC lines showing a heterozygote call for the QTL can be selected. Heterozygous lines with alleles of the two most contrasting parents at the QTL are superior. In parallel, codominant kompetitive allele specific (KASP) markers for this region can be developed. In a next step, the selected lines are grown and their heterozygosity is confirmed by the developed KASP markers. The lines are then selfed and the progenies are screened with the KASP markers to select homozygous individuals. The developed NILs can be used for downstream analysis, such as detailed phenotyping and differential gene expression. Potentially, this process takes just one generation in MAGIC populations. However, in BMWpop, single lines of the $F_{6:8}$ bulks must be genotyped in advance if a heterozygote call at the target region is present because a heterozygote call might not represent an individual heterozygote line but a heterogeneous sample. The development of such NILs may be complicated if the QTL is located in a non-recombining region or only small differences in the effects of the contributing founders are observed. If the NILs have shown strong contrasting phenotypes, developed markers may be very interesting and promising for marker-assisted selection (MAS) breeding.

Peak markers of stable QTL with small SIs possibly represent good candidates for utilization in MAS. A large panel consisting of a set of diverse lines should be used to

validate the ability of markers to distinguish contrasting phenotypes. SNP markers can be converted to KASP markers if the validation was successful. The following SNP peak markers are suggested for validation: IWA3268 and IWA501 for PM, IWA198 and AX-94384624 for STB, and IWB32049 and IAAV3362 for TS.

When the QTL region was large (e.g. *QTs.lfl-4B*) fine-mapping of the genomic region of interest using heterogeneous inbred families (HIFs) can be applied. HIFs show a high identical genetic background combined with a distinct genetic constitution at the genomic region of interest. They can be easily developed from RILs heterozygous at the target region (Tuinstra et al., 1997). BMWpop comprises F_6 SSD lines, which were subsequently advanced as a bulk two times. A mixture of ten individual plants per bulk was used for genotyping. This means, bulks that show a heterozygous call at a target region are promising sources for already established HIFs. Sister lines of HIFs, which differ at the target region, can be intercrossed to build up new mapping populations showing genetic recombination within the target QTL region. These populations are useful to narrow down the target region in fine-mapping studies. Additionally, the QTL phenotype and effect can be accurately investigated in such populations.

3.5 Breeding strategies for resistance to PM, STB, and TS

Resistance to PM, STB, and TS disease appears to be controlled by numerous QTL with varying effect sizes. Most QTL seem to be trait-specific, which means parallel breeding for resistance to PM, STB, and TS is feasible. To achieve durable and broad-spectrum resistance to PM, STB, and TS, it is recommended to stack qualitative resistance genes, such as *Pm3a, Stb6*, and *tsc1*, additionally to multiple quantitative resistance loci, such as *QPm.lfl-6B, QPm.lfl-7D*, *QStb.lfl-1B*, *QStb.lfl-2D*, *QTs.lfl-2D*, and *QTs.lfl-3D*. The major genes confer a strong vertical resistance due to their specific and effective interaction with pathogens. The quantitative resistance loci confer mainly the horizontal partial resistance and are suggested to lead to a more durable resistance in general and to a longer durability of race-specific resistance genes (Brun et al., 2010). Pyramiding qualitative and quantitative genes can be achieved by classical breeding using MAS, which is often time- and labor consuming, or by genome editing. Genome editing technologies are currently the most rapid methods to stack multiple resistance genes in a single genotype. However, plant breeders in Europe have to consider regulations when

using these methods since the judgment of Case C-528/16 in July 2018 (Court of Justice of the European Union, 2018).

Beside trait-specific resistance QTL, which can be easily pyramided, some loci, such as on chromosome 1AS and 7AL, are involved in multiple fungal pathogen-wheat interactions. It has to be clarified whether these observations depend on linkage of multiple strong resistance genes or on pleiotropy with a single gene as key regulator. The very distal part of chromosome 1AS is promising to enhance both, resistance to biotrophic and necrotrophic pathogens. In this region, the allele of the founder 'BAYP4535' reduced susceptibility and the allele of the founder 'Bussard' increased infestation regarding PM, STB, and TS (Stadlmeier et al., 2019). This means, breeders can use the allele of 'BAYP4535' on chromosome 1AS to enhance resistance to all three diseases in parallel. In contrast, on the long arm of chromosome 7A contrary allelic effects for resistance to PM/STB and TS were found. To deal with such loci in breeding, genomic regions of founders, which only marginally influence each disease, should be preferred. Thus, the genomic region of the founder 'Format' appears to be a good choice to circumvent the trade-off between PM/STB and TS on chromosome 7AL. It is likely that this region represents a multi-resistance locus as it was associated with the known multi-resistance locus *Pm1/Lr20/Sr15/Rlnn1* (Ouyang et al., 2014). Therefore, a second promising approach would be to search for BMWpop lines with recombination in this region and to select those, which combine the favorable alleles for resistance to PM, STB, and TS. Editing one allele would be a further approach to combine resistance alleles at this locus.

3.6 Conclusion

The eight-founder multiparental advanced generation intercross population BMWpop is a valuable plant genetic resource with well-described population properties and an appropriate genetic linkage map, which facilitates high precision and power in quantitative trait locus mapping. This resource was successfully used to map 23 QTL for resistance to PM, STB, and TS and 15 QTL for the agro-morphological traits PH, EET, and LAD. QTL mapping for a range of further traits using BMWpop is feasible because of the large genetic diversity present in the population. The combination of results from this and ongoing studies will allow investigating relationships, including possible trade-offs, between various traits, for example between yield and resistance or quality and resistance.

An eight-founder MAGIC population with a modified mating design has to be considered as equivalent to a MAGIC population with an almost fully-realized crossing schema. This applies to the extent of population structure, the total and unique number of recombination events, the parental genomic proportion, the construction of an appropriate genetic linkage map, and high precision QTL mapping. These findings will greatly support time and cost efficient MAGIC populations.

MAGIC populations can be interesting sources for genotypes exhibiting new allelic combinations. The inclusion of synthetics in wheat MAGIC population development is expected to be useful to integrate novel resistance genes with parallel breakage of possible linkage-drags and to increase D genome diversity. Genotypes derived from such crosses may be promising lines in the early steps of breeding.

Resistance to PM, STB, and TS was quantitatively inherited. Most detected QTL were trait-specific. This implies that breeding genotypes combining resistance to PM, STB, and TS is feasible. The genetic region on chromosome 1AS simultaneously conferred resistance to all three diseases and is therefore promising in resistance breeding. The alleles at the QTL on chromosome 7AL showed contrary effects for resistance to PM/STB and TS. It is likely that this region represents a multi-resistance locus. Further efforts should be invested to break linkage of unfavorable allele combinations at this locus.

Several markers associated with pathogen resistance were suggested for validation in an independent panel to investigate their potential in MAS and for the development of diagnostic markers.

Multiple candidate genes were identified for resistance QTL. The majority of genes coded for proteins, which have been described to be involved in plant immunity. The gene products belonged to various protein classes confirming the quantitative and trait-specific character of the analyzed diseases. This enables the utilization of different resistance mechanisms for achieving durable resistance.

4 REFERENCES

Anonymous (2019a). Scribble maps. Make maps differently. Available at: https://www.scribblemaps.com/ [Accessed February 19, 2019].

Anonymous (2019b). The registration and placement of pesticides on the EU market. Available at: https://www.ecpa.eu/regulatory-policy-topics/registration-and-placement-pesticides-eu-market [Accessed February 17, 2019].

Asimit, J., and Zeggini, E. (2010). Rare variant association analysis methods for complex traits. *Annu. Rev. Genet.* 44, 293–308. doi:10.1146/annurev-genet-102209-163421.

Babitha, M. P., Bhat, S. G., Prakash, H. S., and Shetty, H. S. (2002). Differential induction of superoxide dismutase in downy mildew-resistant and -susceptible genotypes of pearl millet. *Plant Pathol.* 51, 480–486. doi:10.1046/j.1365-3059.2002.00733.x.

Badaeva, E. D., Keilwagen, J., Knüpffer, H., Waßermann, L., Dedkova, O. S., Mitrofanova, O. P., et al. (2015). Chromosomal passports provide new insights into diffusion of emmer wheat. *PLoS One* 10, e0128556. doi:10.1371/journal.pone.0128556.

Bandillo, N., Raghavan, C., Muyco, P., Sevilla, M. A. L., Lobina, I. T., Dilla-Ermita, C., et al. (2013). Multi-parent advanced generation inter-cross (MAGIC) populations in rice: progress and potential for genetics research and breeding. *Rice* 6, 11. doi:10.1186/1939-8433-6-11.

Bates, D., Mächler, M., Bolker, B., and Walker, S. (2015). Fitting linear mixed-effects models using lme4. *J. Stat. Softw.* 67. doi:10.18637/jss.v067.i01.

Benjamini, Y., and Hochberg, Y. (1995). Controlling the false discovery rate: A practical and powerful approach to multiple testing. *J. R. Stat. Soc. Ser. B* 57, 289–300. doi:10.2307/2346101.

Bennett, F. G. A. (1984). Resistance to powdery mildew in wheat: a review of its use in agriculture and breeding programmes. *Plant Pathol.* 33, 279–300. doi:10.1111/j.1365-3059.1984.tb01324.x.

Bhatta, M., Morgounov, A., Belamkar, V., Yorgancılar, A., and Baenziger, P. S. (2018). Genome-wide association study reveals favorable alleles associated with common bunt resistance in synthetic hexaploid wheat. *Euphytica* 214, 200. doi:10.1007/s10681-018-2282-4.

Blake, J., Wynn, S., Maumene, C., and Jørgensen, L. N. (2011). Evaluation of the benefits provided by the azole class of compounds in wheat, and the effect of losing all azoles on wheat and potato production in Denmark, France and the UK. Report 1 – Impact of the loss of all azoles. *ADAS UK Ltd.*

Blake, N. K., Lehfeldt, B. R., Lavin, M., and Talbert, L. E. (1999). Phylogenetic reconstruction based on low copy DNA sequence data in an allopolyploid: The B genome of wheat. *Genome* 42, 351–360. doi:10.1139/g98-136.

Borrelli, V. M. G., Brambilla, V., Rogowsky, P., Marocco, A., and Lanubile, A. (2018). The enhancement of plant disease resistance using CRISPR/Cas9 technology. *Front. Plant Sci.* 9, 1245. doi:10.3389/FPLS.2018.01245.

Bowler, C., Montagu, M. V, and Inze, D. (1992). Superoxide dismutase and stress tolerance. *Annu. Rev. Plant Physiol. Plant Mol. Biol.* 43, 83–116. doi:10.1146/annurev.pp.43.060192.000503.

Bozkurt, O., Unver, T., and Akkaya, M. S. (2007). Genes associated with resistance to wheat yellow rust disease identified by differential display analysis. *Physiol. Mol. Plant Pathol.* 71, 251–259. doi:10.1016/j.pmpp.2008.03.002.

Breseghello, F., and Sorrells, M. E. (2006). Association mapping of kernel size and milling quality in wheat (*Triticum aestivum* L.) cultivars. *Genetics* 172, 1165–77. doi:10.1534/genetics.105.044586.

Broman, K. W. (2005). The genomes of recombinant inbred lines. *Genetics* 169, 1133–46. doi:10.1534/genetics.104.035212.

Brown, J. K. M., Chartrain, L., Lasserre-Zuber, P., and Saintenac, C. (2015). Genetics of resistance to *Zymoseptoria tritici* and applications to wheat breeding. *Fungal Genet. Biol.* 79, 33–41. doi:10.1016/j.fgb.2015.04.017.

Brun, H., Chèvre, A.-M., Fitt, B. D., Powers, S., Besnard, A.-L., Ermel, M., et al. (2010). Quantitative resistance increases the durability of qualitative resistance to *Leptosphaeria maculans* in *Brassica napus*. *New Phytol.* 185, 285–299. doi:10.1111/j.1469-8137.2009.03049.x.

Burdon, J. J., and Thrall, P. H. (2008). Pathogen evolution across the agro-ecological interface: implications for disease management. *Evol. Appl.* 1, 57–65. doi:10.1111/j.1752-4571.2007.00005.x.

Bürstmayr, H., Mohler, V., and Kohli, M. (2016). “Advances in control of wheat diseases: Fusarium head blight, wheat blast and powdery mildew.,” in *Achieving sustainable cultivation of wheat.* (Burleigh dodds), 345–370. doi:9781786760166-017.

Carbonell, A., and Carrington, J. C. (2015). Antiviral roles of plant ARGONAUTES. *Curr. Opin. Plant Biol.* 27, 111–117. doi:10.1016/j.pbi.2015.06.013.

Cavanagh, C., Morell, M., Mackay, I., and Powell, W. (2008). From mutations to MAGIC: resources for gene discovery, validation and delivery in crop plants. *Curr. Opin. Plant Biol.* 11, 215–221. doi:10.1016/j.pbi.2008.01.002.

Cavanagh, C. R., Chao, S., Wang, S., Huang, B. E., Stephen, S., Kiani, S., et al. (2013). Genome-wide comparative diversity uncovers multiple targets of selection for improvement in hexaploid wheat landraces and cultivars. *Proc. Natl. Acad. Sci. U. S. A.* 110, 8057–8062. doi:10.1073/pnas.1217133110.

Chen, F., Duan, G.-H., Li, D.-L., and Zhan, J. (2017). Host resistance and temperature-dependent evolution of aggressiveness in the plant pathogen *Zymoseptoria tritici*. *Front. Microbiol.* 8, 1217. doi:10.3389/fmicb.2017.01217.

Chen, L., Huang, L., Min, D., Phillips, A., Wang, S., Madgwick, P. J., et al. (2012). Development and characterization of a new TILLING population of common bread wheat (*Triticum aestivum* L.). *PLoS One* 7, e41570. doi:10.1371/journal.pone.0041570.

Chen, L., Zhang, Z., Liang, H., Liu, H., Du, L., Xu, H., et al. (2008). Overexpression of *TiERF1* enhances resistance to sharp eyespot in transgenic wheat. *J. Exp. Bot.* 59, 4195–4204. doi:10.1093/jxb/ern259.

Cheng, Y. T., and Li, X. (2012). Ubiquitination in NB-LRR-mediated immunity. *Curr. Opin. Plant Biol.* 15, 392–399. doi:10.1016/j.pbi.2012.03.014.

Cheval, P., Siah, A., Bomble, M., Popper, A. D., Reignault, P., and Halama, P. (2017). Evolution of QoI resistance of the wheat pathogen *Zymoseptoria tritici* in Northern

France. *Crop Prot.* 92, 131–133. doi:10.1016/j.cropro.2016.10.017.

Churchill, G. A., and Doerge, R. W. (1994). Empirical threshold values for quantitative trait mapping. *Genetics* 138, 963–971.

Cockram, J., and Mackay, I. (2018). "Genetic mapping populations for conducting high-resolution trait mapping in plants," in *Advances in biochemical engineering/biotechnology*, 109–138. doi:10.1007/10_2017_48.

Cockram, J., Scuderi, A., Barber, T., Furuki, E., Gardner, K. A., Gosman, N., et al. (2015). Fine-mapping the wheat *Snn1* locus conferring sensitivity to the *Parastagonospora nodorum* necrotrophic effector SnTox1 using an eight founder multiparent advanced generation inter-cross population. *G3 Genes|Genomes|Genetics* 5, 2257–66. doi:10.1534/g3.115.021584.

Cools, H. J., and Fraaije, B. A. (2008). Are azole fungicides losing ground against septoria wheat disease? Resistance mechanisms in *Mycosphaerella graminicola*. *Pest Manag. Sci.* 64, 681–684. doi:10.1002/ps.1568.

Cools, H. J., and Fraaije, B. A. (2013). Update on mechanisms of azole resistance in *Mycosphaerella graminicola* and implications for future control. *Pest Manag. Sci.* 69, 150–155. doi:10.1002/ps.3348.

Court of Justice of the European Union (2018). Press Release No 111/18. Available at: https://curia.europa.eu/jcms/upload/docs/application/pdf/2018-07/cp180111en.pdf [Accessed April 17, 2019].

Cui, F., Zhang, N., Fan, X., Zhang, W., Zhao, C., Yang, L., et al. (2017). Utilization of a Wheat660K SNP array-derived high-density genetic map for high-resolution mapping of a major QTL for kernel number. *Sci. Rep.* 7, 3788. doi:10.1038/s41598-017-04028-6.

Czedik-Eysenberg, A., Seitner, S., Güldener, U., Koemeda, S., Jez, J., Colombini, M., et al. (2018). The 'PhenoBox', a flexible, automated, open-source plant phenotyping solution. *New Phytol.* 219, 808–823. doi:10.1111/nph.15129.

Dean, R., van Kan, J. A. L., Pretorius, Z. A., Hammond-Kosack, K. E., Di Pietro, A., Spanu, P. D., et al. (2012). The top 10 fungal pathogens in molecular plant pathology. *Mol. Plant Pathol.* 13, 414–430. doi:10.1111/j.1364-3703.2011.00783.x.

Dell'Acqua, M., Gatti, D. M., Pea, G., Cattonaro, F., Coppens, F., Magris, G., et al. (2015). Genetic properties of the MAGIC maize population: a new platform for high definition QTL mapping in *Zea mays*. *Genome Biol.* 16, 167. doi:10.1186/s13059-015-0716-z.

Denancé, N., Sánchez-Vallet, A., Goffner, D., and Molina, A. (2013). Disease resistance or growth: the role of plant hormones in balancing immune responses and fitness costs. *Front. Plant Sci.* 4. doi:10.3389/fpls.2013.00155.

Dong, N., Liu, X., Lu, Y., Du, L., Xu, H., Liu, H., et al. (2010). Overexpression of *TaPIEP1*, a pathogen-induced ERF gene of wheat, confers host-enhanced resistance to fungal pathogen *Bipolaris sorokiniana*. *Funct. Integr. Genomics* 10, 215–226. doi:10.1007/s10142-009-0157-4.

Doudna, J. A., and Charpentier, E. (2014). The new frontier of genome engineering with CRISPR-Cas9. *Science (80-.).* 346. doi:10.1126/science.1258096.

Drabešová, J., Ryšánek, P., Brunner, P., McDonald, B. A., and Croll, D. (2013).

Population genetic structure of *Mycosphaerella graminicola* and quinone outside inhibitor (QoI) resistance in the Czech Republic. *Eur. J. Plant Pathol.* 135, 211–224. doi:10.1007/s10658-012-0080-8.

Dreisigacker, S., Kishii, M., Lage, J., and Warburton, M. (2008). Use of synthetic hexaploid wheat to increase diversity for CIMMYT bread wheat improvement. *Aust. J. Agric. Res.* 59, 413. doi:10.1071/AR07225.

Dubcovsky, J., and Dvořák, J. (2007). Genome plasticity a key factor in the success of polyploid wheat under domestication. *Science* 316, 1862–1866. doi:10.1126/science.1143986.

Dvořák, J., Luo, M.-C., Yang, Z.-L., and Zhang, H.-B. (1998). The structure of the *Aegilops tauschii* genepool and the evolution of hexaploid wheat. *TAG Theor. Appl. Genet.* 97, 657–670. doi:10.1007/s001220050942.

Dvořák, J., Terlizzi, P. di, Zhang, H.-B., and Resta, P. (1993). The evolution of polyploid wheats: identification of the A genome donor species. *Genome* 36, 21–31. doi:10.1139/g93-004.

Eurostat (2017). Main annual crop statistics. Available at: https://ec.europa.eu/eurostat/statistics-explained/index.php?title=Archive:Main_annual_crop_statistics [Accessed February 12, 2019].

Eurostat (2018). Agriculture, forestry and fishery statistics - 2018 edition. Available at: https://ec.europa.eu/eurostat/documents/3217494/9455154/KS-FK-18-001-EN-N.pdf [Accessed February 12, 2019].

Ewens, W. J., and Spielman, R. S. (2001). Locating genes by linkage and association. *Theor. Popul. Biol.* 60, 135–139. doi:10.1006/TPBI.2001.1547.

Faize, M., Burgos, L., Faize, L., Petri, C., Barba-Espin, G., Díaz-Vivancos, P., et al. (2012). Modulation of tobacco bacterial disease resistance using cytosolic ascorbate peroxidase and Cu,Zn-superoxide dismutase. *Plant Pathol.* 61, 858–866. doi:10.1111/j.1365-3059.2011.02570.x.

Fan, T., Bykova, N. V., Rampitsch, C., and Xing, T. (2016). Identification and characterization of a serine protease from wheat leaves. *Eur. J. Plant Pathol.* 146, 293–304. doi:10.1007/s10658-016-0914-x.

FAOSTAT (2017). Food and Agriculture organization of the United Nations. Crops. Available at: www.fao.org [Accessed February 12, 2019].

Faris, J. D., Liu, Z., and Xu, S. S. (2013). Genetics of tan spot resistance in wheat. *Theor. Appl. Genet.* 126, 2197–2217. doi:10.1007/s00122-013-2157-y.

Figueiredo, J., Sousa Silva, M., and Figueiredo, A. (2018). Subtilisin-like proteases in plant defence: the past, the present and beyond. *Mol. Plant Pathol.* 19, 1017–1028. doi:10.1111/mpp.12567.

Flint-Garcia, S. A., Thornsberry, J. M., and Buckler, E. S. (2003). Structure of linkage disequilibrium in plants. *Annu. Rev. Plant Biol.* 54, 357–374. doi:10.1146/annurev.arplant.54.031902.134907.

Fones, H., and Gurr, S. (2015). The impact of septoria tritici blotch disease on wheat: An EU perspective. *Fungal Genet. Biol.* 79, 3–7. doi:10.1016/j.fgb.2015.04.004.

Fu, Z. Q., Yan, S., Saleh, A., Wang, W., Ruble, J., Oka, N., et al. (2012). NPR3 and NPR4

are receptors for the immune signal salicylic acid in plants. *Nature* 486, 228–232. doi:10.1038/nature11162.

Gardner, K. A., Wittern, L. M., and Mackay, I. J. (2016). A highly recombined, high-density, eight-founder wheat MAGIC map reveals extensive segregation distortion and genomic locations of introgression segments. *Plant Biotechnol. J.* 14, 1406–1417. doi:10.1111/pbi.12504.

Geyer, M., Albrecht, T., Hartl, L., and Mohler, V. (2018). Exploring the genetics of fertility restoration controlled by *Rf1* in common wheat (*Triticum aestivum* L.) using high-density linkage maps. *Mol. Genet. Genomics* 293, 451–462. doi:10.1007/s00438-017-1396-z.

Geyer, M., Bund, A., Albrecht, T., Hartl, L., and Mohler, V. (2016). Distribution of the fertility-restoring gene *Rf3* in common and spelt wheat determined by an informative SNP marker. *Mol. Breed.* 36, 167. doi:10.1007/s11032-016-0592-6.

Gibson, G. (2012). Rare and common variants: twenty arguments. *Nat. Rev. Genet.* 13, 135–45. doi:10.1038/nrg3118.

Gopher, A., Abbo, S., and Yadun, S. L. (2001). The “when”, the “where” and the “why” of the Neolithic revolution in the Levant. *Doc. Praehist.* 28, 49–62. doi:10.4312/dp.28.3.

Götz, M., and Boyle, C. (1998). Haustorial function during development of cleistothecia in *Blumeria graminis* f. sp. *tritici*. *Plant Dis.* 82, 507–511. doi:10.1094/PDIS.1998.82.5.507.

Gower, J. C. (1966). Some distance properties of latent root and vector methods used in multivariate analysis. *Biometrika* 53, 325–338. doi:10.1093/biomet/53.3-4.325.

Griffin, M. J., and Fisher, N. (1985). Laboratory studies on benzimidazole resistance in *Septoria tritici*. *EPPO Bull.* 15, 505–511. doi:10.1111/j.1365-2338.1985.tb00262.x.

Grubbs, F. E. (1950). Sample criteria for testing outlying observations. *Ann. Math. Stat.* 21, 27–58. doi:10.2307/2236553.

Haldane, J. B. S. (1919). The combination of linkage values, and the calculation of distances between the loci of linked factors. *J. Genet.* 8, 299–309.

Hallauer, A., and Miranda, J. (1981). *Quantitative genetics in maize breeding*. Ames IA, USA: Iowa State University Press.

Harlan, J. R., and Zohary, D. (1966). Distribution of wild wheats and barley. *Science* 153, 1074–1080. doi:10.1126/science.153.3740.1074.

Hartmann, A., Czauderna, T., Hoffmann, R., Stein, N., and Schreiber, F. (2011). HTPheno: An image analysis pipeline for high-throughput plant phenotyping. *BMC Bioinformatics* 12, 148. doi:10.1186/1471-2105-12-148.

He, J., Zhao, X., Laroche, A., Lu, Z.-X., Liu, H., and Li, Z. (2014). Genotyping-by-sequencing (GBS), an ultimate marker-assisted selection (MAS) tool to accelerate plant breeding. *Front. Plant Sci.* 5, 484. doi:10.3389/fpls.2014.00484.

Henry, I. M., Nagalakshmi, U., Lieberman, M. C., Ngo, K. J., Krasileva, K. V., Vasquez-Gross, H., et al. (2014). Efficient genome-wide detection and cataloging of EMS-induced mutations using exome capture and next-generation sequencing. *Plant Cell* 26, 1382–1397. doi:10.1105/TPC.113.121590.

Holland, J. B. (2007). Genetic architecture of complex traits in plants. *Curr. Opin. Plant*

Biol. 10, 156–161. doi:10.1016/J.PBI.2007.01.003.

Hovmøller, M. S., Walter, S., and Justesen, A. F. (2010). Escalating threat of wheat rusts. *Science* 329, 369. doi:10.1126/science.1194925.

Hu, P., Liu, J., Xu, J., Zhou, C., Cao, S., Zhou, W., et al. (2018). A malectin-like/leucine-rich repeat receptor protein kinase gene, *Rlk-v* , regulates powdery mildew resistance in wheat. *Mol. Plant Pathol.* 19, 2561–2574. doi:10.1111/mpp.12729.

Huang, B. E., and George, A. W. (2011). R/mpMap: a computational platform for the genetic analysis of multiparent recombinant inbred lines. *Bioinformatics* 27, 727–729. doi:10.1093/bioinformatics/btq719.

Huang, B. E., George, A. W., Forrest, K. L., Kilian, A., Hayden, M. J., Morell, M. K., et al. (2012). A multiparent advanced generation inter-cross population for genetic analysis in wheat. *Plant Biotechnol. J.* 10, 826–839. doi:10.1111/j.1467-7652.2012.00702.x.

Hückelhoven, R., and Panstruga, R. (2011). Cell biology of the plant–powdery mildew interaction. *Curr. Opin. Plant Biol.* 14, 738–746. doi:10.1016/J.PBI.2011.08.002.

Huynh, B.-L., Ehlers, J. D., Huang, B. E., Muñoz-Amatriaín, M., Lonardi, S., Santos, J. R. P., et al. (2018). A multi-parent advanced generation inter-cross (MAGIC) population for genetic analysis and improvement of cowpea (*Vigna unguiculata* L. Walp.). *Plant J.* 93, 1129–1142. doi:10.1111/tpj.13827.

International Wheat Genome Sequencing Consortium (2018). Shifting the limits in wheat research and breeding using a fully annotated reference genome. *Science* 361, eaar7191. doi:10.1126/science.aar7191.

International Wheat Genome Sequencing Consortium (2019). Generating a high quality genome sequence of bread wheat. Available at: http://www.wheatgenome.org/About [Accessed June 13, 2019]

Irving, G., and Holden, J. (2016). How blockchain-timestamped protocols could improve the trustworthiness of medical science. *F1000Research* 5, 222. doi:10.12688/f1000research.8114.3.

Jin, W., and Wu, F. (2015). Characterization of miRNAs associated with *Botrytis cinerea* infection of tomato leaves. *BMC Plant Biol.* 15, 1. doi:10.1186/s12870-014-0410-4.

Jørgensen, L. N., Nielsen, G. C., Ørum, J. E., and Noe, E. (2008). Controlling cereal disease with reduced agrochemical inputs – a challenge for both growers and advisers. Cereal Pathosystems. BSPP Presidential Conference. University of London. 23–33. Available at: http://www.bspp.org.uk/archives/bspp2008/docs/bspppres2008papers.pdf#page=30.

Jørgensen, L. N., Oliver, R. P., and Heick, T. M. (2018). “Occurance and avoidance of fungicide resistance in cereal diseases.,” in *Burleigh Dodds series in Agricultural Science.*, ed. R. P. Oliver doi:DOI: 10.19103/AS.2018.0039.13.

Juliana, P., Singh, R. P., Singh, P. K., Poland, J. A., Bergstrom, G. C., Huerta-Espino, J., et al. (2018). Genome-wide association mapping for resistance to leaf rust, stripe rust and tan spot in wheat reveals potential candidate genes. *Theor. Appl. Genet.* 131, 1405–1422. doi:10.1007/s00122-018-3086-6.

Khazaei, H., Stoddard, F. L., Purves, R. W., and Vandenberg, A. (2018). A multi-parent

faba bean (*Vicia faba* L.) population for future genomic studies. *Plant Genet. Resour. Charact. Util.* 16, 419–423. doi:10.1017/S1479262118000242.

Klittich, C. J. (2008). Milestones in fungicide discovery: Chemistry that changed agriculture. *Plant Heal. Prog.* 9, 31. doi:10.1094/PHP-2008-0418-01-RV.

Klukas, C., Chen, D., and Pape, J.-M. (2014). Integrated analysis platform: An open-source information system for high-throughput plant phenotyping. *Plant Physiol.* 165, 506–518. doi:10.1104/pp.113.233932.

Kollers, S., Rodemann, B., Ling, J., Korzun, V., Ebmeyer, E., Argillier, O., et al. (2014). Genome-wide association mapping of tan spot resistance (*Pyrenophora tritici-repentis*) in European winter wheat. *Mol. Breed.* 34, 363–371. doi:10.1007/s11032-014-0039-x.

Kover, P. X., Valdar, W., Trakalo, J., Scarcelli, N., Ehrenreich, I. M., Purugganan, M. D., et al. (2009). A multiparent advanced generation inter-cross to fine-map quantitative traits in *Arabidopsis thaliana*. *PLoS Genet.* 5, e1000551. doi:10.1371/journal.pgen.1000551.

Krasileva, K. V, Vasquez-Gross, H. A., Howell, T., Bailey, P., Paraiso, F., Clissold, L., et al. (2017). Uncovering hidden variation in polyploid wheat. *Proc. Natl. Acad. Sci. U. S. A.* 114, E913–E921. doi:10.1073/pnas.1619268114.

Ladejobi, O., Elderfield, J., Gardner, K. A., Gaynor, R. C., Hickey, J., Hibberd, J. M., et al. (2016). Maximizing the potential of multi-parental crop populations. *Appl. Transl. Genomics* 11, 9–17. doi:10.1016/J.ATG.2016.10.002.

Lamari, L., and Bernier, C. C. (1989). Evaluation of wheat lines and cultivars to tan spot (*Pyrenophora tritici-repentis*) based on lesion type. *Can. J. Plant Pathol.* 11, 49–56. doi:10.1080/07060668909501146.

Lee, H. Y., Bowen, C. H., Popescu, G. V., Kang, H.-G., Kato, N., Ma, S., et al. (2011). Arabidopsis RTNLB1 and RTNLB2 Reticulon-like proteins regulate intracellular trafficking and activity of the FLS2 immune receptor. *Plant Cell* 23, 3374–91. doi:10.1105/tpc.111.089656.

Leroux, P., and Walker, A.-S. (2011). Multiple mechanisms account for resistance to sterol 14α-demethylation inhibitors in field isolates of *Mycosphaerella graminicola*. *Pest Manag. Sci.* 67, 44–59. doi:10.1002/ps.2028.

Lev-Yadun, S., Gopher, A., and Abbo, S. (2000). The cradle of agriculture. *Science* 288, 1602–1603. doi:10.1126/science.288.5471.1602.

Li, G., Carver, B. F., Cowger, C., Bai, G., and Xu, X. (2018). *Pm223899*, a new recessive powdery mildew resistance gene identified in Afghanistan landrace PI 223899. *Theor. Appl. Genet.*, 1–9. doi:10.1007/s00122-018-3199-y.

Li, Y., Lu, Y.-G., Shi, Y., Wu, L., Xu, Y.-J., Huang, F., et al. (2014a). Multiple rice microRNAs are involved in immunity against the blast fungus *Magnaporthe oryzae*. *Plant Physiol.* 164, 1077–92. doi:10.1104/pp.113.230052.

Li, Z., Lan, C., He, Z., Singh, R. P., Rosewarne, G. M., Chen, X., et al. (2014b). Overview and application of QTL for adult plant resistance to leaf rust and powdery mildew in wheat. *Crop Sci.* 54, 1907. doi:10.2135/cropsci2014.02.0162.

Lindenthal, M., Steiner, U., Dehne, H.-W., and Oerke, E.-C. (2005). Effect of downy mildew development on transpiration of cucumber leaves visualized by digital

infrared thermography. *Phytopathology* 95, 233–240. doi:10.1094/PHYTO-95-0233.

Lipka, A. E., Tian, F., Wang, Q., Peiffer, J., Li, M., Bradbury, P. J., et al. (2012). GAPIT: genome association and prediction integrated tool. *Bioinformatics* 28, 2397–2399. doi:10.1093/bioinformatics/bts444.

Lucas, J. A., Hawkins, N. J., and Fraaije, B. A. (2015). The evolution of fungicide resistance. *Adv. Appl. Microbiol.* 90, 29–92. doi:10.1016/BS.AAMBS.2014.09.001.

Mackay, I. J., Bansept-Basler, P., Barber, T., Bentley, A. R., Cockram, J., Gosman, N., et al. (2014). An eight-parent multiparent advanced generation inter-cross population for winter-sown wheat: creation, properties, and validation. *G3 Genes|Genomes|Genetics* 4, 1603–1610. doi:10.1534/g3.114.012963.

Mackay, I., and Powell, W. (2007). Methods for linkage disequilibrium mapping in crops. *Trends Plant Sci.* 12, 57–63. doi:10.1016/J.TPLANTS.2006.12.001.

Mackintosh, C. A., Lewis, J., Radmer, L. E., Shin, S., Heinen, S. J., Smith, L. A., et al. (2007). Overexpression of defense response genes in transgenic wheat enhances resistance to fusarium head blight. *Plant Cell Rep.* 26, 479–488. doi:10.1007/s00299-006-0265-8.

Mahlein, A.-K., Steiner, U., Hillnhütter, C., Dehne, H.-W., and Oerke, E.-C. (2012). Hyperspectral imaging for small-scale analysis of symptoms caused by different sugar beet diseases. *Plant Methods* 8, 3. doi:10.1186/1746-4811-8-3.

Maier, U. (1996). Morphological studies of free-threshing wheat ears from a Neolithic site in southwest Germany, and the history of the naked wheats. *Veg. Hist. Archaeobot.* 5, 39–55. doi:10.1007/BF00189434.

Marcotuli, I., Gadaleta, A., Mangini, G., Signorile, A., Zacheo, S., Blanco, A., et al. (2017). Development of a high-density SNP-based linkage map and detection of QTL for β-glucans, protein content, grain yield per spike and heading time in durum wheat. *Int. J. Mol. Sci.* 18, 1329. doi:10.3390/ijms18061329.

McDonald, B. A., and Linde, C. (2002). Pathogen population genetics, evolutionary potential, and durable resistance. *Annu. Rev. Phytopathol.* 40, 349–379. doi:10.1146/annurev.phyto.40.120501.101443.

McDonald, B. A., and Martinez, J. P. (1990). DNA restriction fragment length polymorphisms among *Mycosphaerella graminicola* (anamorph *Septoria tritici*) isolates collected from a single wheat field. *Phytopathology* 80, 1368. doi:10.1094/Phyto-80-1368.

McIntosh, R. A. (2009). History and status of the wheat rusts. In: McIntosh RA (ed) Proceedings of the Borlaug global rust initiative 2009 technical workshop BGRI Cd Obregon, Mexico. 11–23. Available at: https://www.globalrust.org/sites/default/files/posters/Mcintosh_2009.pdf.

McIntosh, R. A., Yamazaki, Y., Dubcovsky, J., Rogers, J., Morris, C., Appels, R., et al. (2013). Catalogue of gene symbols for wheat. 12th International wheat genetic symposium. Yokohama, Japan, September.

Miedaner, T., and Flath, K. (2007). Effectiveness and environmental stability of quantitative powdery mildew (*Blumeria graminis*) resistance among winter wheat cultivars. *Plant Breed.* 126, 553–558. doi:10.1111/j.1439-0523.2006.01353.x.

Miedaner, T., and Longin, C. F. H. (2012). *Unterschätzte Getreidearten - Einkorn, Emmer,*

Dinkel & Co. Agrimedia Verlag.

Mohler, V., Bauer, C., Schweizer, G., Kempf, H., and Hartl, L. (2013). *Pm50*: a new powdery mildew resistance gene in common wheat derived from cultivated emmer. *J. Appl. Genet.* 54, 259–263. doi:10.1007/s13353-013-0158-9.

Molina, A., Görlach, J., Volrath, S., and Ryals, J. (1999). Wheat genes encoding two types of PR-1 proteins are pathogen inducible, but do not respond to activators of systemic acquired resistance. *Mol. Plant-Microbe Interact.* 12, 53–58. doi:10.1094/MPMI.1999.12.1.53.

Morton, V., and Staub, T. (2008). A short history of fungicides. *APSnet Featur. Artic.* doi:10.1094/APSnetFeature-2008-0308.

Mott, R., Talbot, C. J., Turri, M. G., Collins, A. C., and Flint, J. (2000). A method for fine mapping quantitative trait loci in outbred animal stocks. *Proc. Natl. Acad. Sci.* 97, 12649–12654. doi:10.1073/pnas.230304397.

Mujeeb-Kazi, A., Rosas, V., and Roldan, S. (1996). Conservation of the genetic variation of *Triticum tauschii* (Coss.) Schmalh. (*Aegilops squarrosa* auct. non L.) in synthetic hexaploid wheats (*T. turgidum* L. s.lat. x *T. tauschii*; 2n=6x=42, AABBDD) and its potential utilization f. *Genet. Resour. Crop Evol.* 43, 129–134. doi:10.1007/BF00126756.

Mullins, J. G. L., Parker, J. E., Cools, H. J., Togawa, R. C., Lucas, J. A., Fraaije, B. A., et al. (2011). Molecular modelling of the emergence of azole resistance in *Mycosphaerella graminicola*. *PLoS One* 6, e20973. doi:10.1371/journal.pone.0020973.

Mutka, A. M., and Bart, R. S. (2015). Image-based phenotyping of plant disease symptoms. *Front. Plant Sci.* 5, 734. doi:10.3389/fpls.2014.00734.

Nalam, V. J., Vales, M. I., Watson, C. J. W., Kianian, S. F., and Riera-Lizarazu, O. (2006). Map-based analysis of genes affecting the brittle rachis character in tetraploid wheat (*Triticum turgidum* L.). *Theor. Appl. Genet.* 112, 373–381. doi:10.1007/s00122-005-0140-y.

Navarro, L., Dunoyer, P., Jay, F., Arnold, B., Dharmasiri, N., Estelle, M., et al. (2006). A plant miRNA contributes to antibacterial resistance by repressing auxin signaling. *Science* 312, 436–439. doi:10.1126/science.1126088.

Niu, J. shan, Jia, H. yan, Yin, J., Wang, B. qin, Ma, Z. qiang, and Shen, T. min (2010). Development of an STS marker linked to powdery mildew resistance genes *PmLK906* and *Pm4a* by gene chip hybridization. *Agric. Sci. China* 9, 331–336. doi:10.1016/S1671-2927(09)60101-2.

O'Driscoll, A., Kildea, S., Doohan, F., Spink, J., and Mullins, E. (2014). The wheat-septoria conflict: a new front opening up? *Trends Plant Sci.* 19, 602–610. doi:10.1016/j.tplants.2014.04.011.

Ogbonnaya, F. C., Halloran, G. M., and Lagudah, E. S. (2005). D genome of wheat – 60 years on from Kihara, Sears and McFadden. *Wheat Inf. Serv.* 100, 205–220. Available at: http://shigen.nig.ac.jp/wheat/wis/No100/p205/p205.1.html.

Olivera Firpo, P. D., Newcomb, M., Flath, K., Sommerfeldt-Impe, N., Szabo, L. J., Carter, M., et al. (2017). Characterization of *Puccinia graminis* f. sp. *tritici* isolates derived from an unusual wheat stem rust outbreak in Germany in 2013. *Plant Pathol.* 66, 1258–1266. doi:10.1111/ppa.12674.

Ongom, P. O., and Ejeta, G. (2018). Mating design and genetic structure of a multiparent advanced generation intercross (MAGIC) population of sorghum (*Sorghum bicolor* L.) Moench). *G3 Genes|Genomes|Genetics* 8, 331–341. doi:10.1534/g3.117.300248.

Orton, E. S., Deller, S., and Brown, J. K. M. (2011). *Mycosphaerella graminicola*: from genomics to disease control. *Mol. Plant Pathol.* 12, 413–424. doi:10.1111/j.1364-3703.2010.00688.x.

Ouyang, S., Zhang, D., Han, J., Zhao, X., Cui, Y., Song, W., et al. (2014). Fine physical and genetic mapping of powdery mildew resistance gene *MlIW172* originating from wild emmer (*Triticum dicoccoides*). *PLoS One* 9, e100160. doi:10.1371/journal.pone.0100160.

Panstruga, R., and Dodds, P. N. (2009). Terrific protein traffic: the mystery of effector protein delivery by filamentous plant pathogens. *Science* 324, 748–750. doi:10.1126/science.1171652.

Paradis, E., Claude, J., and Strimmer, K. (2004). APE: Analyses of phylogenetics and evolution in R language. *Bioinformatics* 20, 289–290. doi:10.1093/bioinformatics/btg412.

Pascual, L., Desplat, N., Huang, B. E., Desgroux, A., Bruguier, L., Bouchet, J.-P., et al. (2015). Potential of a tomato MAGIC population to decipher the genetic control of quantitative traits and detect causal variants in the resequencing era. *Plant Biotechnol. J.* 13, 565–577. doi:10.1111/pbi.12282.

Pilet-Nayel, M.-L., Moury, B., Caffier, V., Montarry, J., Kerlan, M.-C., Fournet, S., et al. (2017). Quantitative resistance to plant pathogens in pyramiding strategies for durable crop protection. *Front. Plant Sci.* 8, 1838. doi:10.3389/fpls.2017.01838.

Plaschke, J., Ganal, M. W., and Röder, M. S. (1995). Detection of genetic diversity in closely related bread wheat using microsatellite markers. *Theor. Appl. Genet.* 91, 1001–1007. doi:10.1007/BF00223912.

Plissonneau, C., Hartmann, F. E., and Croll, D. (2018). Pangenome analyses of the wheat pathogen *Zymoseptoria tritici* reveal the structural basis of a highly plastic eukaryotic genome. *BMC Biol.* 16, 5. doi:10.1186/s12915-017-0457-4.

R Development Core Team (2017). R: A language and environment for statistical computing. R foundation for statistical computing, Vienna, Austria.

Rajaraman, J., Douchkov, D., Hensel, G., Stefanato, F. L., Gordon, A., Ereful, N., et al. (2016). An LRR/malectin receptor-like kinase mediates resistance to non-adapted and adapted powdery mildew fungi in barley and wheat. *Front. Plant Sci.* 7, 1836. doi:10.3389/fpls.2016.01836.

Ran, F. A., Hsu, P. D., Wright, J., Agarwala, V., Scott, D. A., and Zhang, F. (2013). Genome engineering using the CRISPR-Cas9 system. *Nat. Protoc.* 8, 2281–2308. doi:10.1038/nprot.2013.143.

Risser, P., Ebmeyer, E., Korzun, V., Hartl, L., and Miedaner, T. (2011). Quantitative trait loci for adult-plant resistance to *Mycosphaerella graminicola* in two winter wheat populations. *Phytopathology* 101, 1209–1216. doi:10.1094/PHYTO-08-10-0203.

Rodríguez-Moreno, L., Pineda, M., Soukupová, J., Macho, A. P., Beuzón, C. R., Barón, M., et al. (2008). Early detection of bean infection by *Pseudomonas syringae* in asymptomatic leaf areas using chlorophyll fluorescence imaging. *Photosynth. Res.* 96, 27–35. doi:10.1007/s11120-007-9278-6.

Rogers, J. S. (1972). Measures of genetic similarity and genetic distances. *Stud. Genet. VII, Univ. Texas Publ.* 7213, 145–153.

Salamini, F., Özkan, H., Brandolini, A., Schäfer-Pregl, R., and Martin, W. (2002). Genetics and geography of wild cereal domestication in the near east. *Nat. Rev. Genet.* 3, 429–441. doi:10.1038/nrg817.

Sallam, A., and Martsch, R. (2015). Association mapping for frost tolerance using multi-parent advanced generation inter-cross (MAGIC) population in faba bean (*Vicia faba* L.). *Genetica* 143, 501–514. doi:10.1007/s10709-015-9848-z.

San Segundo-Val, I., and Sanz-Lozano, C. S. (2016). "Introduction to the gene expression analysis," in *Methods in molecular biology (Clifton, N.J.)*, 29–43. doi:10.1007/978-1-4939-3652-6_3.

Sanders, P. L., Waard, M. A., and Loerakker, W. M. (1986). Resistance to carbendazim in *Pseudocercosporella herpotrichoides* from Dutch wheat fields. *Netherlands J. Plant Pathol.* 92, 15–20. doi:10.1007/BF01976372.

Sannemann, W., Huang, B. E., Mathew, B., and Léon, J. (2015). Multi-parent advanced generation inter-cross in barley: high-resolution quantitative trait locus mapping for flowering time as a proof of concept. *Mol. Breed.* 35, 86. doi:10.1007/s11032-015-0284-7.

Sannemann, W., Lisker, A., Maurer, A., Léon, J., Kazman, E., Cöster, H., et al. (2018). Adaptive selection of founder segments and epistatic control of plant height in the MAGIC winter wheat population WM-800. *BMC Genomics* 19, 559. doi:10.1186/s12864-018-4915-3.

Schilder, A. M. C., and Bergstrom, G. C. (1992). The dispersal of conidia and ascospores of *Pyrenophora tritici-repentis*. in *Proceedings of 2nd tan spot workshop*, eds. L. J. Francl, J. M. Krupinsky, and M. P. McMullen (Fargo: North Dakota Agricultural Experiment Station), 96–99. Available at: http://agris.fao.org/agris-search/search.do?recordID=US9403897 [Accessed March 11, 2019].

Schwessinger, B., Sperschneider, J., Cuddy, W. S., Garnica, D. P., Miller, M. E., Taylor, J. M., et al. (2018). A near-complete haplotype-phased genome of the dikaryotic wheat stripe rust fungus *Puccinia striiformis* f. sp. *tritici* reveals high interhaplotype diversity. *MBio* 9, e02275-17. doi:10.1128/mBio.02275-17.

Seo, J.-K., Wu, J., Lii, Y., Li, Y., and Jin, H. (2013). Contribution of small RNA pathway components in plant immunity. *Mol. Plant-Microbe Interact.* 26, 617–625. doi:10.1094/MPMI-10-12-0255-IA.

Shah, R., and Huang, B. E. (2017). mpMap2: An R pipeline for genetic map construction. Available at: https://github.com/rohan-shah/mpMap2Paper/releases [Accessed February 15, 2018].

Shah, R., Huang, B. E., Whan, A., Newberry, M., Verbyla, K., Morell, M. K., et al. (2019). The complex genetic architecture of recombination and structural variation in wheat uncovered using a large 8-founder MAGIC population. *bioRxiv*, 594317. doi:10.1101/594317.

Shen, D., Suhrkamp, I., Wang, Y., Liu, S., Menkhaus, J., Verreet, J. A., et al. (2014). Identification and characterization of microRNAs in oilseed rape (*Brassica napus*) responsive to infection with the pathogenic fungus *Verticillium longisporum* using Brassica AA (*Brassica rapa*) and CC (*Brassica oleracea*) as refer. *New Phytol.* 204,

577–594. doi:10.1111/nph.12934.

Simons, K. J., Fellers, J. P., Trick, H. N., Zhang, Z., Tai, Y. S., Gill, B. S., et al. (2006). Molecular characterization of the major wheat domestication gene *Q*. *Genetics*. doi:10.1534/genetics.105.044727.

Singh, R. P., Hodson, D. P., Huerta-Espino, J., Jin, Y., Njau, P., Wanyera, R., et al. (2008). Will stem rust destroy the world's wheat crop? *Adv. Agron.* 98, 271–309. doi:10.1016/S0065-2113(08)00205-8.

Sireesha, Y., and Velazhahan, R. (2017). Analysis of defense genes expression in maize upon infection with *Peronosclerospora sorghi*. *Cereal Res. Commun.* 45, 272–283. doi:10.1556/0806.45.2017.010.

Sood, S., Kuraparthy, V., Bai, G., and Gill, B. S. (2009). The major threshability genes soft glume (*sog*) and tenacious glume (*Tg*), of diploid and polyploid wheat, trace their origin to independent mutations at non-orthologous loci. *Theor. Appl. Genet.* doi:10.1007/s00122-009-1043-0.

Stadlmeier, M., Hartl, L., and Mohler, V. (2018). Usefulness of a multiparent advanced generation intercross population with a greatly reduced mating design for genetic studies in winter wheat. *Front. Plant Sci.* 9, 1825. doi:10.3389/FPLS.2018.01825.

Stadlmeier, M., Jørgensen, L. N., Corsi, B., Cockram, J., Hartl, L., and Mohler, V. (2019). Genetic dissection of resistance to the three fungal plant pathogens *Blumeria graminis*, *Zymoseptoria tritici*, and *Pyrenophora tritici-repentis* using a multiparental winter wheat population. *G3 Genes|Genomes|Genetics* 5, 1745–1757. doi:10.1534/g3.119.400068.

Stammler, G., and Semar, M. (2011). Sensitivity of *Mycosphaerella graminicola* (anamorph: *Septoria tritici*) to DMI fungicides across Europe and impact on field performance. *EPPO Bull.* 41, 149–155. doi:10.1111/j.1365-2338.2011.02454.x.

Stewart, E. L., and McDonald, B. A. (2014). Measuring quantitative virulence in the wheat pathogen *Zymoseptoria tritici* using high-throughput automated image analysis. *Phytopathology* 104, 985–992. doi:10.1094/PHYTO-11-13-0328-R.

Strelkov, S. E., and Lamari, L. (2003). Host–parasite interactions in tan spot (*Pyrenophora tritici-repentis*) of wheat. *Can. J. Plant Pathol.* 25, 339–349. doi:10.1080/07060660309507089.

Suffert, F., Sache, I., and Lannou, C. (2011). Early stages of septoria tritici blotch epidemics of winter wheat: build-up, overseasoning, and release of primary inoculum. *Plant Pathol.* 60, 166–177. doi:10.1111/j.1365-3059.2010.02369.x.

Sugiura, R., Tsuda, S., Tamiya, S., Itoh, A., Nishiwaki, K., Murakami, N., et al. (2016). Field phenotyping system for the assessment of potato late blight resistance using RGB imagery from an unmanned aerial vehicle. *Biosyst. Eng.* 148, 1–10. doi:10.1016/J.BIOSYSTEMSENG.2016.04.010.

Thapa, G., Gunupuru, L. R., Hehir, J. G., Kahla, A., Mullins, E., and Doohan, F. M. (2018). A pathogen-responsive leucine rich receptor like kinase contributes to fusarium resistance in cereals. *Front. Plant Sci.* 9, 867. doi:10.3389/fpls.2018.00867.

Thoen, M. P. M., Kloth, K. J., Wiegers, G. L., Krips, O. E., Noldus, L. P. J. J., Dicke, M., et al. (2016). Automated video tracking of thrips behavior to assess host-plant resistance in multiple parallel two-choice setups. *Plant Methods* 12, 1. doi:10.1186/s13007-016-0102-1.

Tian, D., Traw, M. B., Chen, J. Q., Kreitman, M., and Bergelson, J. (2003). Fitness costs of R-gene-mediated resistance in *Arabidopsis thaliana*. *Nature* 423, 74–77. doi:10.1038/nature01588.

Tommasini, L., Yahiaoui, N., Srichumpa, P., and Keller, B. (2006). Development of functional markers specific for seven *Pm3* resistance alleles and their validation in the bread wheat gene pool. *Theor. Appl. Genet.* 114, 165–175. doi:10.1007/s00122-006-0420-1.

Tuinstra, M. R., Ejeta, G., and Goldsbrough, P. B. (1997). Heterogeneous inbred family (HIF) analysis: a method for developing near-isogenic lines that differ at quantitative trait loci. *Theor. Appl. Genet.* 95, 1005–1011. doi:10.1007/s001220050654.

Uauy, C., Paraiso, F., Colasuonno, P., Tran, R. K., Tsai, H., Berardi, S., et al. (2009). A modified TILLING approach to detect induced mutations in tetraploid and hexaploid wheat. *BMC Plant Biol.* 9, 115. doi:10.1186/1471-2229-9-115.

United Nations (2015). General assembly resolution A/RES/70/1. Transforming our world, the 2030 agenda for sustainable development. Available at: https://sustainabledevelopment.un.org/content/documents/21252030 Agenda for Sustainable Development web.pdf [Accessed February 11, 2019].

Utz, H. (2011). PLABSTAT Version 3A. A computer program for statistical analysis of plant breeding experiments. Institut für Pflanzenzüchtung, Saatgutforschung und Populationsgenetik Universität Hohenheim, Stuttgart, Deutschland.

VanRaden, P. M. (2008). Efficient methods to compute genomic predictions. *J. Dairy Sci.* 91, 4414–4423. doi:10.3168/JDS.2007-0980.

Vilhjálmsson, B. J., and Nordborg, M. (2013). The nature of confounding in genome-wide association studies. *Nat. Rev. Genet.* 14, 1–2. doi:10.1038/nrg3382.

Wang, S., Wong, D., Forrest, K., Allen, A., Chao, S., Huang, B. E., et al. (2014a). Characterization of polyploid wheat genomic diversity using a high-density 90 000 single nucleotide polymorphism array. *Plant Biotechnol. J.* 12, 787–796. doi:10.1111/pbi.12183.

Wang, X., Yang, B., Li, K., Kang, Z., Cantu, D., and Dubcovsky, J. (2016). A conserved *Puccinia striiformis* protein interacts with wheat NPR1 and reduces induction of pathogenesis-related genes in response to pathogens. *Mol. Plant-Microbe Interact.* 29, 977–989. doi:10.1094/MPMI-10-16-0207-R.

Wang, Y., Cheng, X., Shan, Q., Zhang, Y., Liu, J., Gao, C., et al. (2014b). Simultaneous editing of three homoeoalleles in hexaploid bread wheat confers heritable resistance to powdery mildew. *Nat. Biotechnol.* 32, 947–951. doi:10.1038/nbt.2969.

Warnes, G., with contributions from Gorjanc, G., Leisch, F., and Man, M. (2013). Genetics: Population Genetics. R Package Version 1.3.8.1. Available at: https://cran.r-project.org/package=genetics.

Watson, A., Ghosh, S., Williams, M. J., Cuddy, W. S., Simmonds, J., Rey, M.-D., et al. (2018). Speed breeding is a powerful tool to accelerate crop research and breeding. *Nat. Plants* 4, 23–29. doi:10.1038/s41477-017-0083-8.

Wicker, T., Oberhaensli, S., Parlange, F., Buchmann, J. P., Shatalina, M., Roffler, S., et al. (2013). The wheat powdery mildew genome shows the unique evolution of an obligate biotroph. *Nat. Genet.* 45, 1092–1096. doi:10.1038/ng.2704.

Wimmer, V., Albrecht, T., Auinger, H.-J., and Schön, C.-C. (2012). Synbreed: a framework for the analysis of genomic prediction data using R. *Bioinformatics* 28, 2086–2087. doi:10.1093/bioinformatics/bts335.

Wright, A., and De Filippi, P. (2015). Decentralized blockchain technology and the rise of Lex Cryptographia. *SSRN Electron. J.* doi:10.2139/ssrn.2580664.

Xu, Y., Li, P., Yang, Z., and Xu, C. (2017). Genetic mapping of quantitative trait loci in crops. *Crop J.* 5, 175–184. doi:10.1016/j.cj.2016.06.003.

Yan, Y., Hsam, S. L. K., Yu, J. Z., Jiang, Y., Ohtsuka, I., and Zeller, F. J. (2003). HMW and LMW glutenin alleles among putative tetraploid and hexaploid European spelt wheat (*Triticum spelta* L.) progenitors. *Theor. Appl. Genet.* 107, 1321–1330. doi:10.1007/s00122-003-1315-z.

Yang, L., and Huang, H. (2014). Roles of small RNAs in plant disease resistance. *J. Integr. Plant Biol.* 56, 962–970. doi:10.1111/jipb.12200.

Yu, Y., Xu, W., Wang, J., Wang, L., Yao, W., Yang, Y., et al. (2013). The Chinese wild grapevine (*Vitis pseudoreticulata*) E3 ubiquitin ligase *Erysiphe necator*-induced RING finger protein 1 (EIRP1) activates plant defense responses by inducing proteolysis of the VpWRKY11 transcription factor. *New Phytol.* 200, 834–846. doi:10.1111/nph.12418.

Zeng, L.-R., Vega-Sánchez, M. E., Zhu, T., and Wang, G.-L. (2006). Ubiquitination-mediated protein degradation and modification: an emerging theme in plant-microbe interactions. *Cell Res.* 16, 413–426. doi:10.1038/sj.cr.7310053.

Zhang, C., Gao, H., Li, R., Han, D., Wang, L., Wu, J., et al. (2019). GmBTB/POZ, a novel BTB/POZ domain-containing nuclear protein, positively regulates the response of soybean to *Phytophthora sojae* infection. *Mol. Plant Pathol.* 20, 78–91. doi:10.1111/mpp.12741.

Zhao, K., Aranzana, M. J., Kim, S., Lister, C., Shindo, C., Tang, C., et al. (2007). An Arabidopsis example of association mapping in structured samples. *PLoS Genet.* 3, 0071–0082. doi:10.1371/journal.pgen.0030004.

Zheng, Z., Xie, S., Dai, H., Chen, X., and Wang, H. (2017). An overview of blockchain technology: architecture, consensus, and future trends. in *2017 IEEE International Congress on Big Data (BigData Congress)* (IEEE), 557–564. doi:10.1109/BigDataCongress.2017.85.

Zhou, H., Li, S., Deng, Z., Wang, X., Chen, T., Zhang, J., et al. (2007). Molecular analysis of three new receptor-like kinase genes from hexaploid wheat and evidence for their participation in the wheat hypersensitive response to stripe rust fungus infection. *Plant J.* 52, 420–434. doi:10.1111/j.1365-313X.2007.03246.x.

Zhu, C., Gore, M., Buckler, E. S., and Yu, J. (2008). Status and prospects of association mapping in plants. *Plant Genome J.* 1, 5. doi:10.3835/plantgenome2008.02.0089.

5 PUBLICATIONS

This section includes reprints of the two publications underlying this thesis. The two publications, including supplementary material, can be accessed *via* the following links:

Stadlmeier et al. 2018

https://www.frontiersin.org/articles/10.3389/fpls.2018.01825/full

Stadlmeier et al. 2019

https://www.g3journal.org/content/9/5/1745

frontiers in Plant Science

ORIGINAL RESEARCH
published: 06 December 2018
doi: 10.3389/fpls.2018.01825

Usefulness of a Multiparent Advanced Generation Intercross Population With a Greatly Reduced Mating Design for Genetic Studies in Winter Wheat

Melanie Stadlmeier[1,2]*, *Lorenz Hartl*[1] and *Volker Mohler*[1,2]

[1] Bavarian State Research Center for Agriculture, Institute for Crop Science and Plant Breeding, Freising, Germany, [2] TUM School of Life Sciences Weihenstephan, Technical University of Munich, Freising, Germany

Multiparent advanced generation intercross (MAGIC) populations were recently developed to allow the high-resolution mapping of quantitative traits. We present a genetic linkage map of an elite but highly diverse eight-founder MAGIC population in common wheat (*Triticum aestivum* L.). Our MAGIC population is composed of 394 $F_{6:8}$ recombinant inbred lines lacking significant signatures of population structure. The linkage map included 5435 SNP markers distributed over 2804 loci and spanning 5230 cM. The analysis of population parameters, including genetic structure, kinship, founder probabilities, and linkage disequilibrium and congruency to other maps indicated appropriate construction of both the population and the genetic map. It was shown that eight-founder MAGIC populations exhibit a greater number of loci and higher recombination rates, especially in the pericentromeric regions, compared to four-founder MAGIC, and biparental populations. In addition, our greatly simplified eight-parental MAGIC mating design with an additional eight-way intercross step was found to be equivalent to a MAGIC design with all 210 possible four-way crosses regarding the levels of missing founder assignments and the number of recombination events. Furthermore, the MAGIC population captured 71.7% of the allelic diversity available in the German wheat breeding gene pool. As a proof of principle, we demonstrated the application of the resource for quantitative trait loci mapping analyzing seedling resistance to powdery mildew. As wheat is a crop with many breeding objectives, this resource will allow scientists and breeders to carry out genetic studies for a wide range of breeder-relevant parameters in a single genetic background and reveal possible interactions between traits of economic importance.

Keywords: multiparental population, SNP, RIL, linkage map, recombination, wheat

OPEN ACCESS

Edited by:
Thomas Miedaner, University of Hohenheim, Germany

Reviewed by:
Alison Bentley, National Institute of Agricultural Botany (NIAB), United Kingdom
Alex Whan, Commonwealth Scientific and Industrial Research Organisation (CSIRO), Australia

***Correspondence:**
Melanie Stadlmeier
melanie_stadlmeier@mytum.de

Specialty section:
This article was submitted to Plant Breeding, a section of the journal Frontiers in Plant Science

Received: *07 August 2018*
Accepted: *23 November 2018*
Published: *06 December 2018*

Citation:
Stadlmeier M, Hartl L and Mohler V (2018) Usefulness of a Multiparent Advanced Generation Intercross Population With a Greatly Reduced Mating Design for Genetic Studies in Winter Wheat. Front. Plant Sci. 9:1825. doi: 10.3389/fpls.2018.01825

INTRODUCTION

In plant breeding, the detection of quantitative trait loci (QTL) is no longer limited by the availability of genetic marker information and genotyping throughput (Mammadov et al., 2012; Chen et al., 2014; He et al., 2014; Unterseer et al., 2014; Cui et al., 2017), but rather by the genetic material employed (Flint-Garcia et al., 2003; Zhu et al., 2008; Asimit and Zeggini, 2010; Gibson, 2012). In an attempt to counteract this fact, nested association mapping (NAM) and multiparent advanced generation intercross (MAGIC) populations were

established. In crops, Mackay and Powell (2007) and Cavanagh et al. (2008) first discussed the latter population type. In MAGIC designs, multiple inbred founders are intercrossed several times in a well-defined order to combine the genetic material of all the founders in a single line (Cavanagh et al., 2008). This leads to highly diverse genotypes each with a unique mosaic of founder alleles. The higher number of parents and recombination events of a MAGIC population are clear advantages compared to a classical biparental population, while for both designs pedigree and genetic structure are well known. In association mapping (AM) panels, genetic diversity and recombination rates are higher than in MAGIC designs as these panels take advantage of a collection of diverse breeding lines. However, the main factor limiting AM studies is confounding due to population structure based on sampling effects (Flint-Garcia et al., 2003; Caldwell et al., 2006; Vilhjálmsson and Nordborg, 2013) which enhances the risk of detecting false positives (Ewens and Spielman, 2001; Dickson et al., 2010; Korte and Farlow, 2013). Therefore, MAGIC populations represent an intermediate to biparental crosses and diversity panels concerning substructure, allele diversity, the number of traits that can be investigated, resolution, and power (Rakshit et al., 2012; Pascual et al., 2016). To date, MAGIC populations were established in a wide range of various crops including rice (Bandillo et al., 2013), tomato (Pascual et al., 2015), fava bean (Sallam and Martsch, 2015), maize (Dell'Acqua et al., 2015), barley (Sannemann et al., 2015), and sorghum (Ongom and Ejeta, 2018). In wheat, the first described MAGIC population was based on four founder genotypes (Huang et al., 2012). Further wheat MAGIC resources were generated using eight parents by Mackay et al. (2014) and Sannemann et al. (2018). A 16 founder wheat MAGIC population was established in the UK including elite and historical varieties (Fradgley et al., 2017). It is expected that a higher number of parents and initial crosses will result in a better dissection of complex traits (Huang et al., 2012). However, this implies more time and higher costs for population creation. So far, no study has been published investigating a MAGIC population design that involved a greatly reduced number of overall crossings.

Through intensive genetic analysis, we evaluated the impact of a MAGIC mating design with a greatly reduced number of overall crossings. First, we explored the genetic structure of our Bavarian MAGIC wheat population (BMWpop) for the validation of the crossing procedure. Second, we constructed a genetic linkage map, which we evaluated through population parameters and congruency with other maps. For comparative analysis, we used two other wheat MAGIC maps (Cavanagh et al., 2013; Gardner et al., 2016), one biparental map (Geyer et al., 2017), and the IWGSC RefSeq v1.0 (International Wheat Genome Sequencing Consortium, 2018). Recombination fraction, linkage disequilibrium, and founder probabilities were used to address population analysis parameters. Third, as a proof of principle, we demonstrated the application of the resource for QTL mapping using the trait seedling resistance to powdery mildew. The described genetic material will be shared with the scientific community upon request. It will enable scientists and breeders to carry out genetic studies for a wide range of economically relevant winter wheat breeding traits in a single genetic background and to reveal possible interactions.

MATERIALS AND METHODS

Plant Material and Population Development

Eight winter wheat lines 'Event' (A), 'Format' (B), 'BAYP4535' (C), 'Potenzial' (D), 'Ambition' (E), 'Bussard' (F), 'Firl3565' (G), and 'Julius' (H) were selected as founders of an eight-way MAGIC population based on the following criteria: (i) variation for disease resistance, quality, and agronomic traits, (ii) derivation from diverse breeding programs, and (iii) importance within the respective quality group (**Table 1**). All founders originated from wheat breeders in Germany except for the variety 'Ambition', which emerged from the Nordic Seed (Denmark) breeding program. To create F_1 seed, one ear per plant was used in four two-way crosses (AB, CD, EF, and GH) (**Figure 1**). Out of each of the four two-way crosses, one randomly selected F_1 seed was raised and two ears per plant were further mated to four-way crosses (ABCD and EFGH). Out of 32 available four-way crosses, sixteen independent plants were selected and crossed, to obtain eight F_1 populations that involved four reciprocal cross combinations (ABCDEFGH and EFGHABCD). The four eight-way crosses were further hybridized with the four reciprocal eight-way crosses for establishing 16 eight-way intercross combinations (ABCDEFGH/EFGHABCD). The term 'MAGIC group 1–16', as used hereinafter, refers to these 16 subpopulations. The F_1 seeds of BMWpop were progressed to the F_6 generation via single seed descent followed by two generations of bulk propagation in the field. The crossing procedure started in June 2009, and was completed in December 2010 followed by 5 years it took to self the plants to $F_{6:8}$ recombinant inbred lines (RILs).

DNA Extraction and Genotyping

Ten individual primary leaves of each one of the 394 $F_{6:8}$ RILs and all eight founders were harvested, pooled and freeze-dried. Genomic DNA was extracted according to the procedure described by Plaschke et al. (1995). All lines including the parents repeated twice were genotyped using the 15K + 5K Infinium® iSelect® array containing 17267 single nucleotide polymorphism (SNP) markers provided as a service by the company TraitGenetics (Gatersleben, Germany). The array combines markers from the 90K iSelect array (Wang et al., 2014) and the 820K Axiom® array (Winfield et al., 2016). The population was further genotyped with a functional PCR marker for powdery mildew resistance allele *Pm3a* (Tommasini et al., 2006) since the parent 'BAYP4535' is known to carry that gene.

Marker Filtering

The filtering of the genotypic data was carried out with the synbreed package V0.12-6 (Wimmer et al., 2012) in R (R Core Team, 2017). First, all markers were excluded which were monomorphic for the population and for the founders. Further

TABLE 1 | Classification of founder lines of the eight-parent Bavarian MAGIC winter wheat population.

Founder line	Quality			Resistance			Breeder	Registration period
	Group[c]	GPC[d]	Yield[e]	PM[f]	LR[f]	STB[f]		
Event[a]	E	6	7/5	3	4	6	Saatzucht Josef Breun	2009–2015
Format[a]	A	8	6/6	5	5	4	Saatzucht Schweiger	2007–2013
BAYP4535[b]	C	n.d.	7/7	2	2	4	LfL	Not released
Potenzial[a]	A	5	7/7	2	4	5	Deutsche Saatveredelung	2006–present
Ambition[a,b]	C	4	6/7	2	5	4	Nordic Seed	2003–2012
Bussard[a]	E	8	2/3	4	7	6	KWS Lochow	1990–present
Firl3565[b]	A	4	6/7	4	5	4	Saatzucht Firlbeck	Not released
Julius[a]	B	4	8/8	3	3	3	KWS Lochow	2008–present

[a] *Based on the descriptive variety list of the Federal Plant Variety Office 2009 (www.bundessortenamt.de).*
[b] *Based on the assessment of the Bavarian Research Center for Agriculture (LfL).*
[c] *Quality group (bread-making): E (excellent), A (high), B (medium), and C (low/other use).*
[d] *Grain protein content: 1 (low) – 9 (high).*
[e] *Grain yield without growth regulator and fungicide treatment/at high production intensity: 1 (low) – 9 (high).*
[f] *PM (Powdery mildew), LR (Leaf rust), STB (Septoria tritici blotch); rating score: 1 (no disease) – 9 (severe disease).*
n.d., not determined.

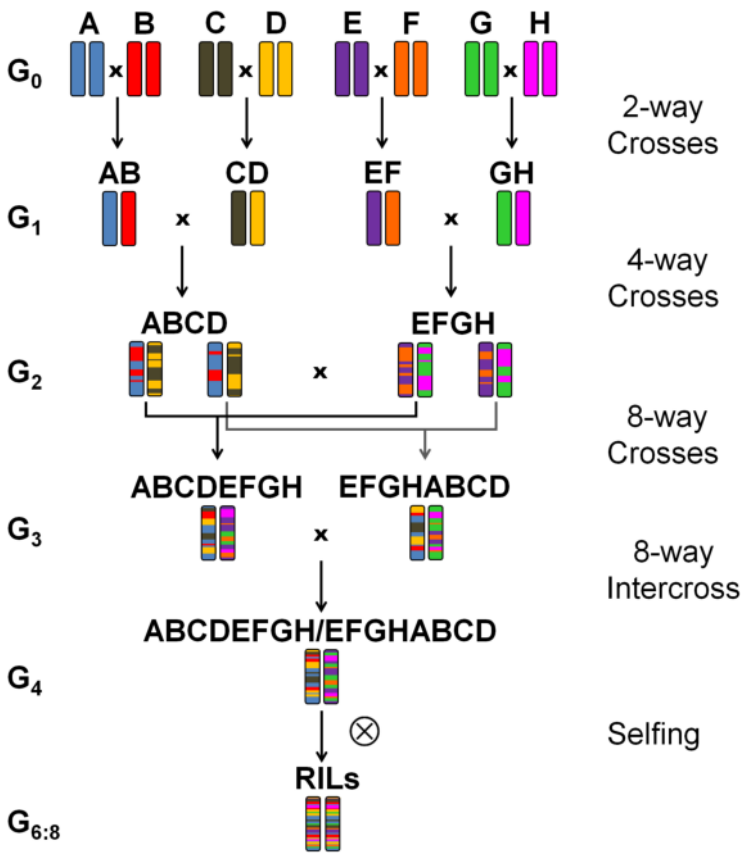

FIGURE 1 | Crossing scheme based on Cavanagh et al. (2008) of the eight-founder BMWpop. **(A)** 'Event', **(B)** 'Format', **(C)** 'BAYP4535', **(D)** 'Potenzial', **(E)** 'Ambition', **(F)** 'Bussard', **(G)** 'Firl3565', **(H)** 'Julius'.

markers were removed based on the following conditions: (i) missing data $\geq$ 5%, (ii) minor allele frequency $\leq$ 5%, (iii) duplicated segregation pattern (marker with the lowest number of missing data was kept), (iv) missing and heterozygous data in founders and (v) different allele calls between the double-genotyped founders. Markers exhibiting segregation distortion were left in the data set, as segregation distortion does not affect recombination fractions (Kjær et al., 1995).

Population Validation

The genotypic validation of BMWpop was based on a subset of 6717 markers (selection procedure see section '2.2 Marker Filtering'). The population structure was investigated with a principle coordinates analysis (PCoA) based on Roger's distance matrix in R/ape V5.0 (Paradis et al., 2004). The kinship matrix K was calculated with the R package Genomic Association and Prediction Integrated Tool (GAPIT Tool 3.0) (Lipka et al., 2012) using the method of VanRaden (2008). Furthermore, we examined the proportion of heterozygote allele calls i.e., the combination of the heterozygosity of each plant and the segregation of the allele within the ten bulked plants of the $F_{6:8}$ lines. The deviation of the observed segregation from the expected ratio of each marker was analyzed after setting all heterozygous data to missing. The multipoint probability of each locus that the observed genotype was inherited from one of the eight founders was calculated based on haplotype structure using the function 'mpprob' implemented in R/mpMap V2.0.2 (Huang and George, 2011). The threshold to determine the parental origin of an allele was set to 0.7. This threshold allowed us to compare the proportion of missing founder probabilities and the number of recombination events with other studies. The number of recombination events in the RILs of BMWpop was compared to the recombination events in the eight-founder MAGIC population NIAB 2015 (Gardner et al., 2016), the four-founder MAGIC design 9kMAGIC (Cavanagh et al., 2013), and the biparental backcross population L19 BC1 (Geyer et al., 2017). Information about the population size and type, the generation of the lines, and the genotyping platform used of the populations mentioned above is given in **Table 2**. Recombination events of RILs in all MAGIC populations were recognized by the change of the origin of parental alleles along the chromosome, whereas in the L19 BC1 lines the change of allele calls from heterozygote to homozygote along the chromosome and vice versa was assessed. Genome-wide recombination counts were available for 9kMAGIC (Huang et al., 2012), whereas for NIAB 2015 data were only published for chromosome 3B. The allelic diversity captured in BMWpop was compared to a panel of 524 common wheat breeding lines provided by six breeding companies (Geyer et al., 2016). This genetic library represents well the germplasm of the German wheat breeding pool and was genotyped with the Illumina® Infinium® 15 k SNP array representing a subset of markers of the 15K + 5K Infinium® iSelect® array.

Map Construction

The construction of the genetic map was based on the two R packages mpMap V2.0.2 (Huang and George, 2011) and mpMap2 V0.0.3[1,2]. Unless otherwise stated, the functions used were from the mpMap package. Heterozygous calls were set to missing. A recombination fraction (rf) matrix between all pairs of markers was calculated using the function 'estimateRF' in the package mpMap2 at default settings. The estimation of the rf matrix was based on identical by descent probabilities given in Broman (2005). Markers were grouped to 200 linkage groups using 'mpgroup' function. The linkage groups were assigned to chromosomes based on the information of published maps (Cavanagh et al., 2013; Wang et al., 2014; Marcotuli et al., 2017). Within linkage groups, markers were ordered in two steps using two-point ordering: First, an overall path order was constructed to minimize total map length using the 'mporder' function; second, fine ordering was performed based on the overall path order using the 'orderCross' function in mpMap2. All linkage groups belonging to the same chromosome were merged based on the consensus map of Cavanagh et al. (2013). Finally, the validity of the marker order over the whole chromosome was examined using the R/qtl ripple function implemented in the 'mporder' function. Genetic map distances were calculated using Haldane mapping function using 'computemap'.

[1]https://github.com/rohan-shah/mpMap2Paper

[2]https://github.com/rohan-shah/mpMap2

Map Validation

Chromosome length and number of markers and loci were compared to the wheat genetic maps of NIAB 2015, 9kMAGIC, and L19 BC1 populations. The congruency of marker order was assessed in relation to the three above-mentioned genetic maps and to the physical marker positions of IWGSC RefSeq v1.0 (International Wheat Genome Sequencing Consortium, 2018) employing a set of markers common between BMWpop and the respective other population.

The rf heatmaps (R/lattice V0.20-35; Sarkar, 2008) were used to visualize marker order. Linkage disequilibrium (LD) was estimated as the squared correlation coefficient between markers using R/genetics V1.3.8.1 (Warnes et al., 2013). The extent of LD decay was analyzed similar to Breseghello and Sorrells (2006): a population-specific r^2 value was determined at the 95th percentile of the square root transformed r^2 value distribution for unlinked markers. r^2 values above this threshold were expected to be caused by genetic linkage. A least square regression (loess) curve was fitted to the LD decay estimation using a smoothing span parameter of 0.10 (R/stats V3.4.3, R Core Team, 2017).

QTL Mapping

Two independent trials were conducted for powdery mildew (PM) seedling resistance in the glasshouse under controlled conditions with a mean relative humidity of 67%, a temperature of 18°C, and 16 h of light per day. For each experiment, the population and the eight founders were sown in multi pot plates in a randomized complete block design with two replicates each. After the primary leaf emerged up to a length of 5 cm, the plants were inoculated with a *B. graminis tritici* isolate mixture by evenly shaking conidia of heavily infected wheat seedlings above the trial. The isolate mixture consisted of two isolates with virulence to the resistance genes *Pm2*, *Pm4b*, *Pm5a*, *Pm6*, and *Pm8* (Mohler et al., 2013). Disease reaction was scored from 1 (no symptoms) to 9 (susceptible) 2 weeks after inoculation. The assessment was based on ten plants per genotype and replicate.

Phenotypic data were adjusted in R/lme4 V1.1-14 (Bates et al., 2014) based on the following model:

$$y_{ijk} = \mu + g_i + l_j + gl_{ij} + r_{kj} + e_{ijk} \quad (1)$$

TABLE 2 | Description of BMWpop and reference populations and linkage map summary statistics.

	BMWpop	NIAB 2015[a]	9kMAGIC[b]	L19 BC1[c]
Population type	**8-founder MAGIC**	**8-founder MAGIC**	**4-founder MAGIC**	**Biparental**
Generation	F6:8	F4:5	F6	BC1
Population size	394	643	1440	230
SNP array	20k	80k	9k	20k
Total marker number	**5436**	**18601**	**4300**	**2100**
Marker number A genome	2185	6832	2055	967
Marker number B genome	2603	9388	1944	906
Marker number D genome	648	2381	301	227
Min number/chromosome	35	80	14	9
Max number/chromosome	483	2327	451	231
Total chromosome length	**5230**	**5405**	**3522**	**2823**
Chromosome length A genome	2012	2009	1420	1283
Chromosome length B genome	2070	2108	1405	1109
Chromosome length D genome	1149	1287	697	579
Min chromosome length	87	126	44	30
Max chromosome length	390	386	300	219
Total loci number	**2804**	**4578**	**1813**	**1920**
Loci A genome	1126	1892	798	874
Loci B genome	1327	2160	878	838
Loci D genome	351	526	137	208
Min loci/chromosome	25	39	11	9
Max loci/chromosome	248	452	202	209
Mean recombination event/RIL	73	–[d]	37	53
Range recombination event/RIL	49–100	–[d]	1–80	23–126

[a] *Mackay et al., 2014; Gardner et al., 2016.*
[b] *Huang et al., 2012; Cavanagh et al., 2013.*
[c] *Geyer et al., 2017.*
[d] *No whole genome data available, only for chromosome 3B.*

where y_{ijk} is the trait observation, μ is the overall mean, g_i is the fixed effect of genotype i, l_j is the random effect of the trial j, gl_{ij} is the random interaction effect of genotype i with trial j, r_{kj} is the random effect of replication k nested within trial j, and e_{ijk} is the random residual error. To obtain variance components, the genotype was fitted as random. Heritability was estimated on a progeny mean basis according to Hallauer and Miranda (1981).

The QTL mapping was carried out using the mpMap package V2.0.2. Simple interval mapping was based on founder probabilities computed as mentioned above (2.4 Population validation). The function 'mpIM' was used for mapping. QTL were detected at a genome-wide significance threshold of $\alpha < 0.001$. The threshold was derived from an empirically null distribution with 1000 simulation runs similar to Churchill and Doerge (1994). All detected QTL of the base model were simultaneously fitted in a full model using the function 'fit'. From this model fit, only QTL were kept with a p-value < 0.05 and the full model was fitted again to obtain additive founder effects relative to Julius and the phenotypic variance explained (R^2) by individual QTL. The QTL support interval (S.I.) was defined as the map distance in cM surrounding a QTL peak at a -log10(p) drop of ± 1.0. The designation of QTL followed the recommended rules for gene symbolization in wheat (McIntosh et al., 2013).

Data and Material Availability

All raw genotypic data and the complete pedigree traceable to two-way crosses are publicly available at http://doi.org/10.14459/2018mp1435172. Seed of all 394 RILs of BMWpop and the eight founders are available for non-commercial use upon request from the Bavarian State Research Center for Agriculture (Freising, Germany).

RESULTS

Construction of the MAGIC Population

The crossing design of the MAGIC population was greatly simplified compared to the maximum number of possible crosses (Mackay et al., 2014); however, it involved an additional eight-way intercross step. Any developed line can be sourced to one of the 16 eight-way intercrosses (MAGIC group 1-16). The RILs built up MAGIC groups of 13 to 58 lines with an average size of 32 lines. Altogether 972 seeds, each representing a unique genotype, were generated during MAGIC crossing procedure. Five hundred sixteen lines were advanced to $F_{6:8}$ generation and a number of 394 lines were selected based on sufficient seed availability for field trials and suitability for experiments in the agricultural environment.

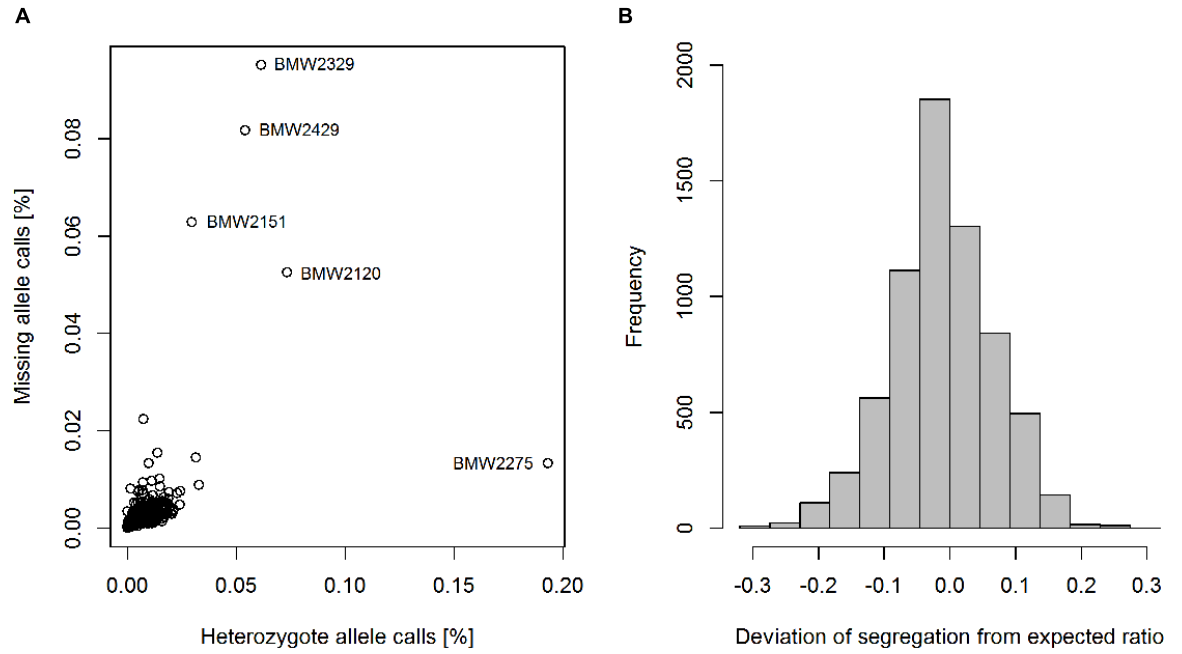

FIGURE 2 | Heterozygosity and proportion of missing marker data of RILs **(A)**, and the segregation ratio of major and minor allele per marker **(B)**.

Genotypic Data Analysis

Of the 17267 SNP markers available on the 15K + 5K Infinium® iSelect® array, 11426 markers (66.2%) were segregating in the population. After marker filtering 6738 SNPs (58.8%) remained. Since founder lines were genotyped twice, a genotyping error rate of 0.1% could be observed. Twenty-two markers were found to be polymorphic in the population but not in the founders. These markers were also excluded from the data set, and a total number of 6716 codominant SNP markers and one dominant PCR marker remained for further analysis. The percentage of missing marker data per line was in the range of 0.0–9.5%, with an overall mean of 0.3% (**Figure 2A**). The four lines 'BMW2329', 'BMW2429', 'BMW2151', and 'BMW2120' showed the highest proportion of missing allele calls (**Figure 2A**). The mean proportion of heterozygote allele calls of the bulk of ten plants per MAGIC RIL was 0.8%. RIL 'BMW2275' showed an unexpected high level of heterozygote allele calls of 19.3%, but also three of the four above-mentioned lines had higher proportions of heterozygote calls (**Figure 2A**). The deviation of the observed segregation from the expected ratio followed a normal distribution with a mean of -0.01 (**Figure 2B**). The range of the deviation was from -0.32 to 0.26. A total of 71.7% of markers segregating in a diversity panel described by Geyer et al. (2016) were also polymorphic in BMWpop.

Structure of the MAGIC Population

The first two principle coordinates of the PCoA accounted for 2.7 and 2.3% of the molecular variation, respectively (**Figure 3**). Individuals of MAGIC groups with the same paternal crossing partner in the 8-way × 8-way cross showed a weak clustering. The kinship showed that all lines were relatives and that there was no kinship structure present although lines built up some more related groups (**Supplementary Figure S1**). Thus, analyses revealed a mild population structure. Average congruency of the marker pattern between all lines was 62.8%. The range of the similarity of the marker pattern of two lines was from 52.2 to 97.6%. The genome-wide founder contributions in BMWpop were analyzed with haplotype probabilities using a threshold of 0.7. Based on the threshold setting, different proportions of founder probabilities per chromosome remained unknown (**Figure 4**). The average amount of missing founder contribution over the whole genome was 31.6%, ranging from 16.0% on chromosome 6B to 70.3% on chromosome 4D with average values of 26.0, 28.2, and 40.5% for the A, B, and D genomes, respectively. Generally, all eight parental genomes contributed to all chromosomes except for chromosome 4D. Based on an eight-founder crossing scheme as used in this study, each founder genome is expected to be represented by 12.5% in the population. In BMWpop, the average founder contribution varied from 7.0 to 9.6%. Generally, for the 18 chromosomes with higher explained contributions (**Figure 4**), the probability explained by the eight founders was quite equally distributed except for chromosome 2B. Here, the parent 'Firl3565' was underrepresented with 0.1%, whereas 'BAYP4535' was overrepresented with 17.8%.

Genetic Map Construction

In total, 5436 markers were assigned to the 21 wheat chromosomes. Summary statistics are shown in **Table 2**. The complete genetic map of BMWpop is presented in **Supplementary Table S1**. The majority of markers of 40.2 and 47.9% were mapped to the A and B genomes, respectively. Only 11.9% of markers were located on the D genome. The number

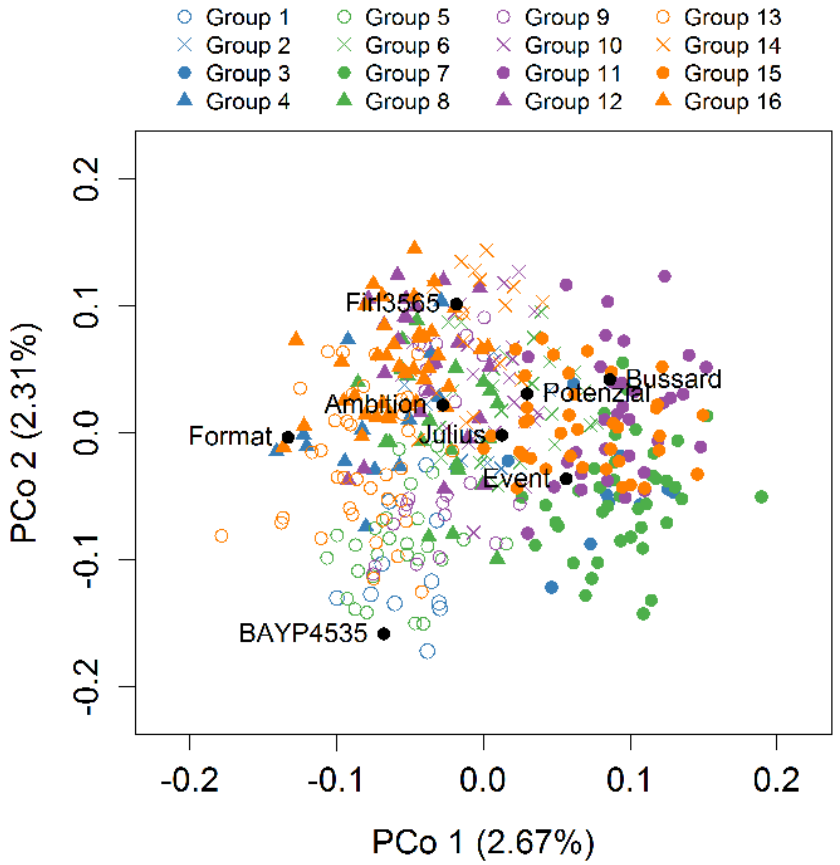

FIGURE 3 | Population structure based on 6717 markers. Genotypes belonging to one of the 16 MAGIC groups are distinguished by color and symbol. The color represents the female crossing partner and the symbol represents the male crossing partner in the 8-way × 8-way crossing step.

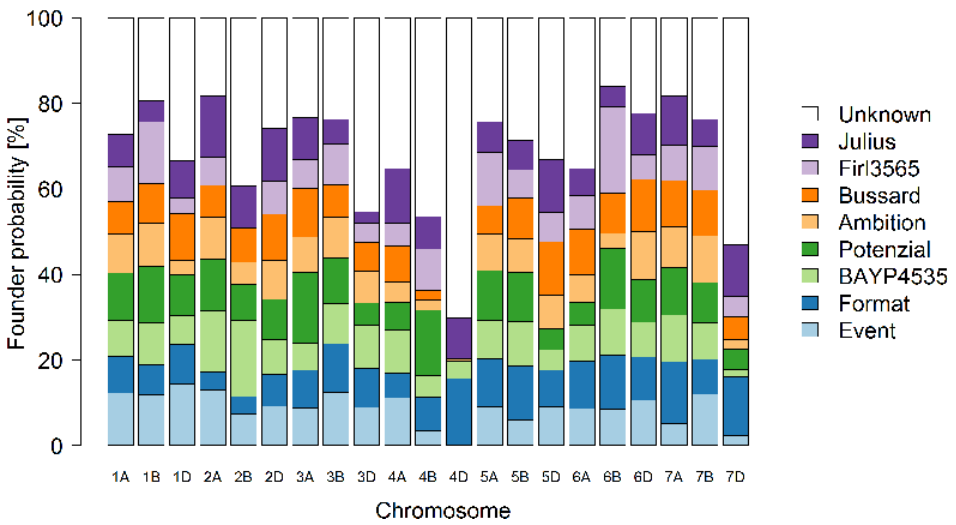

FIGURE 4 | Genome-wide founder representation in the 394 eight-parent MAGIC RILs.

of markers per chromosome varied between 35 on chromosome 4D and 483 on chromosome 5B. The total linkage map spanned 5230 cM. The A and B genomes contributed equally to the map length with 38.4 and 39.6%, respectively, whereas the D genome had only a share of 22.0%. The individual chromosome length ranged from 87.0 cM for chromosome 4D to 389.6 cM

for chromosome 7A. Average chromosome length was 287.4 cM, 295.7 cM, and 164.1 cM for the A, B, and D genomes, respectively. More than half of the mapped markers (2804) represented unique sites across the genome (A genome: 40.2%; B genome: 47.3%; D genome: 12.5%). The number of loci per chromosome was between 25 on chromosome 4D and 248 on chromosome 3B. The average locus distance on the A, B, and D genome was 1.8, 1.6, and 3.3 cM, respectively. A major gap of 53.9 cM was present in the pericentromeric region of chromosome 3A (**Supplementary Figure S2**, Chromosome 3A). In this region, no markers could be mapped because all markers associated with this region were monomorphic between the eight founder lines.

Map Comparisons

Table 2 summarizes the comparison of BMWpop linkage map to three other maps. The eight-founder MAGIC map NIAB 2015 included 3.4× higher number of markers, whereas the maps of the four-founder 9kMAGIC population and the biparental L19 BC1 progeny had 0.8 and 0.4 as many markers, respectively. However, when considering the number of loci, the difference between NIAB 2015 and BMWpop was reduced to 1.6×. The two other maps showed 0.6 (9kMAGIC) and 0.7 (L19 BC1) as many loci. Both eight-founder MAGIC maps showed a similar total map length. The 9kMAGIC and L19 BC1 maps were 0.3× and 0.5× shorter, respectively. With respect to the sub-genome level, a similar trend for all investigated parameters was observed (**Table 2**).

In general, the marker order compared to the other three genetic maps, especially NIAB 2015, and the IWGSC RefSeq v1.0, was similar (**Supplementary Figure S2**). In some instances, local marker order was inverted compared to NIAB 2015 (**Supplementary Figure S2**, Chromosome 2B, panel B). Comparison of the D genome to 9kMAGIC and L19 BC1 was challenging due to an overall low marker number which limited the number of common markers required for the analysis (**Supplementary Figure S2**, Chromosome 3D, panel C,D). The comparison with the physical map clearly indicated lower recombination rates in the centromeric region of all chromosomes (**Supplementary Figure S2**, Chromosome 2A, panel A) except for chromosomes 3B, 5B, and 6B. In the three MAGIC populations, a similar coverage of marker loci was observed near the centromere (**Supplementary Figure S2**, Chromosome 2A, panel B,C), compared to a strong reduction in L19 BC1 (**Supplementary Figure S2**, Chromosome 2A, panel D). Further examination of marker order had the following outcomes: First, chromosome 6B showed low recombination rates in the region between 74.4 cM and 103.0 cM. This corresponds to approximately half of the length of the comparable region in NIAB 2015 that ranged from 101.1 cM to 167.8 cM (**Supplementary Figure S2**, Chromosome 6B, panel B). Second, there was an inversion on the long arm of chromosome 5D compared to NIAB 2015 (**Supplementary Figure S2**, Chromosome 5D, panel B), but not compared to the physical position and the consensus map of Wang et al. (2014) (**Supplementary Figure S3**). The average number of recombination events per RIL of BMWpop was 73.0, with values ranging from 49 to 100 (**Table 2**). There were 2x as many recombination events per line compared to four-founder MAGIC genotypes but just 1.4× as many compared to L19 BC1. For all populations except for the biparental one, average experimental recombination events lagged far behind simulated ones based on a wheat consensus map (Somers et al., 2004) with a total length of ∼2500 cM (Huang et al., 2012). BMWpop, 9kMAGIC, and L19 BC1 showed 71.6, 48.1, and 103.9% of the simulated average recombination number, respectively.

Linkage Map Validation

The overall heatmap of the recombination fraction matrix (**Supplementary Figure S4**) showed a clear diagonal. The analysis of individual chromosomes reflected the signatures for correctly mapped A, B, and D genomes (**Supplementary Figure S5**; Gardner et al., 2016). The A and B genome chromosomes showed a distinct diagonal with small-sized tightly linked blocks (**Supplementary Figure S5**, Chromosome 5, panel A). In some cases, the markers around the centromeric region were all closely linked leading to bigger-sized blocks (**Supplementary Figure S5**, Chromosome 7, panel A). An extreme case of this was seen for chromosome 6B (**Supplementary Figure S5**, Chromosome 6, panel B). This result confirmed the already described truncated map length around the centromeric region of this chromosome (see "Map Comparison"). The rf heatmaps of the D genome chromosomes (**Supplementary Figure S5**, Chromosome 7, panel C) showed a limited number of blocks.

Plots of LD showed a clear pattern of intra-chromosomal LD decay in BMWpop for the genome and for the individual chromosomes (**Supplementary Figures S6, S7**). The mean LD for the genome decreased to $r^2 < 0.2$ within 9.3 cM. Individual chromosome LD decay to $r^2 < 0.2$ ranged from 3.5 cM (chromosome 6D) to 18.5 cM (chromosome 7D). To consider LD between loci due to genetic linkage the r^2 critical population-specific threshold was 0.017. Thus for the genome, markers were assumed to be genetically linked within a distance of 68.6 cM.

Powdery Mildew QTL

The repeatability of PM trials was 81.3 and 81.9% with a correlation between the trials of 0.8 (**Supplementary Table S2**). The residuals of the adjusted means followed a normal distribution (**Supplementary Figure S8A**), a prerequisite for appropriate QTL mapping. The progeny mean was not significantly different ($p < 0.05$) from the parental mean (**Supplementary Table S2**). The adjusted means (**Supplementary Table S3**) did not follow a normal distribution but rather showed a bimodal distribution (**Supplementary Figure S8B**). The heritability estimate was high with 93.0% (**Supplementary Table S2**). Five QTL were detected in simple interval mapping explaining 72.5% of the total phenotypic variance (**Table 3**). The individual R^2 values ranged from 4.5 to 34.1%. The support interval for all QTL was between 0 and 9 cM. The strongest QTL *QPm.lfl-1A* explained 34.1% of the phenotypic variance and coincided with the functional marker for the *Pm3a* gene. The resistance allele was inherited from 'BAYP4535', which is the only founder carrying this gene, and reduced disease severity by 3.6 grades on a scale of 1–9. The QTL on chromosomes 6B and 7A had also high -log(p) values and accounted for 17.4 and

TABLE 3 | QTL for seedling resistance to powdery mildew (PM) in BMWpop.

Trait	QTL	Chr.	Pos. (cM)	S.I. (cM)	*P*-value	R^{2*}	Eff(A)	Eff(B)	Eff(C)	Eff(D)	Eff(E)	Eff(F)	Eff(G)
PM [1–9]						**72.5**							
	QPm.lfl-1A	1A	3	3–3	0.0E+00	34.1	0.1	−3.6	0.1	0.3	0.3	0.5	0.8
	QPm.lfl-1B	1B	142	138–146	4.1E-05	4.5	−1.5	−1.8	−1.4	−1.2	−2.4	−1.2	−1.8
	QPm.lfl-4A	4A	162	160–169	1.2E-08	6.6	−0.1	−1.2	−0.6	0.5	0.0	−0.9	0.1
	QPm.lfl-6B	6B	177	177–177	0.0E+00	17.4	−3.2	0.5	0.0	0.1	0.2	0.3	0.2
	QPm.lfl-7A	7A	379	375–380	0.0E+00	18.3	−0.3	0.2	−2.8	0.0	0.1	−0.1	−0.3

Chromosome (Chr.), position (Pos.), support interval (S.I.), p-value, proportion of phenotypic variance explained (R^2), and additive effects (Eff) of the founders Event (A), BAYP4535 (B), Ambition (C), Firl3565 (D), Format (E), Potenzial (F), and Bussard (G) relative to Julius are presented.

**The explained phenotypic variance of the model fitting all detected QTL simultaneously is presented in bold above the individual R^2 values for each QTL.*

18.3%, respectively, of the variation for PM. The alleles reducing disease severity at *QPm.lfl-6B* and *QPm.lfl-7A* were contributed by 'Event' and 'Ambition', respectively. The QTL *QPm.lfl-1B* explained 4.5% of the phenotypic variance with all founder effects being negative relative to the parent Julius, whereas four parental lines decreased disease severity for *QPm.lfl-4A*.

DISCUSSION

A full eight-founder MAGIC crossing design is built up of 28 two-way crosses, 210 four-way crosses, and 315 eight-way crosses (Mackay et al., 2014). Starting with just four two-way crosses, 32 four-way crosses and eight eight-way crosses our mating design was greatly reduced but it involved sixteen additional eight-way intercrosses to compensate for the low number of overall crosses. We evaluated possible effects of this crossing design on population structure, number of recombination events, genetic map construction, founder probabilities, and QTL mapping.

Our greatly simplified MAGIC design and the small population size of 394 RILs did not cause a considerable structure in the population as indicated by population structure and kinship analyses (**Figure 1** and **Supplementary Figure S1**). This notwithstanding, we observed a negligible impact of the male eight-way intercrossing partner. Possible biased maternal effects (Donohue, 2009; Roach and Wulff, 1987) cannot be ruled out as in our simplified crossing design the parent Event was the ultimate female parent of all 394 RILs. Another parameter that could have been affected is the number of recombination events. Based on a simulation model, the number of recombination events per RIL in a population is expected to increase with the number of founders and the number of crosses involved (Huang et al., 2012; Ladejobi et al., 2016). The average number of 73 recombination events per line in BMWpop compared to 37 in a four-founder MAGIC population (**Table 2**) supported the assumption of the simulation model. Despite this, the experimentally derived number of recombination events lagged for both MAGIC populations behind the simulated ones, possibly due to partially informative SNPs and missing founder assignments. This drawback of MAGIC designs was already described in other studies that used mating designs with a higher number of crosses (Huang et al., 2012; Sannemann et al., 2015; Gardner et al., 2016). A similar number of 1.6 and 1.8 recombination events per line per Morgan was detected on chromosome 3B for NIAB 2015 (Gardner et al., 2016) and BMWpop, respectively. Despite this observation, which is limited to a single chromosome, it could be still possible that in a simplified MAGIC mating design a lower number of unique recombinations is available. A simplified MAGIC design could also have led to lower accuracy in estimation of the rf matrix, which in turn would have adversely affected genetic map construction. Nevertheless, of 6717 markers passing quality control, 5436 markers were mapped to the 21 wheat chromosomes. The rf heatmaps (**Supplementary Figures S4, S5**), and the agreement of BMWpop map to other genetic maps and the IWGSC RefSeq v1.0 (**Supplementary Figure S2**) supported the appropriateness of marker ordering. Of the 1281 unmapped markers, the largest share of 49.3 and 36.0% was rejected due to too many missing values (>20%) in the rf matrix and marker ordering, respectively. The trivialization of both criteria resulted in incorrect marker order and artificially increased map length. Therefore, to ensure accurate mapping in BMWpop, strict quality control of the rf matrix and extensive manual curation during the mapping process was carried out. Similar conclusions were reported by Gardner et al. (2016) who used an almost fully realized mating design for MAGIC population creation. A valid genetic map and a sufficient number of recombinations are prerequisites for the determination of the parental origin of an allele. Increasing the number of crosses and progenies in a MAGIC population would increase the possible number of recombination events and could reduce the amount of missing founder assignments. However, the genome-wide proportion of missing haplotype data of our greatly reduced mating design compared to the mating design of NIAB 2015 with 643 RILs was similar with 17.3 and 18.6%, respectively. Therefore, it appears that a higher number of crosses will not enhance the proportion of alleles assigned to parental origin. Since founder assignments are based on haplotypes, increasing the number of unique founder haplotypes would considerably improve founder assignment. This aim may be achieved for example by using a higher number of SNP markers, including multiallelic marker systems, or new approaches to construct the haplotypes (Gabriel et al., 2002; Pook et al., 2018). Additionally, to keep the error rate low the threshold to determine the parental origin of an allele needs to be set in the upper range strengthening missing founder assignments. Beside technical issues, there could be also genetic reasons for missing founder probabilities such as

a narrow genetic distance of the founder lines. Simulation studies showed that for randomly selected founders in an eight-founder MAGIC population 73.7% of the loci were polymorphic (Ladejobi et al., 2016). This proportion could be increased to 91.6% if the founders were selected based on a maximized number of segregating alleles. The captured allelic diversity of 71.7% in BMWpop indicated that our founders were selected randomly in terms of allelic diversity and a higher degree of polymorphism may have been possible by choosing other parents. The monomorphic region on chromosome 3A of BMWpop supported this finding as lines being polymorphic in this region are available in a German wheat breeding panel (Geyer et al., 2016; data not shown). Finally, the above-mentioned limitations could have touched the dissection of the genetic architecture of seedling resistance to powdery mildew. However, limitations of QTL analysis could not be observed in this study. Three major and two minor QTL with a total explained phenotypic variance of 72.5% were identified (**Table 3**). Additionally, the small support intervals of 0–9 cM obtained provided further evidence for appropriate QTL mapping. The successful genetic analysis of a complex trait demonstrated that our genetic material employed is useful for further gene mapping studies. As MAGIC designs combine the genetic material of several founders, it is possible to investigate multiple traits simultaneously which is usually limited in biparental populations particularly when adapted germplasm is used. Our future work will show whether the genetic analysis of a broad range of traits reveal, from a breeder's perspective, desirable or undesirable genetic relationships which are expected to be described with great accuracy and reliability as suggested by our QTL analysis.

CONCLUSION

It appears that a greatly reduced MAGIC mating design including an additional eight-way intercross step is equivalent to an almost full design. This refers to the total number of recombination events, the ability to construct an appropriate genetic map, and the proportion of missing founder assignments. Furthermore, we could show that QTL mapping for seedling resistance to powdery mildew was successful in the background of this simplified eight-founder MAGIC design. These findings are of great importance for researchers and scientists working on multiparental populations as the effort of developing such a population can be significantly reduced. The eight-founder BMWpop and its genetic linkage map is a valuable genetic resource that could allow scientists and breeders to carry out genetic studies for a wide range of breeder-relevant parameters in a single genetic background.

AUTHOR CONTRIBUTIONS

VM and LH conceived the study. MS conducted the experiments and analyzed the data. VM supervised the research. MS and VM drafted the manuscript. All authors read, edited, and approved the final manuscript.

FUNDING

This study was part of the ERA-CAPS project 'An effector- and genomics-assisted pipeline for necrotrophic pathogen resistance breeding in wheat (EfectaWheat)' funded by the German Research Foundation (DFG; Project No. 263641700).

ACKNOWLEDGMENTS

We deeply thank Sabine Schmidt and the working group Wheat and Oat Breeding of the Bavarian State Research Center for Agriculture for their excellent and accurate technical effort during MAGIC population construction. The authors also gratefully thank Petra Greim of the Bavarian State Research Center for Agriculture for her excellent assistance in the lab. We express deep gratitude to Chris-Carolin Schön and the staff of Plant Breeding, Technical University of Munich (TUM) for the outstanding opportunity of using computing power and office space. We thank Rohan Shah for helpful advice for the use of 'mpMap2' package. We thank the International Wheat Genome Sequencing Consortium (http://www.wheatgenome.org/) for allowing access to the IWGSC RefSeq v1.0 and we gratefully acknowledge Martin Ganal and Jörg Plieske of TraitGenetics for providing unpublished assignments of 15K + 5K Infinium® iSelect® array markers to physical positions based on the IWGSC RefSeq v1.0. The authors thank Beatrice Corsi, Keith Gardner, and James Cockram for the QTL mapping course on multiparental populations at NIAB. We thank the EfectaWheat Consortium for giving us all the time needed to carry out this study.

SUPPLEMENTARY MATERIAL

The Supplementary Material for this article can be found online at: https://www.frontiersin.org/articles/10.3389/fpls.2018.01825/full#supplementary-material

REFERENCES

Asimit, J., and Zeggini, E. (2010). Rare variant association analysis methods for complex traits. *Annu. Rev. Genet.* 44, 293–308. doi: 10.1146/annurev-genet-102209-163421

Bandillo, N., Raghavan, C., Muyco, P., Sevilla, M. A. L., Lobina, I. T., Dilla-Ermita, C., et al. (2013). Multi-parent advanced generation inter-cross (magic) populations in rice: progress and potential for genetics research and breeding. *Rice* 6:11. doi: 10.1186/1939-8433-6-11

Bates, D., Mächler, M., Bolker, B., and Walker, S. (2014). *Fitting Linear Mixed-Effects Models Using Lme4*. Available at: http://arxiv.org/abs/1406.5823

Breseghello, F., and Sorrells, M. E. (2006). Association mapping of kernel size and milling quality in wheat (*Triticum aestivum L.*) cultivars. *Genetics* 172, 1165–1177. doi: 10.1534/genetics.105.044586

Broman, K. W. (2005). The genomes of recombinant inbred lines. *Genetics* 169, 1133–1146. doi: 10.1534/genetics.104.035212

Caldwell, K. S., Russell, J., Langridge, P., and Powell, W. (2006). Extreme population-dependent linkage disequilibrium detected in an inbreeding plant species, Hordeum vulgare. *Genetics* 172, 557–567. doi: 10.1534/genetics.104.038489

Cavanagh, C., Morell, M., Mackay, I., and Powell, W. (2008). From mutations to magic: resources for gene discovery, validation and delivery in crop plants. *Curr. Opin. Plant Biol.* 11, 215–221. doi: 10.1016/j.pbi.2008.01.002

Cavanagh, C. R., Chao, S., Wang, S., Huang, B. E., Stephen, S., Kiani, S., et al. (2013). Genome-wide comparative diversity uncovers multiple targets of selection for improvement in hexaploid wheat landraces and cultivars. *Proc. Natl. Acad. Sci. U. S. A.* 110, 8057–8062. doi: 10.1073/pnas.1217133110

Chen, H., Xie, W., He, H., Yu, H., Chen, W., Li, J., et al. (2014). A high-density snp genotyping array for rice biology and molecular breeding. *Mol. Plant* 7, 541–553. doi: 10.1093/mp/sst135

Churchill, G. A., and Doerge, R. W. (1994). Empirical threshold values for quantitative trait mapping. *Genetics* 138, 963–971.

R Core Team, (2017). *R: A language and environment for statistical computing. R Foundation for Statistical Computing, Vienna, Austria*. Available at: https://www.R-project.org/

Cui, F., Zhang, N., Fan, X., Zhang, W., Zhao, C., Yang, L., et al. (2017). Utilization of a Wheat660K SNP array-derived high-density genetic map for high-resolution mapping of a major QTL for kernel number. *Sci. Rep.* 7:3788. doi: 10.1038/s41598-017-04028-6

Dell'Acqua, M., Gatti, D. M., Pea, G., Cattonaro, F., Coppens, F., Magris, G., et al. (2015). Genetic properties of the magic maize population: a new platform for high definition QTL mapping in Zea mays. *Genome Biol.* 16:167. doi: 10.1186/s13059-015-0716-z

Dickson, S. P., Wang, K., Krantz, I., Hakonarson, H., and Goldstein, D. B. (2010). Rare variants create synthetic genome-wide associations. *PLoS Biol.* 8:e1000294. doi: 10.1371/journal.pbio.1000294

Donohue, K. (2009). Completing the cycle: maternal effects as the missing link in plant life histories. *Philos. Trans. R. Soc. Lond. B. Biol. Sci.* 364, 1059–1074. doi: 10.1098/rstb.2008.0291

Ewens, W. J., and Spielman, R. S. (2001). Locating genes by linkage and association. *Theor. Popul. Biol.* 60, 135–139. doi: 10.1006/TPBI.2001.1547

Flint-Garcia, S. A., Thornsberry, J. M., and Buckler, E. S. (2003). Structure of linkage disequilibrium in plants. *Annu. Rev. Plant Biol.* 54, 357–374. doi: 10.1146/annurev.arplant.54.031902.134907

Fradgley, N., Bentley, A. R., Gardner, K. A., Howell, P. J., Mackay, I., Scott, M., et al. (2017). Development and QTL mapping in a 16 founder wheat magic population. *Cereal Res. Commun.* 45, 13–14. doi: 10.1556/0806.45.2017.100

Gabriel, S. B., Schaffner, S. F., Nguyen, H., Moore, J. M., Roy, J., Blumenstiel, B., et al. (2002). The structure of haplotype blocks in the human genome. *Science* 296, 2225–2229. doi: 10.1126/science.1069424

Gardner, K. A., Wittern, L. M., and Mackay, I. J. (2016). A highly recombined, high-density, eight-founder wheat magic map reveals extensive segregation distortion and genomic locations of introgression segments. *Plant Biotechnol. J.* 14, 1406–1417. doi: 10.1111/pbi.12504

Geyer, M., Albrecht, T., Hartl, L., and Mohler, V. (2017). Exploring the genetics of fertility restoration controlled by Rf1 in common wheat (*Triticum aestivum L.*) using high-density linkage maps. *Mol. Genet. Genom.* 293, 451–462. doi: 10.1007/s00438-017-1396-z

Geyer, M., Bund, A., Albrecht, T., Hartl, L., and Mohler, V. (2016). Distribution of the fertility-restoring gene Rf3 in common and spelt wheat determined by an informative SNP marker. *Mol. Breed.* 36:167. doi: 10.1007/s11032-016-0592-6

Gibson, G. (2012). Rare and common variants: twenty arguments. *Nat. Rev. Genet.* 13, 135–145. doi: 10.1038/nrg3118

Hallauer, A., and Miranda, J. (1981). *Quantitative Genetics in Maize Breeding*. Ames, IA: Iowa State University Press.

He, J., Zhao, X., Laroche, A., Lu, Z.-X., Liu, H., and Li, Z. (2014). Genotyping-by-sequencing (GBS), an ultimate marker-assisted selection (MAS) tool to accelerate plant breeding. *Front. Plant Sci.* 5:484. doi: 10.3389/fpls.2014.00484

Huang, B. E., and George, A. W. (2011). R/mpmap: a computational platform for the genetic analysis of multiparent recombinant inbred lines. *Bioinformatics* 27, 727–729. doi: 10.1093/bioinformatics/btq719

Huang, B. E., George, A. W., Forrest, K. L., Kilian, A., Hayden, M. J., Morell, M. K., et al. (2012). A multiparent advanced generation inter-cross population for genetic analysis in wheat. *Plant Biotechnol. J.* 10, 826–839. doi: 10.1111/j.1467-7652.2012.00702.x

International Wheat Genome Sequencing Consortium (2018). Shifting the limits in wheat research and breeding using a fully annotated reference genome. *Science* 361:eaar7191. doi: 10.1126/science.aar7191

Kjær, B., Jensen, J., and Giese, H. (1995). Quantitative trait loci for heading date and straw characters in barley. *Genome* 38, 1098–1104. doi: 10.1139/g95-146

Korte, A., and Farlow, A. (2013). The advantages and limitations of trait analysis with GWAS: a review. *Plant Methods* 9:29. doi: 10.1186/1746-4811-9-29

Ladejobi, O., Elderfield, J., Gardner, K. A., Gaynor, R. C., Hickey, J., Hibberd, J. M., et al. (2016). Maximizing the potential of multi-parental crop populations. *Appl. Transl. Genom.* 11, 9–17. doi: 10.1016/J.ATG.2016.10.002

Lipka, A. E., Tian, F., Wang, Q., Peiffer, J., Li, M., Bradbury, P. J., et al. (2012). GAPIT: genome association and prediction integrated tool. *Bioinformatics* 28, 2397–2399. doi: 10.1093/bioinformatics/bts444

Mackay, I., and Powell, W. (2007). Methods for linkage disequilibrium mapping in crops. *Trends Plant Sci.* 12, 57–63. doi: 10.1016/J.TPLANTS.2006.12.001

Mackay, I. J., Bansept-Basler, P., Barber, T., Bentley, A. R., Cockram, J., Gosman, N., et al. (2014). An eight-parent multiparent advanced generation inter-cross population for winter-sown wheat: creation, properties, and validation. *G3* 4, 1603–1610. doi: 10.1534/g3.114.012963

Mammadov, J., Aggarwal, R., Buyyarapu, R., and Kumpatla, S. (2012). SNP markers and their impact on plant breeding. *Int. J. Plant Genom.* 2012, 1–11. doi: 10.1155/2012/728398

Marcotuli, I., Gadaleta, A., Mangini, G., Signorile, A., Zacheo, S., Blanco, A., et al. (2017). Development of a high-density SNP-based linkage map and detection of QTL for β-glucans, protein content, grain yield per spike and heading time in durum wheat. *Int. J. Mol. Sci.* 18:1329. doi: 10.3390/ijms18061329

McIntosh, R. A., Yamazaki, Y., Dubcovsky, J., Rogers, J., Morris, C., Appels, R., et al. (2013). *Catalogue of Gene Symbols for Wheat. 12th International Wheat Genetic Symposium*. Minato: Yokohama.

Mohler, V., Bauer, C., Schweizer, G., Kempf, H., and Hartl, L. (2013). Pm50: a new powdery mildew resistance gene in common wheat derived from cultivated emmer. *J. Appl. Genet.* 54, 259–263. doi: 10.1007/s13353-013-0158-9

Ongom, P. O., and Ejeta, G. (2018). Mating design and genetic structure of a multi-parent advanced generation intercross magic population of sorghum (Sorghum bicolor (L.) Moench. *G3* 8, 331–341. doi: 10.1534/g3.117.300248

Paradis, E., Claude, J., and Strimmer, K. (2004). APE: analyses of phylogenetics and evolution in R language. *Bioinformatics* 20, 289–290. doi: 10.1093/bioinformatics/btg412

Pascual, L., Albert, E., Sauvage, C., Duangjit, J., Bouchet, J. P., Bitton, F., et al. (2016). Dissecting quantitative trait variation in the resequencing era: complementarity of bi-parental, multi-parental and association panels. *Plant Sci.* 242, 120–130. doi: 10.1016/J.PLANTSCI.2015.06.017

Pascual, L., Desplat, N., Huang, B. E., Desgroux, A., Bruguier, L., Bouchet, J. P., et al. (2015). Potential of a tomato magic population to decipher the genetic control of quantitative traits and detect causal variants in the resequencing era. *Plant Biotechnol. J.* 13, 565–577. doi: 10.1111/pbi.12282

Plaschke, J., Ganal, M. W., and Röder, M. S. (1995). Detection of genetic diversity in closely related bread wheat using microsatellite markers. *Theor. Appl. Genet.* 91, 1001–1007. doi: 10.1007/BF00223912

Pook, T., Schlather, M., de los Campos, G., Schoen, C. C., and Simianer, H. (2018). Haplo blocker: creation of subgroup specific haplotype blocks and libraries. *bioRxiv* [Preprint]. doi: 10.1101/339788

Rakshit, S., Rakshit, A., and Patil, J. V. (2012). Multiparent intercross populations in analysis of quantitative traits. *J. Genet.* 91, 111–117. doi: 10.1007/s12041-012-0144-8

Roach, D. A., and Wulff, R. D. (1987). Maternal Effects in Plants. *Annu. Rev. Ecol. Syst.* 18, 209–235. doi: 10.1146/annurev.es.18.110187.001233

Sallam, A., and Martsch, R. (2015). Association mapping for frost tolerance using multi-parent advanced generation inter-cross (magic) population in faba bean (*Vicia faba L.*). *Genetica* 143, 501–514. doi: 10.1007/s10709-015-9848-z

Sannemann, W., Huang, B. E., Mathew, B., and Léon, J. (2015). Multi-parent advanced generation inter-cross in barley: high-resolution quantitative trait locus mapping for flowering time as a proof of concept. *Mol. Breed.* 35:86. doi: 10.1007/s11032-015-0284-7

Sannemann, W., Lisker, A., Maurer, A., Léon, J., Kazman, E., Cöster, H., et al. (2018). Adaptive selection of founder segments and epistatic control of plant height in the MAGIC winter wheat population WM-800. *BMC Genomics* 19:559. doi: 10.1186/s12864-018-4915-3

Sarkar, D. (2008). *Lattice: Multivariate Data Visualization with R*. New York, NY: Springer. doi: 10.1007/978-0-387-75969-2

Somers, D. J., Isaac, P., and Edwards, K. (2004). A high-density microsatellite consensus map for bread wheat (*Triticum aestivum L.*). *Theor. Appl. Genet.* 109, 1105–1114. doi: 10.1007/s00122-004-1740-7

Tommasini, L., Yahiaoui, N., Srichumpa, P., and Keller, B. (2006). Development of functional markers specific for seven Pm3 resistance alleles and their validation in the bread wheat gene pool. *Theor. Appl. Genet.* 114, 165–175. doi: 10.1007/s00122-006-0420-1

Unterseer, S., Bauer, E., Haberer, G., Seidel, M., Knaak, C., Ouzunova, M., et al. (2014). A powerful tool for genome analysis in maize: development and evaluation of the high density 600 k SNP genotyping array. *BMC Genomics* 15:823. doi: 10.1186/1471-2164-15-823

VanRaden, P. M. (2008). Efficient methods to compute genomic predictions. *J. Dairy Sci.* 91, 4414–4423. doi: 10.3168/JDS.2007-0980

Vilhjálmsson, B. J., and Nordborg, M. (2013). The nature of confounding in genome-wide association studies. *Nat. Rev. Genet.* 14, 1–2. doi: 10.1038/nrg3382

Wang, S., Wong, D., Forrest, K., Allen, A., Chao, S., Huang, B. E., et al. (2014). Characterization of polyploid wheat genomic diversity using a high-density 90 000 single nucleotide polymorphism array. *Plant Biotechnol. J.* 12, 787–796. doi: 10.1111/pbi.12183

Warnes, G., with contributions from Gorjanc, G., Leisch, F., and Man, M. (2013). *Genetics: Population Genetics. R Package Version 1.3.8.1*. Available at: https://cran.r-project.org/package=genetics

Wimmer, V., Albrecht, T., Auinger, H.-J., and Schön, C.-C. (2012). Synbreed: a framework for the analysis of genomic prediction data using R. *Bioinformatics* 28, 2086–2087. doi: 10.1093/bioinformatics/bts335

Winfield, M. O., Allen, A. M., Burridge, A. J., Barker, G. L. A., Benbow, H. R., Wilkinson, P. A., et al. (2016). High-density SNP genotyping array for hexaploid wheat and its secondary and tertiary gene pool. *Plant Biotechnol. J.* 14, 1195–1206. doi: 10.1111/pbi.12485

Zhu, C., Gore, M., Buckler, E. S., and Yu, J. (2008). Status and prospects of association mapping in plants. *Plant Genome J.* 1:5. doi: 10.3835/plantgenome2008.02.0089

Conflict of Interest Statement: The authors declare that the research was conducted in the absence of any commercial or financial relationships that could be construed as a potential conflict of interest.

G3 Genes | Genomes | Genetics

MULTIPARENTAL POPULATIONS

Genetic Dissection of Resistance to the Three Fungal Plant Pathogens *Blumeria graminis*, *Zymoseptoria tritici*, and *Pyrenophora tritici-repentis* Using a Multiparental Winter Wheat Population

Melanie Stadlmeier,[*,†,1,4] Lise Nistrup Jørgensen,[‡,2] Beatrice Corsi,[§,3] James Cockram,[§,3] Lorenz Hartl,[*,1] and Volker Mohler[*,†,1]

*Bavarian State Research Center for Agriculture, Institute for Crop Science and Plant Breeding, Freising 85354, Germany, †Technical University of Munich, TUM School of Life Sciences Weihenstephan, Freising 85354, Germany, ‡Aarhus University, Department of Agroecology, Slagelse 4200, Denmark, and §John Bingham Laboratory, NIAB, Huntingdon Road, Cambridge CB3 0LE, United Kingdom

ABSTRACT Bread wheat (*Triticum aestivum* L.) is one of the world's most important crop species. The development of new varieties resistant to multiple pathogens is an ongoing task in wheat breeding, especially in times of increasing demand for sustainable agricultural practices. Despite this, little is known about the relations between various fungal disease resistances at the genetic level, and the possible consequences for wheat breeding strategies. As a first step to fill this gap, we analyzed the genetic relations of resistance to the three fungal diseases – powdery mildew (PM), septoria tritici blotch (STB), and tan spot (TS) – using a winter wheat multiparent advanced generation intercross population. Six, seven, and nine QTL for resistance to PM, STB, and TS, respectively, were genetically mapped. Additionally, 15 QTL were identified for the three agro-morphological traits plant height, ear emergence time, and leaf angle distribution. Our results suggest that resistance to STB and TS on chromosome 2B is conferred by the same genetic region. Furthermore, we identified two genetic regions on chromosome 1AS and 7AL, which are associated with all three diseases, but not always in a synchronal manner. Based on our results, we conclude that parallel marker-assisted breeding for resistance to the fungal diseases PM, STB, and TS appears feasible. Knowledge of the genetic co-localization of alleles with contrasting effects for different diseases, such as on chromosome 7AL, allows the trade-offs of selection of these regions to be better understood, and ultimately determined at the genic level.

KEYWORDS
QTL analysis
MAGIC
Powdery mildew
Septoria tritici blotch
Tan spot
Multiparent Advanced Generation Inter-Cross (MAGIC)
multiparental populations
MPP

Common wheat (*Triticum aestivum* L.) is the most important food crop in the European Union with a total share of near half of cereal production (Eurostat 2017). Wheat grain yields can be extremely negatively influenced by abiotic factors like nutrient availability (van der Bom *et al.* 2017) and extreme weather events such as drought, heat, and heavy rainfall (Trnka *et al.* 2014). In addition, biotic constraints like plant pathogens, insects, and weeds can lead to severe yield losses despite the use of fungicides, insecticides, and herbicides (Singh *et al.* 2016; Deutsch *et al.* 2018). Therefore, and especially in times of an increasing demand for sustainable agriculture (European Parliament 2009, Altieri 2018), the development of improved wheat cultivars must address resistance to diseases in addition to primary breeding targets such as grain yield and quality. In Germany, new winter wheat cultivars need to pass a three-year evaluation, including assessment of disease resistance, before achieving registration as a new marketable variety. Among other fungal pathogens, wheat susceptibility to *Blumeria graminis* (the causal agent of powdery mildew, PM), *Zymoseptoria tritici* (septoria tritici blotch, STB), and *Pyrenophora tritici-repentis* (tan spot, TS) is assessed during registration trials (Bundessortenamt 2016).

B. graminis is an obligate biotrophic fungus that reproduces only on living cell tissue and infects wheat from the seedling stage to ear emergence. The infection not only adversely impacts quality parameters, due to altered composition of the grain content and depletion of carbohydrate reserves, but also yield components such as thousand kernel weight (Gao *et al.* 2018). Currently, more than 100 PM resistance

alleles are described in the literature, distributed over almost all 21 wheat chromosomes (Buerstmayr *et al.* 2016; Li *et al.* 2018). In addition, genetic studies have identified at least 119 quantitative trait loci (QTL) associated with adult plant resistance to PM (Li *et al.* 2014). Despite the large number of known PM resistance genes and QTL, the need to breed new resistant varieties is an ongoing task, as the pathogen possesses a diverse haplotype pool that underpins continual adaption of the fungus to improvements in host genetic resistance (Wicker *et al.* 2013).

STB, caused by the necrotrophic fungus *Z. tritici*, is one of the most damaging fungal diseases in regions with humid climates (Fones and Gurr 2015). Infection via wind-dispersed ascospores, which originate from stubble and wheat volunteers, takes place during early wheat developmental stages (Suffert *et al.* 2011). In a second stage of the fungal life cycle, infection mainly occurs by splash-dispersed pycnidiospores from basal leaf layers (Suffert *et al.* 2011). The long latent period, which typically lasts 3-4 weeks, makes it difficult for farmers to react sufficiently early to STB infection (Orton *et al.* 2011). In addition the intensive use of fungicides for controlling STB increases problems with fungicide resistance. In recent years, target site mutations have been found to evolve in the *Z. tritici* populations to commonly used fungicide groups including azoles, succinate dehydrogenase inhibitors, and strobilurins, providing increasing problems with effective control (Jørgensen *et al.* 2018). Genetic analyses investigating STB resistance have previously identified 21 major genes and at least 89 QTL (Brown *et al.* 2015). Despite this, there is still a lack of a broad range of commercially relevant wheat germplasms which show adequate resistance to *Z. tritici* infection (O'Driscoll *et al.* 2014).

Another economically significant residue-born wheat disease worldwide is TS, caused by the necrotrophic fungus *P. tritici-repentis*. Reduced tillage and retaining stubble, which are partly practices to stabilize the soil in sustainable agricultural approaches, increase the risk of infection due to the presence of *P. tritici-repentis* spores in stubble from previous season crops (Bockus and Shroyer 1998). The main symptoms are yellowish brown leaf spots surrounded by chlorotic and necrotic areas (Lamari and Bernier 1989). Disease development results in coalescence of spots, and consequently in a reduced assimilation rate and yield losses (Faris *et al.* 2013). The symptoms are mainly associated with the three *P. tritici-repentis* necrotrophic fungal protein effectors ToxA, ToxB, and ToxC (Strelkov and Lamari 2003), with further effectors also thought to be involved (Faris *et al.* 2013). Based on the ability of *P. tritici-repentis* to produce these three virulence factors, isolates are classified into eight different races (Strelkov and Lamari 2003). In wheat, allelic variation at the three effector sensitivity loci *Tsn1*, *Tsc1* and *Tsc2*, and the four tan spot resistance loci *Tsr2*, *Tsr3*, *Tsr4*, and *Tsr5* are known to confer qualitative resistance (Faris *et al.* 2013). Additionally, race-nonspecific QTL have been identified for TS resistance (Kollers *et al.* 2014; Juliana *et al.* 2018).

Because new wheat varieties need to be resistant to multiple fungal pathogens, it is of great interest whether simultaneously breeding for resistance to PM, STB, and TS is feasible without taking into account possible genetic interactions between resistance loci for these pathogens. So far, genetic studies in wheat have addressed the relationship of genetic resistance to multiple diseases mainly within bi-parental mapping populations and genome-wide association panels (Lillemo *et al.* 2008; Gurung *et al.* 2012, 2014; Li *et al.* 2014; Jighly *et al.* 2016; Juliana *et al.* 2018). Some describe genetic regions that are associated with multiple disease resistances such as to leaf rust, stripe rust, and PM (Li *et al.* 2014) or leaf rust, stripe rust, and TS (Juliana *et al.* 2018). However, the absence of genetic relations (Gurung *et al.* 2014) and the existence of antagonistic relations between different disease resistances are also propagated (Brown and Rant 2013; Jighly *et al.* 2016).

Simultaneous genetic analysis of resistance to the important wheat fungal diseases PM, STB, and TS at high genetic resolution, which can be achieved using multiparental populations, is of interest for resistance breeding. To address this, we carried out QTL mapping for disease resistance to PM, STB, and TS using a winter wheat multiparent advanced generation intercross (MAGIC) population. The population was constructed using eight founders, which differ in susceptibility to the three target diseases. First, using phenotypic data from MAGIC field trials at six sites over two seasons, we undertook QTL analysis for resistance to PM, STB, TS, and the agro-morphological traits plant height (PH), ear emergence time (EET), and leaf angle distribution (LAD), using four different genetic mapping approaches. Second, we analyzed coinciding QTL based on overlap of support intervals, and explored their relationships. Third, we identified and discuss potential genes underlying the traits of interest, which can serve as a starting point for further studies.

MATERIAL AND METHODS

Plant material and genetic map

An eight-founder MAGIC population of winter wheat (termed the 'BMWpop') comprising 394 $F_{6:8}$ lines was used (Stadlmeier *et al.* 2018). The eight founders 'Event,' 'BAYP4535,' 'Ambition,' 'Firl3565,' 'Format,' 'Potenzial,' 'Bussard,' and 'Julius' differed in various agro-morphological and disease traits. A genetic linkage map including 5435 single nucleotide polymorphism (SNP) markers and a functional marker for the powdery mildew resistance gene *Pm3a* was used for QTL analyses (Stadlmeier *et al.* 2018).

Field trials and trait evaluations

Field trials for assessing reactions to PM, STB, and TS were conducted in Germany and Denmark during 2016 and 2017 (Table 1). The field trial design in each year–location combination was an incomplete block design with two replicates each. The trial at Roggenstein consisted of plots 1.5 m × 3 m in size with ~1300 plants per plot. All other locations used double rows containing ~15 plants per row. Each trait was assessed plotwise as the mean of all plants per plot. Thus, trait evaluation is based on 1300 and 30 plants at Roggenstein and the remaining locations, respectively. Founders, control varieties, and checks differing in susceptibility were included with at least two replicates each in all field trials except for Roggenstein. At Roggenstein only founders were included. Fertilization and pest management, except fungicide treatment, followed the standard agronomic procedures at each location.

doi: https://doi.org/10.1534/g3.119.400068
Manuscript received February 8, 2019; accepted for publication March 20, 2019; published Early Online March 22, 2019.

Supplemental material available at Figshare: https://doi.org/10.25387/g3.7862531.
[1]Present address: Bavarian State Research Center for Agriculture, Institute for Crop Science and Plant Breeding, Freising, 85354, Germany.
[2]Present address: Aarhus University, Department of Agroecology, Slagelse 4200, Denmark
[3]Present address: John Bingham Laboratory, NIAB, Huntingdon Road, Cambridge CB3 0LE, United Kingdom
[4]Corresponding author: Am Gereuth 6, D-85354 Freising, Germany, E-mail: melanie.stadlmeier@mytum.de

Table 1 Overview of field trial environments and traits scored

Year	Location	GPS[a]	Abbreviation	Inoculation	Traits scored[b]
2016	Freising (DEU)	48°24′45.3″N 11°43′21.1″E	16FS1	*Z. tritici* conidia	PH, EET, LAD, STB
2016	Freising (DEU)	48°24′01.8″N 11°42′46.4″E	16FS2	None	PH, EET, LAD, TS
2016	Roggenstein (DEU)	48°10′51.9″N 11°19′07.3″E	16RG	None	PM
2017	Freising (DEU)	48°24′43.9″N 11°43′20.1″E	17FS1	*Z. tritici* conidia	PH, EET, LAD, PM, STB
2017	Freising (DEU)	48°24′38.6″N 11°43′27.9″E	17FS2	*P. tritici-repentis* infected straw	PH, EET, TS
2017	Slagelse (DNK)	55°25′06.9″N 11°22′54.7″E	17SL	*P. tritici-repentis* infected straw	PH, EET, LAD, TS

[a] Global Positioning System (GPS) coordinates.
[b] Traits are plant height (PH), ear emergence time (EET), leaf angle distribution (LAD), septoria tritici blotch (STB), tan spot (TS), and powdery mildew (PM).

Powdery mildew: Field trials were conducted in Germany during 2016 and 2017 (Table 1). In both years, powdery mildew infection occurred naturally without the use of susceptible varieties as spreaders. No fungicides were used before scoring time point for controlling other fungal diseases. Whole-plot disease severity was scored from 1 (no disease) to 9 (severe disease) according to the guidelines of the German Seed Board (Bundessortenamt 2000, Mohler *et al.* 2013, Table S1) when the ligule of the flag leaf was just visible (Feekes 9).

Septoria tritici blotch: Ten *M. graminicola* single-spore isolates, collected by the company EpiLogic GmbH (Freising, Germany) across Germany in 2015, and two historical isolates BAZ 6/1/04 and BAZ 8/8/04 (Risser *et al.* 2011), kindly provided by the Julius-Kühn-Institute (Quedlinburg, Germany), were screened for strong isolate growth and sporulation on media and virulence to all eight founders of BMWpop at the seedling stage. Single spore isolates were cultivated on yeast-glucose-malt agar (4 g yeast, 4 g malt, 4 g glucose, and 15 g agar per liter of distilled water) for five to seven days under white and ultraviolet light for 16 h at 20° and 8 h in darkness at 12° in an MLR-351 incubator (Sanyo Electric Co., Osaka, Japan). These plates were used as starter cultures for mass propagation in liquid yeast-glucose-malt medium (4 g yeast, 4 g malt, and 4 g glucose per liter of distilled water) as described in Risser *et al.* (2011). Fresh conidia of the isolates were concentrated using a separating funnel. The conidia concentration was determined using a Fuchs-Rosenthal hemocytometer (depth 0.2 mm; Laboroptik GmbH, Friedrichsdorf, Germany). The inoculum concentration was adjusted to $1x10^6$ conidia/ml consisting of equal shares of the four isolates St-SN-002, St-SN-004, BAZ 6/1/04, and BAZ 8/8/04. The inoculum was supplemented with 0.05% (v/v) Tween80. The BMWpop for analysis of STB resistance was cultivated in Germany in 2016 and 2017 (Table 1). In 2016, two weeks before inoculation the fenpropimorph fungicide Corbel was applied preventively with a reduced spray rate of 0.75 l per hectare. In 2017, seven days before inoculation a reduced application rate of 0.5 l per hectare was applied. The fungicidal activity of Corbel is against yellow and brown rust and powdery mildew (Anonymous 2018). The trials were artificially inoculated when the sheath of the flag leaf was completely grown out (Feekes 10-10.1). Inoculation was carried out two times at one-week intervals with 660 l inoculum per hectare during cloudy afternoons. An hour after the first inoculation, mist irrigation was applied with a one-hour break for each two hours of irrigation from 8:00 AM to 6:00 PM for the duration of eleven days. Six weeks after inoculation when the trait of interest showed a maximum of differentiation within the population, disease development on the flag leaf was assessed plotwise. Scoring was based on visually assessing the percentage leaf area covered by lesions exhibiting pycnidia using a rating scale from 0% (no symptoms) to 100% (severe disease).

Tan spot: In 2016, a field trial was carried out at a location in Germany where wheat after wheat was sown for over ten years with reduced tillage. Two additional field experiments were conducted in Denmark and Germany in the 2017 cropping season (Table 1). The experiments in the second year were both inoculated with 50 g/m^2 naturally *P. tritici-repentis* infected straw. The spreading of this straw litter took place in Denmark in December 2016 and in Germany in March 2017 when two to five leaves were unfolded (Feekes 1.2-1.5). In 2016 and 2017 in Germany, the fenpropimorph fungicide Corbel was applied preventively with a reduced spray rate of 0.75 and 0.5 l per hectare, respectively, before Feekes growth stage 8. In Denmark, the trial was treated with a reduced spray rate of 0.5 l pyraclostrobin fungicide Comet 200 per hectare at Feekes growth stage 7.1-7.4 to prevent the trial from rust infection. It is known that the level of resistance to the strobilurins fungicides within the *P. tritici-repentis* population is very high in the Danish test population and therefore, the control of tan spot using Comet 200 has to be considered as insignificant (Sierotzki *et al.* 2007). Two weeks after the first symptoms appeared, the infection of the flag leaf was visually assessed based on the percentage leaf area exhibiting brown to black spots surrounded by necrotic and chlorotic areas using a rating scale from 0% (no infestation) to 100% (severe disease).

Agro-morphological traits: The three agro-morphological traits, plant height, ear emergence time, and leaf angle distribution, were assessed in almost all trials (Table 1). PH was measured in cm from ground level to the top of the ears (excluding scurs) from Feekes developmental stage 11.3 to the end of cropping season. EET was recorded when half of the ear emerged above the flag leaf ligule (Feekes 10.3) for half of all plants per plot and converted into number of days after 1st May. The LAD score combined the leaf angle between the stem and the proximal third of the leaf and the overhanging of the distal part of the leaf. The rating was carried out in odd numbers from 1 (erectophile, $<45°$; no overhanging) to 9 (planophile, $>45°$; overhanging) at anthesis (Feekes 10.51-10.53).

Phenotypic data analysis

Outlying observations were identified within the raw phenotypic datasets according to Grubbs (1950) and removed only under obvious incorrect scoring or known problems with the specific plot. Each year–location combination was treated as an individual test environment (TE). All phenotypic data analysis were performed using R/lme4 (Bates *et al.* 2014; R Development Core Team 2017). The residuals of all traits in individual and across TEs were analyzed with residual diagnostic plots. Phenotypic data analysis and repeatability in individual TEs was based on a reduced model (equation 1) without consideration of the TE and the genotype * TE interaction effect. Phenotypic data across the TEs were adjusted based on the following model:

$$y_{ijkm} = \mu + g_i + l_j + gl_{ij} + r_{kj} + b_{mkj} + e_{ijkm}. \quad (1)$$

where y_{ijkm} is the trait observation, μ is the overall mean, g_i is the fixed effect of genotype i, l_j is the random effect of TE j, gl_{ij} is the random interaction effect of genotype i with TE j, r_{kj} is the random effect of replication k nested within TE j, b_{mkj} is the random effect of incomplete block m nested within replication k nested within TE j and e_{ijkm} is the random residual error. To obtain variance components, the genotype was fitted as random. The repeatability was the ratio of the genotypic variance and the sum of the genotypic and residual error variance. The heritability was estimated on an entry mean basis according to Hallauer and Miranda (1981). The Pearson's phenotypic correlation between traits was calculated based on the adjusted means across the TEs. Genotypic correlation coefficients were calculated in PLABSTAT Version 3Awin (Utz 2011) using adjusted means from common individual TEs and fitting genotype and TE as random.

QTL analysis

The adjusted means estimated in the individual TEs and in the combined analysis across TEs represented the phenotypic input data for QTL detection. The simple interval mapping (SIM) approach implemented in the package mpMap V2.0.2 (Huang and George 2011) was applied as the main QTL detection method (Figure 1). A subset of 2804 markers representing unique positions on the BMWpop genetic map (Stadlmeier *et al.* 2018) was used in interval mapping. The QTL mapping was based on founder probabilities computed using the mpMap function 'mpprob' implemented in R/mpMap (Huang and George 2011) at a threshold of 0.7. The function 'mpIM' was used for interval mapping. QTL were detected at a genome-wide significance threshold of $\alpha < 0.001$. This threshold was derived from an empirically null distribution with 1,000 simulation runs similar to Churchill and Doerge (1994). All detected QTL were simultaneously fitted in a full model using the function 'fit.' From this model fit, only QTL were kept with a p-value < 0.10 and the full model was fitted again to obtain the phenotypic variance explained (R^2) and the additive founder effects relative to 'Julius.' The QTL support interval (SI) was determined as the map distance in cM surrounding a QTL peak at a -log10(p) fall-off of ± 1.0. If QTL SIs overlapped, QTL were declared coinciding QTL (cQTL). QTL detected in SIM analysis were named following the recommendations for gene symbolization in wheat (McIntosh *et al.* 2013). To determine the physical position of each QTL in the wheat reference genome assembly, the sequence of the peak marker was used as a query against the IWGSC RefSeq v1.0 genome assembly (International Wheat Genome Sequencing Consortium 2018) using BLASTn analysis (Altschul *et al.* 1990). For composite interval mapping (CIM) (Figure 1), only linkage groups found to be significant in SIM were used. The CIM analysis was based on a forward selection procedure using the Akaike information criteria (Huang and George 2011). The number of selected cofactors was set to the number of detected QTL in SIM.

Another QTL mapping approach, a single marker analysis similar to Sannemann *et al.* (2015), was addressed to support the outcome of simple interval mapping. For this approach, all 5436 available markers were integrated. Generally, two different methods were used (Figure 1). In the identical by state (IBS) method, a regression against the binary allelic state (homozygote allele A, homozygote allele B) of each marker was conducted and the additive effect of the minor allele was estimated. In the identical by descent (IBD) method, a regression was conducted against the founder probabilities of each marker. Founder probabilities were calculated as stated above, and additive founder effects were estimated relative to 'Julius.' In both single marker regression methods, a random effect for MAGIC group assignment of each genotype was included initially. When this term was not significant, it was excluded from the final analysis. The derived p-values were corrected for multiple testing according to Benjamini and Hochberg (1995). Marker-trait associations (MTAs) were declared significant at a false discovery rate (FDR) of 0.01. Adjacent significant SNPs on a linkage group were assumed to represent the same QTL whenever the direction of additive effects was the same. Further QTL on the same linkage group were accepted when a MTA was at least 30 cM from another one. The MTA with the most significant FDR value was chosen as the QTL peak position. Finally, a full model including all detected QTL was fitted to estimate the overall R^2.

A QTL in SIM analysis was declared detected with other approaches when the SIs overlapped.

Data availability statement

Genotypic data are publically available at http://doi.org/10.14459/2018mp1435172. File Figure S1 contains the distribution of phenotypic data within test environments. File Figure S2 represents the residual diagnostic plots of phenotypic data. File Figure S3 shows the density plots of adjusted means. Supplementary Table S1 shows the rating scale for PM. Supplementary Tables S2 and S3 represent the phenotypic data within and across test environments, respectively. Supplementary Table S4 contains the correlation coefficients. Files Table S5-S8 show detailed mapping results for all traits analyzed. Supplemental material available at Figshare: https://doi.org/10.25387/g3.7862531.

RESULTS

Quantitative genetic analysis

The repeatability of trait measurements in the field trials ranged from 0.57 to 0.92 (Table 2). The correlation of the adjusted means (Table S2) between TEs was significant ($P < 0.001$) for each trait (Table 2). The highest values were observed for PH (0.93) and EET (0.84), while for the remaining traits the correlations ranged from 0.28 (LAD) to 0.63 (STB). The severity of infection between the TEs differed significantly at $P < 0.05$ for all three disease traits (Figure S1). The residuals of the adjusted means across TE's (Table S3) followed approximately a normal distribution (Figure S2). Box-Cox and log transformations were applied but did not improve the normality

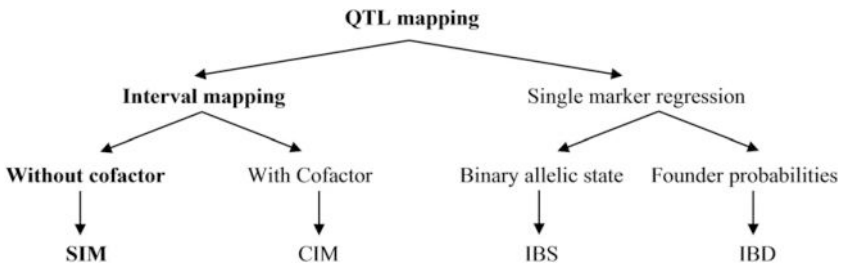

Figure 1 Overview of the QTL detection methods used.

Table 2 Estimates of the repeatability, the phenotypic correlation between test environments (TEs), the mean (± SE) of the population, the range of the population, the mean (± SE) of the founders, the genetic, the genotype * TE interaction, and the residual variance component ($\hat{\sigma}^2_g$, $\hat{\sigma}^2_{gl}$, $\hat{\sigma}^2_e$), the heritability ($\hat{h}^2$), and the number of test environments (No.TE) of the traits investigated

Trait[a]	No.TE	Repeatability	Cor(TE_x,TE_y)**	Mean(pop)	Range(pop)	Mean(found)	$\hat{\sigma}^2_g$*	$\hat{\sigma}^2_{gl}$*	$\hat{\sigma}^2_e$	$\hat{h}^2$
PM	2	0.57, 0.75	0.56	2.8 ± 0.08	0.6 - 7.7	2.5 ± 0.53	1.6	1.2	1.2	0.64
STB	2	0.83, 0.85	0.63	38.8 ± 0.88	8.5 - 91.5	36.8 ± 9.30	253.2	104.4	68.0	0.79
TS	3	0.39 - 0.67	0.34 - 0.61	38.6 ± 0.52	16.5 - 74.8	36.3 ± 3.09	74.4	42.4	102.6	0.70
PH	5	0.85 - 0.92	0.87 - 0.93	94.9 ± 0.42	72.3 - 113.4	90.3 ± 2.45	82.1	3.9	9.0	0.98
EET	5	0.67 - 0.85	0.60 - 0.84	34.8 ± 0.09	30.2 - 41.6	35.4 ± 0.49	3.6	0.6	1.1	0.94
LAD	4	0.44 - 0.59	0.28 - 0.49	5.3 ± 0.07	1.8 - 8.5	5.2 ± 0.30	1.3	0.7	1.8	0.77

[a] Powdery mildew (PM, score 1-9), septoria tritici blotch (STB, %), tan spot (TS, %), plant height (PH, cm), ear emergence time (EET, DaM), and leaf angle distribution (LAD, score 1-9).
*Significant at $P < 0.01$.
**Significant at $P < 0.001$.

and homoscedasticity of the data. Therefore, untransformed data was used for all analyses. The population mean was not significantly different from the parental mean for all traits (Table 2). However, transgressive segregation was identified for all traits except for STB (Figure S3). The full range of reaction scores was found for PM and STB compared to TS, for which the range was from 17 to 75% (Figure S3). The genotypic and genotype * TE variance components were significant at $P < 0.01$ for all traits in the combined analysis across TEs (Table 2). The heritability estimates for PM, STB, TS, and LAD were 0.64, 0.79, 0.70, and 0.77, respectively (Table 2); they were high for PH and EET with 0.98 and 0.93, respectively. Phenotypic data for STB was significantly correlated with PM and TS with 0.22 and 0.33, respectively (Table S4). However, the latter two diseases did not correlate phenotypically. PH and EET revealed significant negative phenotypic and genotypic correlation coefficients with STB and TS (Table S4). Although LAD showed no significant phenotypic correlations, genotypic correlations with STB and TS were significant with 0.32 and -0.20, respectively.

QTL mapping

SIM analysis of the disease and agro-morphological traits identified 22 and 15 QTL across TEs, respectively (Figure 2 and Table 3). The number of detected QTL for individual traits was between three (PH) and nine (TS). For each trait, the QTL collectively explained about 30% of the total phenotypic variance except for TS and PH with a total R^2 value of 40.5% and 53.0%, respectively (Table 3). In general, all mapping approaches explained comparable proportions of the phenotypic variance, although the IBS method always showed slightly lower values. An overview of the QTL detection with SIM is shown in Table 3 and detailed information including allelic effects and the detection within single TEs is given in the Table S5. The results of CIM, IBD, and IBS analysis are presented in Table S6, S7, and S8,

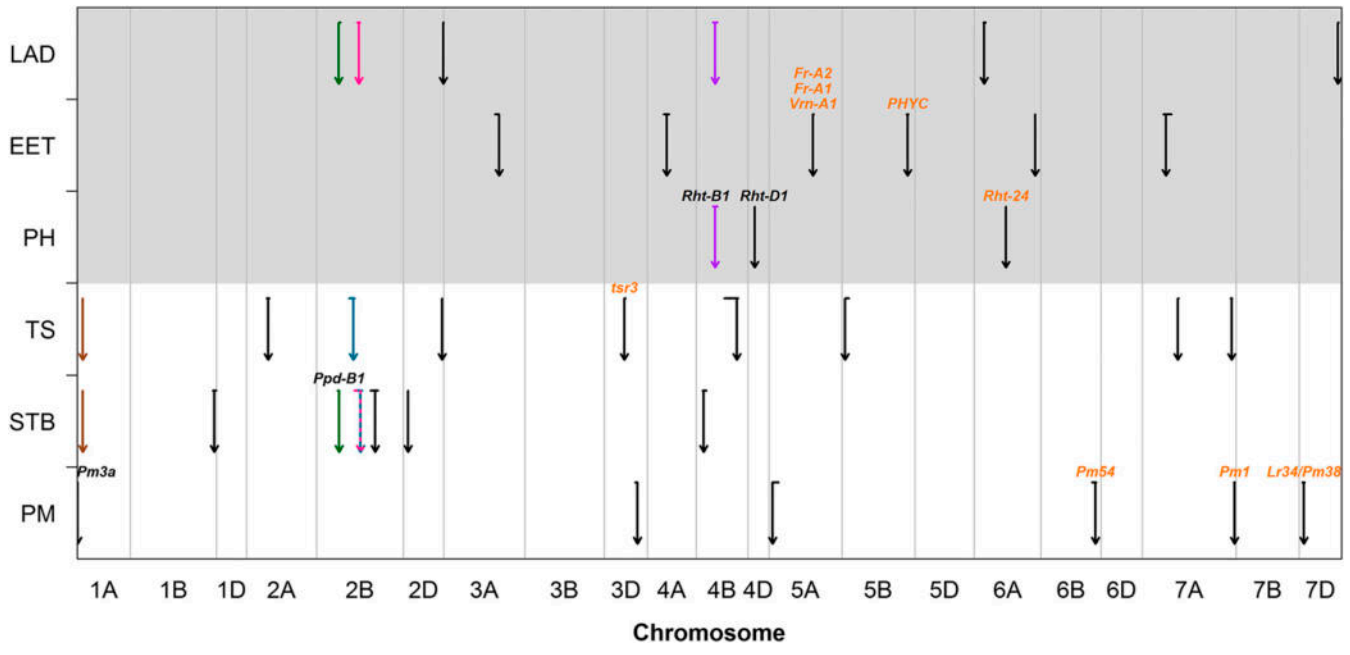

Figure 2 QTL detected in SIM analysis across test environments. The results are shown for the traits powdery mildew (PM), septoria tritici blotch (STB), tan spot (TS), plant height (PH), ear emergence time (EET) and leaf angle distribution (LAD). The arrows indicate the exact localization on the chromosome and the horizontal line above each arrow represents the support interval (SI) of the respective QTL. Overlapping QTL are labeled using the same color. Gene assignments based on functional markers are indicated in black and gene assignments based on physical positions are indicated in orange.

Table 3 Summary of QTL detected in SIM analysis across test environments. Chromosome (Chr.), position (Pos.), support interval (SI), -log(p) value, proportion of phenotypic variance explained (R^2), and the number of TEs (No.TE) in which a QTL was detected are given. Additionally, it is indicated whether QTL were also detected by composite interval mapping (CIM), identical by descent (IBD), and identical by state (IBS) approaches

Trait[a]	QTL	Chr.	Pos. (cM)	Pos (Mbp)	SI (cM)	-log(p)	R^2 [b]	No.TE	Method
PM [1-9]							**31.5**		
	QPm.lfl-1A	1A	3	–	2-3	6.4	9.4	1	CIM, IBD, IBS
	QPm.lfl-3D	3D	137	570	128-137	1.9	4.8	—	—
	QPm.lfl-5A	5A	16	19	14-38	1.2	4.9	—	—
	QPm.lfl-6B	6B	227	710	211-230	4.4	6.7	2	CIM, IBD, IBS
	QPm.lfl-7A	7A	382	730	379-384	5.2	12.8	2	CIM, IBD, IBS
	QPm.lfl-7D	7D	19	–	12-22	1.0	5.3	—	IBD
STB [%]							**27.1**		
	QStb.lfl-1A	1A	23	9	23-23	1.2	6.1	—	IBD
	QStb.lfl-1B	1B	347	690	341-356	2.2	5.9	1	CIM
	QStb.lfl-2B.1	2B	94	57	86-94	1.1	5.3	1	IBD
	QStb.lfl-2B.2	2B	181	440	155-188	1.2	4.7	1	—
	QStb.lfl-2B.3	2B	243	700	222-254	3.5	6.3	2	CIM, IBD, IBS
	QStb.lfl-2D	2D	20	10	20-20	5.4	8.5	2	CIM, IBD, IBS
	QStb.lfl-4B	4B	31	24	27-43	1.5	4.3	—	—
TS [%]							**40.5**		
	QTs.lfl-1A	1A	23	9	23-23	5.1	6.8	—	CIM, IBD
	QTs.lfl-2A	2A	90	71	83-94	4.7	6.6	1	CIM, IBD, IBS
	QTs.lfl-2B	2B	151	130	135-157	3.9	4.6	—	IBD
	QTs.lfl-2D	2D	160	640	160-160	4.5	6.7	2	IBD, IBS
	QTs.lfl-3D	3D	82	210	81-88	4.4	7.1	2	CIM, IBD
	QTs.lfl-4B	4B	170	600	117-175	1.6	5.2	—	IBD
	QTs.lfl-5B	5B	28	41	28-31	2.5	5.0	—	IBD, IBS
	QTs.lfl-7A.1	7A	148	130	148-151	3.5	10.6	2	CIM, IBD, IBS
	QTs.lfl-7A.2	7A	371	710	366-373	3.5	4.5	—	—
PH [cm]							**53.0**		
	QHt.lfl-4B	4B	80	63	68-90	∞	9.2	5	CIM, IBD, IBS
	QHt.lfl-4D	4D	27	–	27-27	∞	33.6	5	CIM, IBD, IBS
	QHt.lfl-6A	6A	130	450	130-130	10.8	12.6	2	IBD, IBS
EET [DaM]				0			**25.9**		
	QEet.lfl-3A	3A	230	650	213-230	4.2	8.8	5	CIM, IBD, IBS
	QEet.lfl-4A	4A	80	560	67-89	1.9	5.2	1	—
	QEet.lfl-5A	5A	182	550	180-185	3.5	7.6	4	CIM, IBD, IBS
	QEet.lfl-5B	5B	273	690	268-276	1.5	5.7	1	—
	QEet.lfl-6A	6A	251	600	250-252	2.9	5.0	1	IBS
	QEet.lfl-7A	7A	99	85	87-122	2.0	5.5	3	IBD
LAD [1-9]							**32.3**		
	QLad.lfl-2B.1	2B	92	53	92-100	1.4	5.8	—	—
	QLad.lfl-2B.2	2B	174	190	167-180	9.0	14.4	2	CIM, IBD, IBS
	QLad.lfl-2D	2D	166	640	164-167	3.7	5.6	1	CIM, IBD, IBS
	QLad.lfl-4B	4B	80	90	70-89	2.5	6.4	1	IBD, IBS
	QLad.lfl-6A	6A	40	19	36-46	4.7	6.6	1	CIM, IBD
	QLad.lfl-7D	7D	160	600	160-163	2.3	4.6	1	—

[a] Powdery mildew (PM), septoria tritici blotch (STB), tan spot (TS), plant height (PH), ear emergence time (EET), and leaf angle distribution (LAD).
[b] For each trait, the explained phenotypic variance of the model fitting all detected QTL simultaneously is given in bold values above the individual R^2 values for each QTL.
- No marker sequence for BLASTn query was available.
— QTL in no test environment or with no other method detected.
∞ P-value is zero.

respectively. The below-mentioned additive allelic effects are stated relative to the founder 'Julius'.

Powdery mildew: The QTL analysis of PM across TEs identified six QTL, which were located on chromosomes 1A, 3D, 5A, 6B, 7A, and 7D (Figure 2 and Table 3). The most significant QTL *QPm.lfl-1A* accounted for 9.4% of the phenotypic variance and coincided with the functional marker for the *Pm3a* gene. The resistance allele was contributed by the parent 'BAYP4535' which is the only founder carrying this allele (Stadlmeier *et al.* 2018). Two other highly significant QTL on chromosomes 7A and 6B explained 12.8% and 6.7% of the phenotypic variance, respectively. On chromosome 7A, the founders 'Event' and 'Ambition' and on chromosome 6B, the founder 'Ambition' decreased disease severity. Both QTL were identified by all mapping approaches and in all TEs (Table S5-S8).

Septoria tritici blotch: Seven QTL controlling resistance to STB were mapped to chromosomes 1A, 1B, 2B, 2D, and 4B in the analysis across

TEs (Figure 2 and Table 3). The two most significant QTL *QStb.lfl-2B.3* and *QStb.lfl-2D*, which were identified in all TEs and with all detection methods (Table S5-S8), explained 8.5% and 6.3% of the phenotypic variance, respectively (Table 3). At *QStb.lfl-2B.3*, the alleles of the founders 'Ambition' and 'Firl3565' decreased disease severity by 10.1% and 14.1%, respectively (Table S5). The 'Format' allele at *QStb.lfl-2D* increased disease severity by 10.1% (Table S5). The three QTL *QStb.lfl-1B*, *QStb.lfl-2B.1*, and *QStb.lfl-2B.2* were detected additionally to the combined analysis across environments in one of two TEs (Table S5). The peak marker of *QStb.lfl-2B.1* corresponded to a functional marker diagnostic for the late-heading allele at the photoperiod response gene, *Photoperiod-B1* (*Ppd-B1*).

Tan spot: For TS, nine QTL across environments were detected on chromosomes 1A, 2A, 2B, 2D, 3D, 4B, 5B, and 7A (Figure 2 and Table 3). The most significant QTL *QTs.lfl-1A* explained 6.8% of the phenotypic variation for this trait. The 'Bussard' allele increased TS infestation by 14.1% at this locus (Table S5). The QTL *QTs.lfl-7A.1*, *QTs.lfl-3D*, and *QTs.lfl-2D* also explained high proportions of the phenotypic variance of 10.6%, 7.1%, and 6.7%, respectively. These QTL were identified using several mapping approaches, and in two of three TEs each (Table 3 and Table S5-S8). The QTL *QTs.lfl-2A* on chromosome 2A explained 6.6% of the phenotypic variance and was mapped across TEs by all analysis methods and in one of three TEs (Table S5-S8).

Agro-morphological traits: Three PH QTL were identified on chromosomes 4B, 4D, and 6A (Figure 2 and Table 3). The two most significant QTL, *QHt.lfl-4D* and *QHt.lfl-4B*, explained 33.6% and 9.2% of the phenotypic variance, respectively (Table 3). The SIs of *QHt.lfl-4D* and *QHt.lfl-4B* coincided with the dwarfing genes *Reduced height-D1* (*Rht-D1*) and *Rht-B1*, respectively. The effects of the founders 'BAYP4535,' 'Firl3565,' 'Format,' and 'Bussard,' all carriers of the wild-type *Rht-D1a* allele, increased PH by up to 29 cm. The mildly dwarfing *Rht-B1b* allele possessed by 'BAYP4535' decreased PH by 9.9 cm (Table S5). The QTL *QHt.lfl-6A* was also highly significant and explained 12.6% of the phenotypic variation for this trait. Alleles from 'Ambition' and 'Potenzial' decreased PH by more than 9 cm at this QTL (Table S5).

The QTL analysis for EET detected six QTL on chromosomes 3A, 4A, 5A, 5B, 6A, and 7A (Figure 2 and Table 3). The two most significant QTL, *QEet.lfl-3A* and *QEet.lfl-5A*, explained 8.8% and 7.6% of the phenotypic variance, respectively. They were mapped with all approaches and in almost all TEs (Table S5-S8). *QEet.lfl-3A* alleles from 'Format,' 'Firl3565,' and 'Ambition' delayed EET by up to 1.6 days, while at *QEet.lfl-5A* the 'Bussard,' 'Potenzial,' and 'BAYP4535' alleles delayed EET by up to 1.5 days (Table S5). The QTL *QEet.lfl-7A* was observed in three of five TEs, explaining 5.5% of the phenotypic variance (Table 3 and Table S5).

Six QTL controlling LAD were identified on chromosomes 2B, 2D, 4B, 6A, and 7D (Figure 2 and Table 3). The most significant QTL *QLad.lfl-2B.2* explained 14.4% of the phenotypic variation and was identified by all methods (Table 3 and Table S5-S8). The 'Event' allele at this locus was associated with a more erectophile LAD (Table S5). The QTL *QLad.lfl-2D*, which explained 5.6% of the phenotypic variance, was also observed by all mapping approaches (Table 3 and Table S5-S8). The allele, which was associated with a more erectophile LAD, originated from 'Bussard' and showed an effect of 2.3 grades (Table S5).

Coinciding QTL

In total, five cQTL were identified on chromosomes 1A, 2B, and 4B (Figure 2). Two QTL overlaps each were detected for STB – TS and STB – LAD. One QTL overlap was observed on chromosome 4B for PH and LAD. The perfect overlap of *QStb.lfl-1A* and *QTs.lfl-1A* on chromosome 1A was pinpointed to 23 cM of the genetic map (Table 3). The 'Bussard' allele increased both STB and TS severity by 11.6% and 14.1%, respectively. The allelic effects of the remaining parents were not clearly opposite, except for the founder 'Event' (Table S5). The second cQTL between STB and TS was located on chromosome 2B. *QStb.lfl-2B.2* and *QTs.lfl-2B* showed just a small overlap of 2 cM and the respective peak markers were located 30 cM away from each other (Table 3). The alleles of 'BAYP4535' and 'Ambition' decreased both STB and TS severity by up to 6.1% and 10.8%, respectively. However, the alleles of the founders 'Event' and 'Potenzial' showed strong opposite effects with a difference of over 20% for the two diseases (Table S5). On chromosome 2B, an overlap between the already mentioned QTL *QStb-lfl.2B.2* for STB and the QTL *QLad.lfl-2B.2* for LAD was present. The SI of the LAD QTL with a size of 13 cM was completely embedded in the other one (Table 3). Especially the allelic effects of 'Event' revealed that a decrease in STB infestation came along with a more erectophile LAD but also the effects of the parents 'Ambition,' 'Potenzial,' and 'Bussard,' showed this behavior (Table S5). A second cQTL for STB and LAD was identified on the short arm of chromosome 2B, and coincides with the location of the major photoperiod response locus *Ppd-B1*. Although there was just a small overlap of 2 cM between *QStb.lfl-2B.1* and *QLad.lfl-2B.1*, the peak markers were located just 2 cM away from each other (Table 3). Despite this fact, the allelic effects showed no clear relational pattern of STB and LAD (Table S5). A further cQTL was located on chromosome 4B for PH and LAD. The SI of *QLad.lfl-4B* completely overlapped with the SI of *QHt.lfl-4B*. The allele of the founder 'BAYP4535', which is carrier of the *Rht-B1b* dwarfing allele, reduced height and was associated with a more planophile LAD. The alleles of the other parents showed no distinct relations (Table S5).

DISCUSSION

Field trials

In total, six field trials for the three diseases PM, STB, and TS were conducted. Except for the trial 17FS1, in each trial, a single disease was assessed and additional infections with other leaf diseases were not observed. In 17FS1 PM and STB were scored in the same field experiment but at different times. After scoring PM and several days before inoculation with STB, a fungicide against PM was applied. Although PM was scored in the STB trial in 2017, no genotype was so heavily infected that individual plants died before STB infestation. However, it appears unlikely that PM infestation had an influence on STB disease development, as the phenotypic correlation between PM scored in 16RG and STB scored in 16FS1 and 17FS1 was similar with 0.14 and 0.12, respectively. In addition, the correlation between PM scored in 17FS1 and STB scored in 16FS1 and 17FS1 was similar at 0.23 and 0.19, respectively.

Comparison of applied QTL mapping approaches

In parallel with the development of multiparental population designs, appropriate statistical methods have also been developed to analyze such populations accurately. In addition to advanced mixed linear model approaches for genome-wide association mapping (Bandillo *et al.* 2013; Sannemann *et al.* 2015), various software packages for interval mapping such as R/HAPPY (Mott *et al.* 2000), R/mpMap (Huang and George 2011), R/mpwgaim (Verbyla *et al.* 2014), and R/qtl2 (Broman *et al.* 2019) are now available. Zhang *et al.* (2017) introduced a two-stage QTL mapping strategy for four-way crosses to control the background genetic variation.

We mapped QTL with the single marker regression methods IBD and IBS and with the interval mapping approaches SIM and CIM implemented in R/mpMap (Figure 1). Although the statistical power of CIM is stronger than of SIM, we chose to use SIM as the main QTL detection method as cofactor selection in CIM remains challenging (Li *et al.* 2007; Wei and Xu 2016). We tried to counteract this issue by including only significant linkage groups of SIM in CIM and by setting the number of cofactors equal to the number of detected QTL in SIM. Our results (Table S6) suggest that this methodology is robust and can deal with this issue although it may result in missing of QTL only detectable in CIM.

The total number of QTL mapped with the different approaches strongly varied with the trait. An increased number of QTL for TS (IBS: 17, IBD: 23) and a reduced number of QTL for PM (IBS: 3, IBD: 5) and STB (IBS: 3, IBD: 5) were detected in single marker analysis compared to interval mapping. The IBS method identified 49% and 52% and the IBD method 70% and 68% of the SIM and CIM QTL, respectively. It is known that multiple testing increases the probability of detecting false positives when the statistical significance is not adjusted properly. For IBS and IBD method, we chose a FDR of 0.01 for all traits of interest. Therefore, our results indicate that a trait-specific significance threshold that accounts for the genetic architecture of the respective trait would have been more appropriate for IBS and IBD mapping.

The SIs of IBS and both interval mapping approaches were comparable (as measured in cM), whereas the SIs of IBD were generally longer (Table S7). For the single marker analysis, greater SIs were similarly detected by Sannemann *et al.* (2015) when using haplotype probabilities instead of the allelic state. They suggested that this is due to the haplotype blocks that expand over a genetic distance of several cM. These results indicate that IBD SIs might remain larger, until small haplotype blocks are generated by the mating design and the statistical methods used.

In general, the estimated effects based on founder probabilities were greater than the estimates based on the allelic state. This observation has previously been noted in a barley MAGIC population using a mixed linear model approach with an incorporated multi-locus procedure (Sannemann *et al.* 2015). In addition, we found out that the additive effects in linkage analyses are generally stronger than in IBD. As an example, at *QHt.lfl-4D*, the difference of the additive effects of PH between the two most contrasting parents 'Event' and 'Firl3565' was 31.7 cm, 32.3 cm, 26.5 cm, and 12.5 cm for SIM, CIM, IBD, and IBS, respectively (Table S5-S8). This raises the question whether the effects estimated using IBD are underestimated, or whether the effects of the linkage analysis are overestimated. Linkage analysis in bi-parental populations provides an unbiased estimate of the QTL effect compared to single-point analysis due to simultaneously analyzed linked markers (Lander and Botstein 1986). Therefore, it is more likely that the additive effects of interval mapping in MAGIC designs are unbiased, and that the haplotype-based founder probabilities are insufficient for estimating unbiased QTL effects in single-point analyses.

Despite the weaknesses of each method, strong and environmentally stable QTL were in most instances mapped with all approaches used here. This indicates that the combined use of these different methods may act as a tool to find robust QTL.

Strength and weakness of multiparental populations in QTL mapping

MAGIC designs are characterized by a high number of recombination events due to several rounds of inter-crossing (Kover *et al.* 2009; Cockram and Mackay 2018; Stadlmeier *et al.* 2018). Therefore, the probability of recombination between linked genetic loci is increased (Holland 2015). Smaller linkage blocks lead to higher accuracy and smaller SIs in linkage mapping (Li *et al.* 2005). In this study, 38% of the detected QTL in SIM and 60% of the QTL mapped in CIM showed SIs $\leq$ 5 cM. QTL results of other advanced intermated populations support our findings (Balint-Kurti *et al.* 2007; Huang *et al.* 2010). However, some QTL studies in bi-parental mapping populations also reported small SIs (0-20 cM) (Windju *et al.* 2017; Ren *et al.* 2017; Jia *et al.* 2018). Additionally, higher recombination rates have been suggested to break the linkage of two small-effect QTL, which subsequently may complicate their detection individually (Huang *et al.* 2010). Despite this potential drawback of MAGIC populations, we were able to map QTL with $<$ 5% of the explained phenotypic variance and minor additive effects such as *QPm.lfl-5A*, *QTs.lfl-2A*, and *QTs.lfl-2B* in addition to large QTL with high R^2 values and high additive effects (Table 3 and Table S5). A QTL study analyzing seed size and seed number using *Arabidopsis thaliana* MAGIC lines also did not observe reduced ability to detect small effect QTL (Gnan *et al.* 2014). Another concern stated about the statistical power of linkage mapping in MAGIC is related to a possible decrease in the number of QTL detectable due to the complex genetic background (Keurentjes *et al.* 2011). Some studies using multiparental populations detected fewer QTL compared to linkage analysis in bi-parental populations for the same trait (Kover *et al.* 2009; Huang *et al.* 2011). However, other studies have found no differences in the number of QTL detected (Gnan *et al.* 2014). Other studies have reported the detection of new QTL, likely due to the increased genetic variation introduced by several founders (Sannemann *et al.* 2015; Pascual *et al.* 2015). For the three diseases PM, STB, and TS, we mapped six, seven and nine QTL using SIM, respectively, and a slightly lower number using CIM. The QTL number for each trait is comparable to bi-parental linkage analyses that reported in the most cases 2-6 QTL for PM (Chantret *et al.* 2001; Börner *et al.* 2002; Bougot *et al.* 2006; Qu *et al.* 2018), 3-10 QTL for STB (Eriksen *et al.* 2003; Risser *et al.* 2011; Tabib Ghaffary *et al.* 2012; Naz *et al.* 2015; Adhikari *et al.* 2015) and 3-7 QTL for TS (Friesen and Faris 2004; Faris and Friesen 2005; Chu *et al.* 2008, 2010; Zwart *et al.* 2010). One study for a segregating wheat x spelt population described eleven QTL for PM but this was because of using a population constructed from a cross between two subspecies (Keller *et al.* 1999). In addition, the number of QTL for PH (3 in SIM and CIM) and EET (6 in SIM and 5 in CIM) was similar to other studies (Börner *et al.* 2002; Klahr *et al.* 2007; Zhang *et al.* 2008; Bai *et al.* 2013). For LAD, no comparison was possible, as this trait has not been widely studied in wheat. Based on these results, we did not find a reduction in power for detecting QTL in multiparental populations. However, especially for PM and STB, we observed a partially strongly reduced proportion of the total explained phenotypic variance of up to 50% compared to the total R^2 value in bi-parental populations. This could not be explained by the number of detected QTL as it was similar between the studies (Chantret *et al.* 2001; Eriksen *et al.* 2003; Friesen and Faris 2004; Li *et al.* 2005; Bougot *et al.* 2006; Risser *et al.* 2011). R^2 values depend on both the phenotypic variance, and on the genetic variance. The genetic variance is a function of the QTL effect and the allele frequency of the QTL (Falconer and Mackay 1996). Simulation studies demonstrated that a low minor allele frequency decreases the estimated proportion of the explained phenotypic variance of a QTL independently from the true R^2 value, given that the QTL effect is constant (Uemoto *et al.* 2015). Unlike the case in bi-parental populations, there is a higher probability for markers of lower minor allele frequencies in MAGIC designs. In the extreme case, only one founder contributes a specific allele to the population, which leads to a minor allele frequency of 1/8 in an

eight-founder MAGIC design. This may be responsible for the decreased explained phenotypic variances observed in multiparent crosses. Therefore, it seems obvious that mapping rare QTL variants combined with small effects will be more challenging in MAGIC populations (Kover *et al.* 2009).

Identification of candidate genes and multitrait loci

To find out whether the QTL detected in this study possibly represent known genes and genetic loci, the physical positions of the QTL peak markers in BMWpop and the markers linked to mapped genes were compared (Figure 2).

QPm.lfl-7D was mapped to the same genetic region as the multi-resistance gene *Lr34/Yr18/Sr57/Pm38*. However, the QTL peak marker was located 34 Mbp distal to the race non-specific gene *Lr34* (Krattinger *et al.* 2009). However, it is likely that *QPm.lfl-7D* corresponds to the gene *Lr34*: first, based on parental information (Serfling *et al.* 2011), we know that the parent 'Potenzial' possesses this gene, and second, *QPm.lfl-7D* was not mapped in seedling stage (Stadlmeier *et al.* 2018). This is in agreement with the fact that *Lr34* is classified as an adult plant resistance gene. *QPm.lfl-7A* was mapped on the long arm of chromosome 7A. In this region, a number of PM resistance loci have been previously mapped (Ouyang *et al.* 2014). *QPm.lfl-7A* was physically located between the two markers *Xwmc525* and *Xcdo347*. The QTL was 12 Mbp distal to the marker *Xwmc525* and 1 Mbp proximal to the marker *Xcdo347*. The latter is linked to the gene *Pm1* that is associated with the *Lr20/Sr15/Rlnn1* multi-resistance locus (Jayatilake *et al.* 2013; Ouyang *et al.* 2014). Based on the physical localization, it is likely that *QPm.lfl-7A* represents the *Pm1* gene. The *QPm.lfl-6B* peak marker was located 6 Mbp distal from the marker *Xbarc134*, which is linked to the race-specific resistance gene *Pm54* (Hao *et al.* 2015). The gene was recently described in the common winter wheat variety 'AGS 2000' as an all-stage resistance gene (Hao *et al.* 2015). Besides the *PmG3M* gene which, however, originated from *T. dicoccoides* (Xie *et al.* 2012), no additional PM genes are known in this region. Therefore, it is likely that the QTL represents the *Pm54* gene, particularly as *QPm.lfl-6B* was also mapped at the seedling stage (Stadlmeier *et al.* 2018).

The STB QTL *QStb.lfl-2B.3* on the long arm of chromosome 2B was mapped to the same genetic region as the *Stb9* gene. The QTL was physically mapped 61 Mbp proximal to the marker *Xwmc317* that is linked to the *Stb9* gene (Chartrain *et al.* 2009). This gene was reported to be active at the seedling stage. As we selected our isolates regarding the absence of seedling resistance, *QStb.lfl-2B.3* is assumed to represent an adult plant stage resistance locus and not *Stb9*. Our QTL was located 14 Mbp distal and 29 Mpb proximal to two other QTL described in literature for field resistance to STB (Eriksen *et al.* 2003; Miedaner *et al.* 2012). The proximal QTL was shown to be active only at the adult plant stage. Therefore, it appears that some way proximal of the seedling resistance gene *Stb9*, an adult plant stage resistance locus exists.

On the short arm of chromosome 2B, *QTs.lfl-2B* and the toxin insensitive locus *Tsc2* were located in the distal region (Faris *et al.* 2013). However, *tsc2* does not segregate in the population, as all founders of BMWpop are insensitive to ToxB (data not shown). However, it has been suggested that adjacent to *Tsc2*, another gene conferring resistance to several races of *P. tritici-repentis* might be present (Li *et al.* 2011). Based on the physical map positions, we conclude that this novel gene is located about 100 Mbp proximal to *Tsc2*. The qualitative TS resistance gene *Tsr3* on the short arm of chromosome 3D is located distal to the marker *Xbarc42* (Tadesse *et al.* 2007). *QTs.lfl-3D* was mapped 300 Mbp distal to this marker. Although the physical distance is large, it is still conceivable that the QTL corresponds to *Tsr3* as *Xbarc42* is not closely linked to that gene (Tadesse *et al.* 2007) and the genetic region is considered to possess a very low recombination rate. The ToxC effector insensitivity locus *Tsc1* is located very distal on the short arm of chromosome 1A (Faris *et al.* 2013), where *QTs.lfl-1A* was also mapped. A comparison based on physical position was not possible due to the lack of publically available sequences for the markers linked to *Tsc1*. However, it could be viewed as unlikely that *QTs.lfl-1A* corresponds to *Tsc1* as the QTL perfectly overlaps with *QStb.lfl-1A* and it has not been reported yet that *Z. tritici* produces the necrotrophic toxin ToxC.

Würschum *et al.* (2017) reported that almost all markers that have been significantly associated with the reduced-height gene *Rht24* have been located in the physical region between 400 and 450 Mbp on chromosome 6A. Our PH QTL on chromosome 6A was mapped to 452 Mbp, indicating that *QHt.lfl-6A* corresponds to *Rht24*.

The frost-tolerance loci *Fr-A1* and *Fr-A2* span a distance of 74 Mbp on chromosome 5A (McIntosh *et al.* 2013). The EET QTL *QEet.lfl-5A* was located in the center of this interval. Furthermore, only 1 Mbp distal to *Fr-A1* the vernalization locus *Vrn-A1* is located. Although functional markers showed that the BMWpop is monomorphic for the *Vrn-A1* allele, the *Vrn-A1* locus can still be considered as a candidate locus for *QEet.lfl-5A*. It was shown that copy number variation of *Vrn-A1* controls flowering time in winter varieties (Díaz *et al.* 2012). Therefore, it is likely that *QEet.lfl-5A* represents one of these three loci. On chromosome 5B, *QEet.lfl-5B* was located in the same genetic region as the vernalization gene *Vrn-B1* but 115 Mbp distal (Yan *et al.* 2003). However, winter wheat varieties normally carry homozygote recessive 'winter' alleles at the *Vrn* loci (Stelmakh 1987; Watson-Haigh *et al.* 2018). The closely linked flowering pathway gene *PHYTOCHROME C* (*PHYC*) has been shown via studies of artificial mutants in the tetraploid wheat *T. durum* to play a role in the control of flowering time (Chen *et al.* 2014). Therefore, it is uncertain whether *QEet.lfl-5B* corresponds to the *Vrn-B1* gene, or to another linked locus such as *PHYC*.

On chromosome 2B, three QTL for STB were mapped. However, *QStb.lfl-2B.1* and *QStb.lfl-2B.2* appear to represent resistance loci conditioned by leaf morphology because both overlapped with QTL for LAD. A relationship of LAD and STB could be expected since spray inoculation took place from the top of the canopy. It is already known that morphological traits such as PH and EET can be linked to STB resistance QTL (Eriksen *et al.* 2003). Besides the two aforementioned QTL, no further cQTL between disease and agro-morphological traits were detected, despite the fact that PH and EET were significantly correlated with STB and TS. However, we can assume that *QStb.lfl-2B.1* represents a resistance locus mainly conditioned, beside the leaf morphology, by heading date, as the peak marker is a functional marker for the major photoperiod response gene, *Ppd-B1*. Although this locus was segregating in the population, it was not possible to detect a QTL for EET in this region in the analysis across TEs. *Ppd-B1* was only mapped in the TE 16FS1 as a QTL for EET. This may be explained by the significant genotype * environment interaction.

Two genetic regions on the short arm of chromosome 1A (1AS) and the long arm of chromosome 7A (7AL) were identified to be associated with all three diseases. On chromosome 1A, the QTL for STB and TS showed a perfect overlap and the PM QTL was about 5 Mbp distally located. Based on the additive effects of the founders, a higher level of resistance to PM came along with a higher level of resistance to both necrotrophic diseases. On chromosome 7AL, the peak marker for *QPm.lfl-7A* was mapped 14 Mbp distal to *QTs.lfl-7A.2*. In the analysis across TEs, no QTL for STB was detected. However, in the TE 16FS1 a QTL for STB was mapped 5 Mbp distal to *QPm.lfl-7A*. While the

founder effects for PM and STB showed a similar trend, the effects for TS were antagonistic. This implies that the genetic region on chromosome 7AL simultaneously confers resistance to PM and STB and susceptibility to TS.

Recombinant inbred lines, which are selfed to around the F_5 generation, are valuable resources for developing heterogeneous inbred families (HIFs; Tuinstra *et al.* 1997). HIFs are characterized by a high identical genetic background combined with a different genetic constitution at the genomic region of interest. Pairs of progenies of such a family, which carry contrasting alleles at a target QTL, serve as a tool for an accurate investigation of the effects of these alleles. Additionally, crossing such pairs of progeny together in order to generate genetic recombination within the target QTL interval can be used to narrow the QTL target region to resolutions that may enable identification of the underlying gene and genetic variant. Accordingly, the future development of HIFs for QTL identified in this study will allow the precise phenotypic and molecular investigations of Mendalized QTL to be undertaken.

In summary, we validated the BMWpop MAGIC population as valuable plant genetic resource to investigate the genetic relations between various traits within a single population. We identified two genetic regions on chromosome 1AS and 7AL, which are associated with all three diseases. We conclude that parallel breeding for resistance to PM, STB, and TS appears feasible, although specific genetic regions such as on chromosomes and 7AL with contrasting effects for the different diseases should be kept in mind.

ACKNOWLEDGMENTS

We sincerely thank Josef Erl, Andreas Graßl, Mahira Duran, Sabine Schmidt, Adalbert Bund and the working group Wheat and Oat Breeding of the Bavarian State Research Center for Agriculture for their excellent assistance and accurate technical effort in the execution of the field trials in Germany. Big thanks goes to Michael Hess, Phytopathology, Technical University of Munich (TUM), for providing us a field side for the TS trial in 2016 and the straw for TS inoculation in Germany in 2017. The authors thank Bernhard Jaser and Friedrich Felsenstein for kindly providing single-spore isolates of *Z. tritici* and *P. tritici-repentis*. We gratefully thank Chris-Carolin Schön and the staff of Plant Breeding Chair, Technical University of Munich (TUM) for the ongoing opportunity of using computer capacity and office space and for their valuable advices throughout the duration of this effort. The authors would also like to thank Keith Gardner for kindly sharing the QTL mapping pipeline. We thank Annemarie Fejer Justesen, Min Lin, Morten Lillemo, and Richard Oliver for the fruitful cooperation.

Results have been achieved within the framework of the 2nd call ERA-NET for Coordinating Plant Sciences, with funding from the Deutsche Forschungsgemeinschaft (DFG, HA 5798/2-1), the Danish Council of Strategic Research (case number 5147-00002B) and the Biotechnology and Biological Sciences Research Council (BBSRC, grant BB/N00518X/1).

LITERATURE CITED

Anonymous, 2018 Corbel. A fungicide for use on winter and spring wheat, durum wheat, winter and spring barley, winter and spring oats, rye and triticale. https://www.agricentre.basf.co.uk/Documents/2018-Product-Files/Corbel.pdf. Accessed 2019–03–15.

Adhikari, T. B., S. Mamidi, S. Gurung, and J. M. Bonman, 2015 Mapping of new quantitative trait loci (QTL) for resistance to septoria tritici blotch in spring wheat (*Triticum aestivum* L.). Euphytica 205: 699–706. https://doi.org/10.1007/s10681-015-1393-4

Altieri, M. A., 2018 *Agroecology. The science of sustainable agriculture*, CRC Press, Boca Raton, FL. https://doi.org/10.1201/9780429495465

Altschul, S. F., W. Gish, W. Miller, E. W. Myers, and D. J. Lipman, 1990 Basic local alignment search tool. J. Mol. Biol. 215: 403–410. https://doi.org/10.1016/S0022-2836(05)80360-2

Bai, C., Y. Liang, and M. J. Hawkesford, 2013 Identification of QTLs associated with seedling root traits and their correlation with plant height in wheat. J. Exp. Bot. 64: 1745–1753. https://doi.org/10.1093/jxb/ert041

Balint-Kurti, P. J., J. C. Zwonitzer, R. J. Wisser, M. L. Carson, M. A. Oropeza-Rosas *et al.*, 2007 Precise mapping of quantitative trait loci for resistance to southern leaf blight, caused by *Cochliobolus heterostrophus* race O, and flowering time using advanced intercross maize lines. Genetics 176: 645–657. https://doi.org/10.1534/genetics.106.067892

Bandillo, N., C. Raghavan, P. Muyco, M. A. L. Sevilla, I. T. Lobina *et al.*, 2013 Multi-parent advanced generation inter-cross (MAGIC) populations in rice: progress and potential for genetics research and breeding. Rice (N. Y.) 6: 11. https://doi.org/10.1186/1939-8433-6-11

Bates, D., M. Mächler, B. Bolker, and S. Walker, 2014 Fitting linear mixed-effects models using lme4.

Benjamini, Y., and Y. Hochberg, 1995 Controlling the false discovery rate: A practical and powerful approach to multiple testing. J. R. Stat. Soc. B 57: 289–300.

Bockus, W. W., and J. P. Shroyer, 1998 The impact of reduced tillage on soilborne plant pathogens. Annu. Rev. Phytopathol. 36: 485–500. https://doi.org/10.1146/annurev.phyto.36.1.485

Börner, A., E. Schumann, A. Fürste, H. Cöster, B. Leithold *et al.*, 2002 Mapping of quantitative trait loci determining agronomic important characters in hexaploid wheat (*Triticum aestivum* L.). Theor. Appl. Genet. 105: 921–936. https://doi.org/10.1007/s00122-002-0994-1

Bougot, Y., J. Lemoine, M. T. Pavoine, H. Guyomar'ch, V. Gautier *et al.*, 2006 A major QTL effect controlling resistance to powdery mildew in winter wheat at the adult plant stage. Plant Breed. 125: 550–556. https://doi.org/10.1111/j.1439-0523.2006.01308.x

Broman, K. W., D. M. Gatti, P. Simecek, N. A. Furlotte, P. Prins *et al.*, 2019 R/qtl2: software for mapping quantitative trait loci with high-dimensional data and multi-parent populations. Genetics 211: 495–502. https://doi.org/10.1534/genetics.118.301595

Brown, J. K. M., L. Chartrain, P. Lasserre-Zuber, and C. Saintenac, 2015 Genetics of resistance to *Zymoseptoria tritici* and applications to wheat breeding. Fungal Genet. Biol. 79: 33–41. https://doi.org/10.1016/j.fgb.2015.04.017

Brown, J. K. M., and J. C. Rant, 2013 Fitness costs and trade-offs of disease resistance and their consequences for breeding arable crops. Plant Pathol. 62: 83–95. https://doi.org/10.1111/ppa.12163

Bundessortenamt, 2000 Richtlinien für die Durchführung von landwirtschaftlichen Wertprüfungen und Sortenversuchen. http://www.bundessortenamt.de/internet30/fileadmin/Files/PDF/Richtlinie_LW2000.pdf. Accessed 2019–03–12.

Bundessortenamt, 2016 Richtlinien für die Durchführung von landwirtschaftlichen Wertprüfungen und Sortenversuchen. http://www.bundessortenamt.de/internet30/fileadmin/Files/PDF/RILI_201602_Getreide.pdf. Accessed 2018–11–07.

Buerstmayr, H., V. Mohler, and M. Kohli, 2016 Advances in control of wheat diseases: Fusarium head blight, wheat blast and powdery mildew, pp. 345–370 in *Achieving sustainable cultivation of wheat*., Burleigh dodds, Cambridge, UK.

Chantret, N., D. Mingeot, P. Sourdille, M. Bernard, J. M. Jacquemin *et al.*, 2001 A major QTL for powdery mildew resistance is stable over time and at two development stages in winter wheat. Theor. Appl. Genet. 103: 962–971. https://doi.org/10.1007/s001220100645

Chartrain, L., P. Sourdille, M. Bernard, and J. K. M. Brown, 2009 Identification and location of *Stb9*, a gene for resistance to septoria tritici blotch in wheat cultivars courtot and tonic. Plant Pathol. 58: 547–555. https://doi.org/10.1111/j.1365-3059.2008.02013.x

Chen, A., C. Li, W. Hu, M. Y. Lau, H. Lin *et al.*, 2014 *Phytochrome C* plays a major role in the acceleration of wheat flowering under long-day photoperiod. Proc. Natl. Acad. Sci. USA 111: 10037–10044. https://doi.org/10.1073/pnas.1409795111

Chu, C.-G., S. Chao, T. L. Friesen, J. D. Faris, S. Zhong *et al.*, 2010 Identification of novel tan spot resistance QTLs using an SSR-based linkage map of tetraploid wheat. Mol. Breed. 25: 327–338. https://doi.org/10.1007/s11032-009-9335-2

Chu, C.-G., T. L. Friesen, S. S. Xu, and J. D. Faris, 2008 Identification of novel tan spot resistance loci beyond the known host-selective toxin insensitivity genes in wheat. Theor. Appl. Genet. 117: 873–881. https://doi.org/10.1007/s00122-008-0826-z

Churchill, G. A., and R. W. Doerge, 1994 Empirical threshold values for quantitative trait mapping. Genetics 138: 963–971.

Cockram, J., and I. Mackay, 2018 Genetic mapping populations for conducting high-resolution trait mapping in plants. Adv. Biochem. Eng. Biotechnol. 164: 109–138. https://doi.org/10.1007/10_2017_48

Deutsch, C. A., J. J. Tewksbury, M. Tigchelaar, D. S. Battisti, S. C. Merrill *et al.*, 2018 Increase in crop losses to insect pests in a warming climate. Science 361: 916–919. https://doi.org/10.1126/science.aat3466

Díaz, A., M. Zikhali, A. S. Turner, P. Isaac, and D. A. Laurie, 2012 Copy number variation affecting the *photoperiod-B1* and *vernalization-A1* genes is associated with altered flowering time in wheat (*Triticum aestivum*). PLoS One 7: e33234. https://doi.org/10.1371/journal.pone.0033234

Eriksen, L., F. Borum, and A. Jahoor, 2003 Inheritance and localisation of resistance to *Mycosphaerella graminicola* causing septoria tritici blotch and plant height in the wheat (*Triticum aestivum* L.) genome with DNA markers. TAG Theor. Appl. Genet. 107: 515–527. https://doi.org/10.1007/s00122-003-1276-2

European Parliament, 2009 Directive 2009/128/EC of the European Parliament and of the Council. https://eur-lex.europa.eu/LexUriServ/LexUriServ.do?uri=OJ:L:2009:309:0071:0086:en:PDF. Accessed 2019–01–03.

Eurostat Agriculture, forestry and fishery statistics - 2017 edition. https://ec.europa.eu/eurostat/en/web/products-statistical-books/-/KS-FK-17–001. Accessed 2018–10–29.

Falconer, D., and T. Mackay, 1996 *Introduction to quantitative genetics*, Longman, Harlow, UK.

Faris, J. D., and T. L. Friesen, 2005 Identification of quantitative trait loci for race-nonspecific resistance to tan spot in wheat. Theor. Appl. Genet. 111: 386–392. https://doi.org/10.1007/s00122-005-2033-5

Faris, J. D., Z. Liu, and S. S. Xu, 2013 Genetics of tan spot resistance in wheat. Theor. Appl. Genet. 126: 2197–2217. https://doi.org/10.1007/s00122-013-2157-y

Fones, H., and S. Gurr, 2015 The impact of septoria tritici blotch disease on wheat: An EU perspective. Fungal Genet. Biol. 79: 3–7. https://doi.org/10.1016/j.fgb.2015.04.004

Friesen, T. L., and J. D. Faris, 2004 Molecular mapping of resistance to *Pyrenophora tritici-repentis* race 5 and sensitivity to Ptr ToxB in wheat. Theor. Appl. Genet. 109: 464–471. https://doi.org/10.1007/s00122-004-1678-9

Gao, H., J. Niu, and S. Li, 2018 Impacts of wheat powdery mildew on grain yield & quality and its prevention and control methods. Am. J. Agric. For. 6: 141–147.

Gnan, S., A. Priest, and P. X. Kover, 2014 The genetic basis of natural variation in seed size and seed number and their trade-off using *Arabidopsis thaliana* MAGIC lines. Genetics 198: 1751–1758. https://doi.org/10.1534/genetics.114.170746

Grubbs, F. E., 1950 Sample criteria for testing outlying observations. Ann. Math. Stat. 21: 27–58. https://doi.org/10.1214/aoms/1177729885

Gurung, S., J. M. Hansen, J. M. Bonman, A. I. N. Gironella, and T. B. Adhikari, 2012 Multiple disease resistance to four leaf spot diseases in winter wheat accessions from the USDA national small grains collection. Crop Sci. 52: 1640. https://doi.org/10.2135/cropsci2011.08.0408

Gurung, S., S. Mamidi, J. M. Bonman, M. Xiong, G. Brown-Guedira *et al.*, 2014 Genome-wide association study reveals novel quantitative trait loci associated with resistance to multiple leaf spot diseases of spring wheat. PLoS One 9: e108179. https://doi.org/10.1371/journal.pone.0108179

Hallauer, A., and J. Miranda, 1981 *Quantitative genetics in maize breeding*, Iowa State University Press, Ames, IA.

Hao, Y., R. Parks, C. Cowger, Z. Chen, Y. Wang *et al.*, 2015 Molecular characterization of a new powdery mildew resistance gene *Pm54* in soft red winter wheat. Theor. Appl. Genet. 128: 465–476. https://doi.org/10.1007/s00122-014-2445-1

Holland, J. B., 2015 MAGIC maize: a new resource for plant genetics. Genome Biol. 16: 163. https://doi.org/10.1186/s13059-015-0713-2

Huang, B. E., and A. W. George, 2011 R/mpMap: a computational platform for the genetic analysis of multiparent recombinant inbred lines. Bioinformatics 27: 727–729. https://doi.org/10.1093/bioinformatics/btq719

Huang, Y.-F., D. Madur, V. Combes, C. L. Ky, D. Coubriche *et al.*, 2010 The genetic architecture of grain yield and related traits in *Zea maize* L. revealed by comparing intermated and conventional populations. Genetics 186: 395–404. https://doi.org/10.1534/genetics.110.113878

Huang, X., M.-J. Paulo, M. Boer, S. Effgen, P. Keizer *et al.*, 2011 Analysis of natural allelic variation in Arabidopsis using a multiparent recombinant inbred line population. Proc. Natl. Acad. Sci. USA 108: 4488–4493. https://doi.org/10.1073/pnas.1100465108

International Wheat Genome Sequencing Consortium, 2018 Shifting the limits in wheat research and breeding using a fully annotated reference genome. Science. 361: eaar7191.

Jayatilake, D. V., E. J. Tucker, H. Bariana, H. Kuchel, J. Edwards *et al.*, 2013 Genetic mapping and marker development for resistance of wheat against the root lesion nematode *Pratylenchus neglectus*. BMC Plant Biol. 13: 230. https://doi.org/10.1186/1471-2229-13-230

Jia, A., Y. Ren, F. Gao, G. Yin, J. Liu *et al.*, 2018 Mapping and validation of a new QTL for adult-plant resistance to powdery mildew in Chinese elite bread wheat line Zhou8425B. Theor. Appl. Genet. 131: 1063–1071. https://doi.org/10.1007/s00122-018-3058-x

Jighly, A., M. Alagu, F. Makdis, M. Singh, S. Singh *et al.*, 2016 Genomic regions conferring resistance to multiple fungal pathogens in synthetic hexaploid wheat. Mol. Breed. 36: 127. https://doi.org/10.1007/s11032-016-0541-4

Jørgensen, L. N., R. P. Oliver, and T. M. Heick, 2018 Occurance and avoidance of fungicide resistance in cereal diseases. pp. 235–259 in Integrated disease management of wheat and barley. *Burleigh Dodds series in Agricultural Science,* edited by Oliver, R. P. Burleigh Dodds Science Publishing, Cambridge, UK.

Juliana, P., R. P. Singh, P. K. Singh, J. A. Poland, G. C. Bergstrom *et al.*, 2018 Genome-wide association mapping for resistance to leaf rust, stripe rust and tan spot in wheat reveals potential candidate genes. Theor. Appl. Genet. 131: 1405–1422. https://doi.org/10.1007/s00122-018-3086-6

Keller, M., B. Keller, G. Schachermayr, M. Winzeler, J. E. Schmid *et al.*, 1999 Quantitative trait loci for resistance against powdery mildew in a segregating wheat×spelt population. TAG Theor. Appl. Genet. 98: 903–912. https://doi.org/10.1007/s001220051149

Keurentjes, J. J. B., G. Willems, F. van Eeuwijk, M. Nordborg, and M. Koornneef, 2011 A comparison of population types used for QTL mapping in *Arabidopsis thaliana*. Plant Genet. Resour. 9: 185–188. https://doi.org/10.1017/S1479262111000086

Klahr, A., G. Zimmermann, G. Wenzel, and V. Mohler, 2007 Effects of environment, disease progress, plant height and heading date on the detection of QTLs for resistance to fusarium head blight in an European winter wheat cross. Euphytica 154: 17–28. https://doi.org/10.1007/s10681-006-9264-7

Kollers, S., B. Rodemann, J. Ling, V. Korzun, E. Ebmeyer *et al.*, 2014 Genome-wide association mapping of tan spot resistance (*Pyrenophora tritici-repentis*) in European winter wheat. Mol. Breed. 34: 363–371. https://doi.org/10.1007/s11032-014-0039-x

Kover, P. X., W. Valdar, J. Trakalo, N. Scarcelli, I. M. Ehrenreich *et al.*, 2009 A multiparent advanced generation inter-cross to fine-map quantitative traits in *Arabidopsis thaliana*. PLoS Genet. 5: e1000551. https://doi.org/10.1371/journal.pgen.1000551

Krattinger, S. G., E. S. Lagudah, W. Spielmeyer, R. P. Singh, J. Huerta-Espino *et al.*, 2009 A putative ABC transporter confers durable resistance to multiple fungal pathogens in wheat. Science 323: 1360–1363. https://doi.org/10.1126/science.1166453

Lamari, L., and C. C. Bernier, 1989 Evaluation of wheat lines and cultivars to tan spot (*Pyrenophora tritici-repentis*) based on lesion type. Can. J. Plant Pathol. 11: 49–56. https://doi.org/10.1080/07060668909501146

Lander, E. S., and D. Botstein, 1986 Mapping complex genetic traits in humans: New methods using a complete RFLP linkage map. Cold Spring Harb. Symp. Quant. Biol. 51: 49–62. https://doi.org/10.1101/SQB.1986.051.01.007

Li, G., B. F. Carver, C. Cowger, G. Bai, and X. Xu, 2018 *Pm223899*, a new recessive powdery mildew resistance gene identified in Afghanistan landrace PI 223899. Theor. Appl. Genet. 131: 2775–2783. https://doi.org/10.1007/s00122-018-3199-y

Li, Z., C. Lan, Z. He, R. P. Singh, G. M. Rosewarne *et al.*, 2014 Overview and application of QTL for adult plant resistance to leaf rust and powdery mildew in wheat. Crop Sci. 54: 1907. https://doi.org/10.2135/cropsci2014.02.0162

Li, R., M. A. Lyons, H. Wittenburg, B. Paigen, G. A. Churchill *et al.*, 2005 Combining data from multiple inbred line crosses improves the power and resolution of quantitative trait loci mapping. Genetics 169: 1699–1709. https://doi.org/10.1534/genetics.104.033993

Li, H. B., W. Yan, G. R. Liu, S. M. Wen, and C. J. Liu, 2011 Identification and validation of quantitative trait loci conferring tan spot resistance in the bread wheat variety Ernie. Theor. Appl. Genet. 122: 395–403. https://doi.org/10.1007/s00122-010-1455-x

Li, H., G. Ye, and J. Wang, 2007 A modified algorithm for the improvement of composite interval mapping. Genetics 175: 361–374. https://doi.org/10.1534/genetics.106.066811

Lillemo, M., B. Asalf, R. P. Singh, J. Huerta-Espino, X. M. Chen *et al.*, 2008 The adult plant rust resistance loci *Lr34/Yr18* and *Lr46/Yr29* are important determinants of partial resistance to powdery mildew in bread wheat line Saar. Theor. Appl. Genet. 116: 1155–1166. https://doi.org/10.1007/s00122-008-0743-1

McIntosh, R. A., Y. Yamazaki, J. Dubcovsky, J. Rogers, C. Morris *et al.*, 2013 Catalogue of gene symbols for wheat. 12th International wheat genetic symposium. Yokohama, Japan, September.

Miedaner, T., P. Risser, S. Paillard, T. Schnurbusch, B. Keller *et al.*, 2012 Broad-spectrum resistance loci for three quantitatively inherited diseases in two winter wheat populations. Mol. Breed. 29: 731–742. https://doi.org/10.1007/s11032-011-9586-6

Mohler, V., C. Bauer, G. Schweizer, H. Kempf, and L. Hartl, 2013 *Pm50*: a new powdery mildew resistance gene in common wheat derived from cultivated emmer. J. Appl. Genet. 54: 259–263. https://doi.org/10.1007/s13353-013-0158-9

Mott, R., C. J. Talbot, M. G. Turri, A. C. Collins, and J. Flint, 2000 A method for fine mapping quantitative trait loci in outbred animal stocks. Proc. Natl. Acad. Sci. USA 97: 12649–12654. https://doi.org/10.1073/pnas.230304397

Naz, A. A., M. Klaus, K. Pillen, and J. Léon, 2015 Genetic analysis and detection of new QTL alleles for septoria tritici blotch resistance using two advanced backcross wheat populations. Plant Breed. 134: 514–519.

O'Driscoll, A., S. Kildea, F. Doohan, J. Spink, and E. Mullins, 2014 The wheat-septoria conflict: a new front opening up? Trends Plant Sci. 19: 602–610. https://doi.org/10.1016/j.tplants.2014.04.011

Orton, E. S., S. Deller, and J. K. M. Brown, 2011 *Mycosphaerella graminicola*: from genomics to disease control. Mol. Plant Pathol. 12: 413–424. https://doi.org/10.1111/j.1364-3703.2010.00688.x

Ouyang, S., D. Zhang, J. Han, X. Zhao, Y. Cui *et al.*, 2014 Fine physical and genetic mapping of powdery mildew resistance gene *MlIW172* originating from wild emmer (*Triticum dicoccoides*). PLoS One 9: e100160. https://doi.org/10.1371/journal.pone.0100160

Pascual, L., N. Desplat, B. E. Huang, A. Desgroux, L. Bruguier *et al.*, 2015 Potential of a tomato MAGIC population to decipher the genetic control of quantitative traits and detect causal variants in the resequencing era. Plant Biotechnol. J. 13: 565–577. https://doi.org/10.1111/pbi.12282

Qu, C., Y. Guo, F. Kong, Y. Zhao, H. Li *et al.*, 2018 Molecular mapping of two quantitative trait loci for adult-plant resistance to powdery mildew in common wheat (*Triticum aestivum* L.). Crop Prot. 114: 137–142. https://doi.org/10.1016/j.cropro.2018.08.030

R Development Core Team, 2017 *R: A language and environment for statistical computing*. R foundation for statistical computing, Vienna, Austria.

Ren, Y., W. Hou, C. Lan, B. R. Basnet, R. P. Singh *et al.*, 2017 QTL analysis and nested association mapping for adult plant resistance to powdery mildew in two bread wheat populations. Front. Plant Sci. 8: 1212. https://doi.org/10.3389/fpls.2017.01212

Risser, P., E. Ebmeyer, V. Korzun, L. Hartl, and T. Miedaner, 2011 Quantitative trait loci for adult-plant resistance to *Mycosphaerella graminicola* in two winter wheat populations. Phytopathology 101: 1209–1216. https://doi.org/10.1094/PHYTO-08-10-0203

Sannemann, W., B. E. Huang, B. Mathew, and J. Léon, 2015 Multi-parent advanced generation inter-cross in barley: high-resolution quantitative trait locus mapping for flowering time as a proof of concept. Mol. Breed. 35: 86. https://doi.org/10.1007/s11032-015-0284-7

Serfling, A., I. Krämer, V. Lind, E. Schliephake, and F. Ordon, 2011 Diagnostic value of molecular markers for *Lr* genes and characterization of leaf rust resistance of German winter wheat cultivars with regard to the stability of vertical resistance. Eur. J. Plant Pathol. 130: 559–575. https://doi.org/10.1007/s10658-011-9778-2

Sierotzki, H., R. J. Frey, S. Wullschleger, S. Palermo, S. Karlin *et al.*, 2007 *Cytochrome b* gene sequence and structure of *Pyrenophora teres* and *P. tritici-repentis* and implications for QoI resistance. Pest Manag. Sci. 63: 225–233. https://doi.org/10.1002/ps.1330

Singh, R. P., P. K. Singh, J. Rutkoski, D. P. Hodson, X. He *et al.*, 2016 Disease impact on wheat yield potential and prospects of genetic control. Annu. Rev. Phytopathol. 54: 303–322. https://doi.org/10.1146/annurev-phyto-080615-095835

Stadlmeier, M., L. Hartl, and V. Mohler, 2018 Usefulness of a multiparent advanced generation intercross population with a greatly reduced mating design for genetic studies in winter wheat. Front. Plant Sci. 9: 1825. https://doi.org/10.3389/fpls.2018.01825

Stelmakh, A. F., 1987 Growth habit in common wheat (*Triticum aestivum* L. em. Thell.). Euphytica 36: 513–519. https://doi.org/10.1007/BF00041495

Strelkov, S. E., and L. Lamari, 2003 Host–parasite interactions in tan spot (*Pyrenophora tritici-repentis*) of wheat. Can. J. Plant Pathol. 25: 339–349. https://doi.org/10.1080/07060660309507089

Suffert, F., I. Sache, and C. Lannou, 2011 Early stages of septoria tritici blotch epidemics of winter wheat: build-up, overseasoning, and release of primary inoculum. Plant Pathol. 60: 166–177. https://doi.org/10.1111/j.1365-3059.2010.02369.x

Tabib Ghaffary, S. M., J. D. Faris, T. L. Friesen, R. G. F. Visser, T. A. J. van der Lee *et al.*, 2012 New broad-spectrum resistance to septoria tritici blotch derived from synthetic hexaploid wheat. Theor. Appl. Genet. 124: 125–142. https://doi.org/10.1007/s00122-011-1692-7

Tadesse, W., M. Schmolke, S. L. K. Hsam, V. Mohler, G. Wenzel *et al.*, 2007 Molecular mapping of resistance genes to tan spot [*Pyrenophora tritici-repentis* race 1] in synthetic wheat lines. Theor. Appl. Genet. 114: 855–862. https://doi.org/10.1007/s00122-006-0484-y

Trnka, M., R. P. Rötter, M. Ruiz-Ramos, K. C. Kersebaum, J. E. Olesen *et al.*, 2014 Adverse weather conditions for European wheat production will become more frequent with climate change. Nat. Clim. Chang. 4: 637–643. https://doi.org/10.1038/nclimate2242

Tuinstra, M. R., G. Ejeta, and P. B. Goldsbrough, 1997 Heterogeneous inbred family (HIF) analysis: a method for developing near-isogenic lines that differ at quantitative trait loci. Theor. Appl. Genet. 95: 1005–1011. https://doi.org/10.1007/s001220050654

Uemoto, Y., S. Sasaki, T. Kojima, Y. Sugimoto, and T. Watanabe, 2015 Impact of QTL minor allele frequency on genomic evaluation using real genotype data and simulated phenotypes in Japanese Black cattle. BMC Genet. 16: 134. https://doi.org/10.1186/s12863-015-0287-8

Utz, H., 2011 *PLABSTAT Version 3A. A computer program for statistical analysis of plant breeding experiments*, Institut für Pflanzenzüchtung,

Saatgutforschung und Populationsgenetik Universität Hohenheim, Stuttgart, Deutschland.
van der Bom, F., J. Magid, and L. S. Jensen, 2017 Long-term P and K fertilisation strategies and balances affect soil availability indices, crop yield depression risk and N use. Eur. J. Agron. 86: 12–23. https://doi.org/10.1016/j.eja.2017.02.006
Verbyla, A. P., A. W. George, C. R. Cavanagh, and K. L. Verbyla, 2014 Whole-genome QTL analysis for MAGIC. Theor. Appl. Genet. 127: 1753–1770. https://doi.org/10.1007/s00122-014-2337-4
Watson-Haigh, N. S., R. Suchecki, E. Kalashyan, M. Garcia, and U. Baumann, 2018 DAWN: a resource for yielding insights into the diversity among wheat genomes. BMC Genomics 19: 941. https://doi.org/10.1186/s12864-018-5228-2
Wei, J., and S. Xu, 2016 A random-model approach to QTL mapping in multiparent advanced generation intercross (MAGIC) populations. Genetics 202: 471–486. https://doi.org/10.1534/genetics.115.179945
Wicker, T., S. Oberhaensli, F. Parlange, J. P. Buchmann, M. Shatalina *et al.*, 2013 The wheat powdery mildew genome shows the unique evolution of an obligate biotroph. Nat. Genet. 45: 1092–1096. https://doi.org/10.1038/ng.2704
Windju, S. S., K. Malla, T. Belova, R. C. Wilson, J. A. Dieseth *et al.*, 2017 Mapping and validation of powdery mildew resistance loci from spring wheat cv. Naxos with SNP markers. Mol. Breed. 37: 61. https://doi.org/10.1007/s11032-017-0655-3
Würschum, T., S. M. Langer, C. F. H. Longin, M. R. Tucker, and W. L. Leiser, 2017 A modern green revolution gene for reduced height in wheat. Plant J. 92: 892–903. https://doi.org/10.1111/tpj.13726
Xie, W., R. Ben-David, B. Zeng, A. Distelfeld, M. S. Röder *et al.*, 2012 Identification and characterization of a novel powdery mildew resistance gene *PmG3M* derived from wild emmer wheat, *Triticum dicoccoides*. Theor. Appl. Genet. 124: 911–922. https://doi.org/10.1007/s00122-011-1756-8
Yan, L., A. Loukoianov, G. Tranquilli, M. Helguera, T. Fahima *et al.*, 2003 Positional cloning of the wheat vernalization gene *VRN1*. Proc. Natl. Acad. Sci. USA 100: 6263–6268. https://doi.org/10.1073/pnas.0937399100
Zhang, S., L. Meng, J. Wang, and L. Zhang, 2017 Background controlled QTL mapping in pure-line genetic populations derived from four-way crosses. Heredity (Edinb) 119: 256–264. https://doi.org/10.1038/hdy.2017.42
Zhang, K., J. Tian, L. Zhao, and S. Wang, 2008 Mapping QTLs with epistatic effects and QTL × environment interactions for plant height using a doubled haploid population in cultivated wheat. J. Genet. Genomics 35: 119–127. https://doi.org/10.1016/S1673-8527(08)60017-X
Zwart, R. S., J. P. Thompson, A. W. Milgate, U. K. Bansal, P. M. Williamson *et al.*, 2010 QTL mapping of multiple foliar disease and root-lesion nematode resistances in wheat. Mol. Breed. 26: 107–124. https://doi.org/10.1007/s11032-009-9381-9

Communicating editor: S. Pearce

6 ACKNOWLEDGEMENTS

First of all, I would like to express my deep gratitude to my supervisor Prof. Dr. Volker Mohler for the shared interest in the most interesting research topic, his valuable advices, and his constant and dedicated support throughout all my PhD project phases. Thanks to his encouragement and excellent guidance on research, I could gain and extend my knowledge in various subjects such as plant population types, genetics of plant disease resistances, and scientific writing skills. I also would like to thank him for interesting discussions, which went beyond the topic of my thesis.

I would like to gratefully acknowledge and sincerely thanks Prof. Dr. Chris-Carolin Schön for her constant and unconditional support and for her excellent and extremely helpful encouragement and assistance since the time, I have been interested in plant breeding. I would like to thank for the outstanding opportunity of using computing power and office space and to be part of her chair. Her extensive mentoring and knowledge significantly accelerated and enriched my PhD project.

Thanks a lot also to Prof. Dr. Andreas Graner for being engaged on my graduate committee and to Prof. Dr. Ralph Hückelhoven for chairing my PhD thesis committee.

Many thanks to Dr. Peter Doleschel and Dr. Lorenz Hartl for giving me the opportunity to work on this most interesting topic at the Bavarian State research Center at the working group wheat and oat within the framework of the international EfectaWheat project. This research was funded by the Deutsche Forschungsgemeinschaft (DFG, HA 5798/2-1) within the framework of the 2nd call ERA-NET for Coordinating Plant Science.

I also like to thank Dr. Michael Hess for initiating this project and for his support during TS trials in Germany.

Many thanks to the EfectaWheat project partners, especially, Dr. Beatrice Corsi, Min Lin, Dr. Lise Nistrup Jørgensen, and Dr. James Cockram, for their encouraged collaboration and fruitful discussions. I also thank Dr. Keith Gardner for providing source files of the NIAB 2015 MAGIC population.

I wish to express my deep gratitude to my colleagues Sabine Schmidt, Mahira Duran, Josef Erl, Andreas Graßl, Konrad Wallner, Benedikt Puschmann, Adalbert Bund, and the working group wheat and oat at the Bavarian State Research Center for their excellent and accurate work and assistance during the development of BMWpop and the experimental part of my PhD project. I thank Petra Greim for her excellent work in the

molecular lab. I also would like to thank the complete working group for the nice working atmosphere.

I cordially acknowledge all former and present members of the Plant Breeding Chair for their scientific discussions and the nice working environment. Special thanks go to my office mate Anne Stache and our tea/coffee break group for always having an open ear for various issues and for their encouraging words. I also greatly thank Armin Hölker for proof reading this thesis.

I want to express my special thanks to my friends Babsi, Willi, and Jeanette for their unconditional willingness to listen and discuss things that touched me emotionally during this time and for their continuous encouraging words and stories.

My most heartfelt and deepest gratitude goes to my family whose unconditional love, welfare, confidence, and support have been with me since I have been here on earth. Words cannot express my gratefulness to have you as family. Without you – mum, dad, and Martina – I would not be the person who I am today!